THE UNIVERSITY OF CHICAGO

FUNCTIONAL MORPHOLOGY AND EVOLUTION OF THE BALISTIFORM SWIMMING MODE

A DISSERTATION SUBMITTED TO
THE FACULTY OF THE DIVISION OF THE BIOLOGICAL SCIENCES
AND THE PRITZKER SCHOOL OF MEDICINE
IN CANDIDACY FOR THE DEGREE OF
DOCTOR OF PHILOSOPHY

GRADUATE PROGRAM IN INTEGRATIVE BIOLOGY

BY

ANDREW BRADLEY GEORGE

CHICAGO, ILINOIS

JUNE 2020

TABLE OF CONTENTS

LIST OF TABLES

LIST OF FIGURES

ACKNOWLEDGEMENTS

My dissertation research would not have been possible without the support of many people and institutions. First, I would like to thank the members of my thesis committee. My thesis advisor, Mark Westneat has been a great mentor throughout my graduate career. Mark has always enthusiastically encouraged me to pursue my research interests at my own pace and to allow my thesis to evolve as each project revealed new, interesting avenues that I hadn't considered in my thesis proposal. Mark introduced me to tropical reef field research early on in my grad career when we searched for balistoid ectoparasites in Okinawa, Japan during a pilot study for a parasitology project. He encouraged me to continue pursuing field research opportunities to fully understand the ecological context of my lab experiments, and our future trips to French Polynesia solidified my interest in and dramatically improved my understanding of fish ecomorphology. Mark has also been an excellent grant writing mentor, an invaluable skill that I will carry with me for the rest of my career. Finally, the academic freedom that Mark provided me with in both the lab and the field greatly increased my confidence in my ability to design and conduct independent research projects.

I am grateful for Melina Hale's support and advice throughout my dissertation, even as the focus of my research drifted away from sensory biomechanics. The summer that I spent studying fin neuroanatomy in the Hale lab during my first year at the University of Chicago helped me understand the neural control behind the swimming kinematics I researched during my thesis. My thesis chair, Callum Ross, also provided valuable discussions and advice as my research progressed. I am particularly appreciative of Callum's suggestion to use the DeepLabCut program to digitize my swimming kinematics videos, as this program made it possible for me to describe more detailed fin motions than would have been possible with manual digitization alone. The neuromechanics course taught by Melina and Callum during my first year at the university played

a large role in my development of a thesis research agenda aimed at comprehensively studying the biomechanics, functional morphology and ecology of balistoid fishes.

I am also appreciative of the wonderful fishes, education and action department staff at the Field Museum of Natural History. Working closely with scientists and educators at the Field Museum has been a highlight of my graduate career. Caleb McMahan, Susan Mochel and Kevin Swagel were incredibly welcoming in the fishes collections and provided a fun and engaging work environment to conduct my morphometrics and ecology literature survey research. They smoothly facilitated my use of fish specimens for both research and educational programming. Caleb and I also had many interesting discussion about fish morphometrics. I enjoyed developing and submitting conservation postdoc grant and fellowship proposals with Caleb, Lesley de Souza and Michelle Thompson, and I learned a lot from these experiences. Finally, I thoroughly enjoyed working on fishes education events with Susan, Kevin, Caleb and Ed Schweitzer. The opportunities that Ed provided for me to directly interact with the public in a variety of contexts have been invaluable to my graduate experience. It was always inspiring and grounding to talk with children about natural history and evolution. I'm excited to continue these scientific and educational collaborations during my postdoc position at the Field Museum.

I was fortunate to be surrounded by a supportive group of graduate students in the Darwin Cluster. I cannot thank Aaron Olsen enough for his constant support, technical advice and friendship during our time working together in the Westneat lab and for years after Aaron moved on to his postdoc position. I consider Aaron to be one of my most influential scientific mentors and an inspiring role model. I used his R package StereoMorph for every chapter of my thesis, as well as most of my side projects from morphometrics to swimming kinematics and field behavior experiments. Brett Aiello has also been a great academic mentor through training me on the high

speed video equipment, providing technical advice, and even road tripping across the America Southwest with me to teach a desert ecology field course. Chloe Nash has been a close collaborator throughout the second half of my graduate career, and our conversations have broadened my research scope to include global and life history trends in my research. Our field and functional biogeography work together has resulted in some of the most interesting and exciting projects to come out of my graduate career. I am grateful for the time Chloe has spent discussing technical research details and helping me improve my coding skills. Chloe and I spent a lot of time planning for and conducting field work in Moorea, French Polynesia together towards the end of my time at the University of Chicago. This experience greatly improved my scientific diving and project management skills, and I enjoyed the opportunity to work on these field projects together.

The other graduate student and postdoc members of the Westneat lab, Charlie McCord, Katie Whitlow, Sam Gartner and Lily Hughes have also been delightful people to work with and learn from. Charlie McCord has been a great academic mentor and provided me with lots of helpful triggerfish and morphometrics knowledge. Additionally, the balistoid phylogeny that she published during her thesis work with Mark Westneat served as the backbone of all phylogenetic comparative methods in my research, allowing for rigorous evolutionarily-informed analyses. Katie Whitlow has been a great friend and lab mate. Our overlapping fish functional morphology research interests have led to numerous conversations that have improved my understanding of biomechanics research techniques and phylogenetic comparative methods in a functional context. Similarly, it has been fun to chat about fish biomechanics and functional morphology with Sam Gartner. Adam Hardy has been a great friend and colleague throughout my entire time at the university. I have really enjoyed designing and constructing biomechanics equipment with Adam in the lab and spending time with him and his family outside of work. A number of undergraduate

students, high school students, and lab technicians including Hannah Weller, Jacob Feingold, Guillermo Zapata, Nicholas Slimmon and Isaac Krone aided in the design, filming, digitization, and analyses of the swimming kinematics experiments in this thesis. I learned a lot from these lab mates and look forward to continuing to work with them on biomechanics projects in the future. Additionally, I have really enjoyed working with the undergraduates Mireille Farjo and Sofia Garrick on their fish evolutionary morphology independent study projects.

Finally, I a owe a special thank you to Westneat Lab alumnus Brad Wright for his foundational work on balistiform locomotor biomechanics that set the stage for much of my thesis work. Brad's previous research on the functional morphology and hydrodynamics of triggerfish swimming allowed me to develop my hypotheses and select avenues of research that allowed for fruitful, detailed morphological, ecological and biomechanical research in a large evolutionary context that make up the bulk of this thesis.

I have also had numerous teaching opportunities while at the University of Chicago, for which I am truly grateful. I have spent dozens of hours teaching comparative anatomy lecture and lab courses with Mark Westneat, and these teaching experiences are some of my fondest graduate school memories. Mark has encouraged me to pursue my passion for teaching, and I am very thankful that he supported my decisions to spend so much time teaching and taking pedagogy courses through the Chicago Center for Teaching (CCT). The teaching certificate program offered through the CCT has dramatically improved my teaching effectiveness, and Mark has always encouraged me to integrate new teaching techniques learned in these CCT courses my teaching in his courses. I am also thankful for the opportunity to teach biological ethics with Vicky Prince. This course offered a very different teaching experience from the small format comparative

anatomy lab courses, and Vicky and Melissa Lindberg made a large effort to allow teaching assistants to participate in the development and constant evolution of the course.

Eric Larsen's desert ecology lecture and field courses provided me with some of the most memorable experiences of my life. Eric allowed me to take complete control of the content and delivery of two full lectures for a large lecture course, an opportunity that solidified my interest in college teaching. Eric's three-week desert ecology field course provided me with yet another unique teaching experience set in the blazing hot deserts of the American Southwest with a small group of enthusiastic undergraduate students and an amazing cohort of graduate student teaching assistants. Despite ending up in the hospital along the way, this trip was a highlight of my graduate career and taught me that I am capable of effectively teaching and connecting with students in just about any academic setting. Eric's passionate commitment to teaching was also inspiring and exciting to be a part of. Finally, I am thankful to Daniel Bataller for asking me to guest lecture in his interdisciplinary museum studies course at the University of Illinois at Chicago (UIC). The opportunity to freely develop a biological collections research curriculum that fit into an art history course for a group of humanities-major students was a challenging and rewarding experience. My conversations with the students in the course and Daniel about the success of these lectures were incredibly valuable as I developed my pedagogy skills.

I also have many funding sources and organizations to thank. The majority of my research was funded by the National Science Foundation through research grants to Mark Westneat (grants: 1425049 and 1541547) and fellowship support in the form of the Graduate Research Fellowship Program (GRFP). The funding provided by the GRFP (grants: 1144082 and 1746045) allowed me to develop and freely adapt my research agenda in order to best answer the series of questions that I found most important and interesting to pursue. This academic freedom allowed me the

independence to incorporate new and exciting research methods into my thesis as they were developed. I also received one year of fellowship support through the U.S. Department of Education's Graduate Assistance in Areas of National Need (GAANN) program in Integrative Neuromechanics (grant: P200A150077). I am thankful for the research funds provided by the Committee on Evolutionary Biology's Henry Hinds Fund that allowed me to purchase the fishes used in swimming performance and biomechanics studies. A large France and Chicago Collaborating in the Sciences (FACCTS) research grant from the University of Chicago's France Chicago Center provided me with the invaluable opportunity to study reef fish behavior and kinematics in the wild in Moorea, French Polynesia. A number of natural history museums provided photographs, specimen data, and ecological data used in this thesis. These museums include the Field Museum of Natural History, the National Museum of Natural History (NMNH), the Royal Ontario Museum (ROM), the University of Michigan Museum of Zoology (UMMZ), I am particularly thankful for Dr. Hiroshi Senou and Mr. Hiroaki Hayashi providing scaled specimen photos from the Kanagawa Prefectural Museum of Natural History and for Dr. Jack Randall and Dr. Jeff Williams providing so many high quality photographs for my morphometrics work.

Finally, this thesis would not have been possible without the constant support and love from my partner Rachel, my parents, and my siblings Liz, Laura, and Ian.

ABSTRACT

Fishes have evolved a wide variety of fin and body shapes and inhabit nearly every aquatic habitat on Earth. Understanding associations between fish morphologies and functional traits that facilitate their occupation of these diverse ecosystems is a general goal of many evolutionary ichthyologists. Exploring these relationships in the context of swimming can be especially informative, as most fishes rely on swimming performance for nearly all aspects of their lives. This thesis examines the functional morphology of triggerfishes (family: Balistidae) and filefishes (family: Monacanthidae) in the superfamily Balistoidea in the contexts of endurance swimming performance, ecology, and steady swimming biomechanics. Despite high morphological and ecological diversity, all balistoid fishes power slow steady swimming using their median dorsal and anal fins in a swimming mode termed balistiform locomotion and transition to a gait dominated by body and caudal fin undulations at high speeds.

First, I use swimming performance experiments and geometric morphometrics of 13 balistoid species to explore relationships among fin and body shapes, gait transition strategies, and endurance swimming performance (George and Westneat 2019). This research reveals that balistoid fishes use several biomechanical strategies to achieve high endurance swimming performance. Balistiform specialists possess long, large median fins capable of powering high-speed locomotion using the median fins alone. Conversely, body/ caudal fin specialists possess short, small median fins, ill-suited for high-speed balistiform locomotion, but narrow caudal peduncles capable of facilitating high-speed caudal fin-powered locomotion. Species with large, high aspect ratio fins exhibit the highest overall endurance swimming performance.

In the second study, I explore patterns of morphological evolution, fin asymmetry, and ecomorphology among 80 balistoid species. Morphologies range from deep-bodied forms with

high aspect ratio median fins to elongate forms with low aspect ratio, rectangular median fins. Ancestral state estimations reveal an early morphological divergence between families, with the filefish common ancestor exhibiting low dorsal, anal, and caudal fin aspect ratios and the triggerfish ancestor possessing high aspect ratio median fins. Dorsal and anal fin aspect ratios then underwent widespread convergence events within and between families. High aspect ratio fins are associated with pelagic and planktivorous species that benefit from high endurance swimming performance. Finally, this chapter reveals widespread morphological asymmetries between dorsal and anal fins.

Next, I use high-speed video to study three-dimensional dorsal and anal fin kinematics during steady balistiform locomotion of the gilded triggerfish, *Xanthichthys auromarginatus*. This work reveals differences in nearly every kinematic property between dorsal and anal fins and along their lengths, with the exception of all fin rays oscillating at the same frequency. Leading edge fin rays provide nearly half the total propulsive effort, and the dorsal fin provides greater effort than the anal fin. Given the relatively morphologically symmetrical fins of *X. auromarginatus*, these biomechanical fin asymmetries likely occur in many balistoid species, challenging the long-standing assumption of symmetrical balistiform median fin biomechanics. In the concluding chapter, I review the implications of these results for the evolution of the balistiform swimming mode and discuss an ongoing balistiform swimming maneuverability field project.

CHAPTER ONE: INTRODUCTION

Among the roughly 34,000 extant species, fishes exhibit an incredible degree of morphological and functional diversity, facilitating their successful occupation of nearly every aquatic ecosystem on Earth (Froese and Pauly 2019). Fish locomotor diversity provides a particularly stunning example of the vast assortment of morphological and biomechanical specializations that fishes have evolved for life in these disparate habitats. Of course, the vast majority of fishes swim through the water column using their bodies and fins as their primary means of locomotion (Breder 1926), but some fishes have evolved the unique fin and body morphologies that allow them to glide through the air (Fish 1990; Breder 1926), walk along underwater (King et al. 2011; Jamon et al. 2007; Pace and Gibb 2009; Rade 2013) and terrestrial (Pace and Gibb 2009) substrates, and even climb waterfalls (Schoenfuss and Blob 2003; Blob et al. 2006). Even among the swimmers, species exhibit an extraordinary variety of biomechanically distinct swimming modes to power aquatic locomotion, and this functional diversity is often reflected by the morphologies of the fishes. Accordingly, fish swimming modes have been defined based on to the parts of the body involved in forward thrust production during steady swimming.

The classically defined swimming modes consist of two broad groups: body/caudal fin (BCF) locomotion and median/paired fin (MPF) locomotion (Figure 1.1). Body/caudal fin swimmers use axial muscle contractions to undulate sinusoidal body bending waves anteriorly to posteriorly along their bodies, or simply oscillate their caudal fins (Figure 1.1 A). Conversely, MPF swimmers undulate or oscillate their median (dorsal and anal) and/ or paired (pectoral and pelvic) fins to power forward propulsion, with little to no contribution from the axial body musculature at most swimming speeds (Figure 1.1 B).

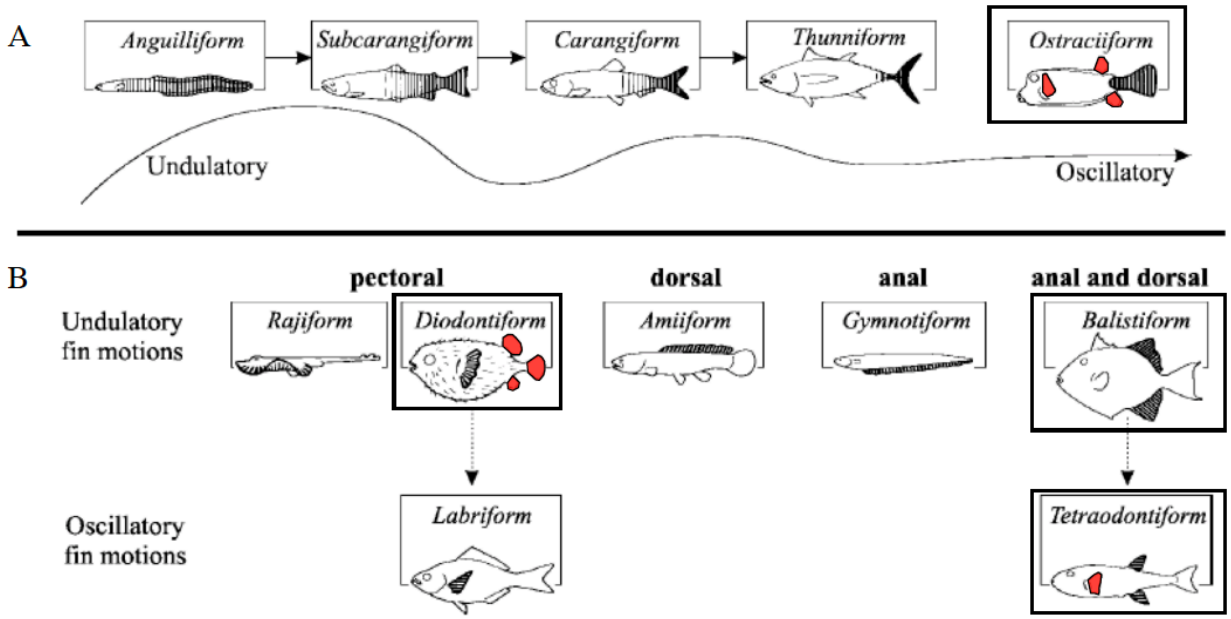

Figure 1.1. Classically defined fish swimming modes.
Black shaded regions indicate the parts of the body and fins used to power propulsion. (A) Body/caudal fin locomotion. (B) Median/paired fin locomotion. Swimming modes named after fish families in the order Tetraodontiformes are indicated by dark black boxes, and red shading indicates fins determined to be involved in thrust production based on resent research (Plaut and Chen 2003; Hove et al. 2001; Arreola and Westneat 1996). Figure adapted from Sfakiotakis, Lane, and Davies (1999) and Lindsey (1978).

Many BCF swimmers are capable of large thrust production and efficient high-speed cruising, a trend thought to facilitate their success in open ocean and fast flowing river habitats, while many MPF swimmers are capable of highly efficient slow swimming and extraordinary maneuverability thought to play a role in their successful occupation of structurally complex habitats (reviewed in Sfakiotakis, Lane, and Davies 1999). These associations between swimming modes and habitat use are best explained in the context of biomechanics and functional morphology, or the relationships between organismal form and function. Perhaps the most widespread and extensively studied fish swimming functional morphology relationship is the association between high aspect ratio fins and increased endurance swimming performance (Nursall 1958; Drucker and Jensen 1996; Walker and Westneat 2002; Wainwright, Bellwood, and

Westneat 2002; C. J. Fulton and Bellwood 2004; M. J. Lighthill 1970; Karpouzian, Spedding, and Cheng 1990; Xin and Wu 2013). Aspect ratio is a measure of how 'wing-like' an air- or hydrofoil is, and in the context of fish swimming it is typically defined as the maximum span of the fin squared, divided by the surface area of the fin (Nursall 1958; M. J. Lighthill 1970). However, fin aspect ratio measurements have a long history in the study of fish morphology and biomechanics, and have been calculated in a number of different ways over the years, making direct comparisons of fin aspect ratios difficult between studies and fin groups. This complication as well as potential solutions are discussed in detail at the end of this introduction.

Despite differences in the exact methods used to calculate fin aspect ratios, it is clear from modelling (M. J. Lighthill 1970; Karpouzian, Spedding, and Cheng 1990; Xin and Wu 2013; Bushnell and Moore 1991) and experimental (Drucker and Jensen 1996; Walker and Westneat 2002; Wainwright, Bellwood, and Westneat 2002; C. J. Fulton and Bellwood 2004) biomechanics studies that increased fin aspect ratios facilitate increased endurance in swimming performance across BCF and MPF locomotor modes that rely on fin oscillations for thrust production. This relationship can be explained by decreased production of destabilizing fin tip vortices and decreased drag due to lift with increasing aspect ratios of an oscillating hydrofoil (Bushnell and Moore 1991; Vogel 1994). However, these hydrodynamic relationships between fin aspect ratios and swimming performance remain largely unstudied in the context of undulating fish fins.

Fishes in the order Tetraodontiformes exhibit a particularly broad array of swimming modes, many of which rely on fin undulations. In fact, 4 of the 12 classically defined swimming modes (boxed in Figure 1.1) are named after families from this order, and when taking recent kinematic research into account (Hove et al. 2001), it is evident that all tetraodontiform fishes utilize some form of undulatory MPF locomotion to power steady swimming. The great kinematic

diversity of swimming modes observed among the Tetraodontiformes is mirrored by the high degree of morphological fin and body diversity found in this group. Tetraodontiform body morphologies range from the wide, soft-bodied pufferfishes (family: Tetraodontidae) and rigid boxfishes (family: Ostraciidae), to the deep, laterally compressed bodies of triggerfishes (family: Balistidae), filefishes (family: Monacanthidae), and the enormous ocean sunfishes (family: Molidae). Perhaps the most interesting axis of morphological variation among these MPF swimmers is the large degree of variation observed in tetraodontiform median fin shapes, which these fishes use to power locomotion. The broad-bodied boxfishes, pufferfishes, and burrfishes employ various combinations of relatively short and stout, low aspect ratio median fins to power locomotion (Blake 2004; Plaut and Chen 2003; Hove et al. 2001; Arreola and Westneat 1996). On the other hand, all 150 triggerfish and filefish species comprising the laterally compressed, monophyletic superfamily Balistoidea power slow steady swimming using elongate median dorsal and anal fins, spanning a wide range of aspect ratios, in a swimming mode termed balistiform locomotion (Blake 1978).

Balistiform locomotion is a particularly interesting swimming mode due to the high ecological and morphological diversity of the balistoid fishes that use this swimming gait. Balistoid fishes are found in a variety of marine habitats including coral reefs, seagrass beds, barren sand flats and even the open ocean and acquire food using a number of different feeding strategies such as benthic grazing, planktivory and even predation of elusive prey. Balistoid body shapes range from slender and elongate forms to deep, rounded forms. Median fin morphologies exhibit particularly high diversity include high aspect ratio, posteriorly tapering fins, short and rounded fins of intermediate aspect ratios, and elongate, low aspect ratio fins (Dornburg et al. 2011; Wright 2000) (Figure 1.2).

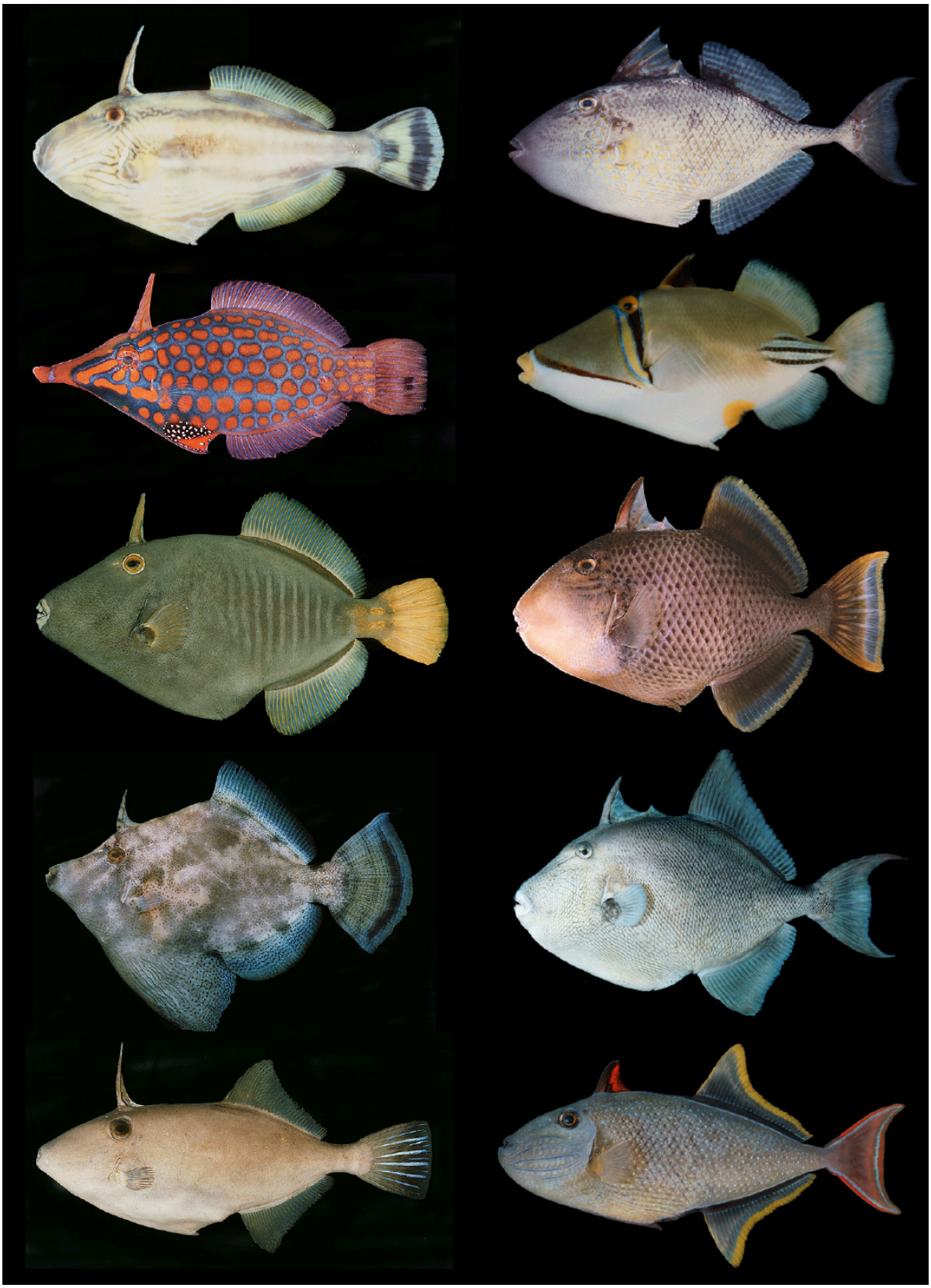

Figure 1.2 continued on page 6.

Figure 1.2. Morphological diversity of balistoid fishes.
Photos in the left column depict filefishes (Monacanthidae) and photos in the right column depict triggerfishes (Balistidae). Images are not to scale. From top to bottom, filefish species in the left column are: *Meuschenia freycineti* (USNM FIN030886), *Oxymonacanthus longirostris* (USNM FIN030896), *Cantherhines dumerilii* (USNM FIN030870), *Monacanthus chinensis* (USNM FIN030892) and *Thamnaconus modestoides* (USNM FIN030944). From top to bottom, triggerfish species in the right column are: *Abalistes stellaris* (USNM FIN026716), *Rhinecanthus assasi* (USNM FIN026751), *Pseudobalistes flavimarginatus* (USNM FIN026741), *Balistes polylepis* (USNM_FIN026721), and *Xanthichthys mento* (USNM FIN026776). All photos were taken by John E. Randall and accessed through the USNM online ichthyology collections database. Reproduced with permission.

In addition to this ecological and morphological diversity, balistoid fishes lie on a biomechanical continuum from swimming powered by broad oscillations to precise undulations of the median fins, and past research has indicated relationships between median fin shapes and swimming biomechanics strategies among triggerfishes (Wright 2000). Moreover, balistoid fishes undergo a gait transition from balistiform locomotion alone at low speeds to a gait dominated by body and caudal fin undulations at high swimming speeds, further increasing the biomechanical complexity of swimming diversity in this group (Wright 2000; Korsmeyer, Steffensen, and Herskin 2002). Finally, the recent advances in our understanding of the phylogenetic relationships among balistoid fishes (Dornburg, Santini, and Alfaro 2008; Santini, Sorenson, and Alfaro 2013; McCord and Westneat 2016b) set the stage nicely for broad comparative studies of the superfamily Balistoidea. Ultimately, the evolution and subsequent biomechanical diversification of the balistiform swimming mode and associated fin and body morphologies within an ecologically diverse superfamily of fishes serves as an ideal system in which to explore ecomorphological trends in the evolution of a unique swimming mode.

This thesis examines the evolutionary functional morphology of the triggerfishes (family: Balistidae) and filefishes (family: Monacanthidae) in the superfamily Balistoidea in the contexts of endurance swimming performance, habitat and feeding ecology, and steady swimming

biomechanics. This research is comprised of three major datasets that together reveal extensive evolutionary patterns in the biomechanics and ecological utility of the balistiform swimming mode.

First, this thesis explores relationships between balistoid fin and body shapes, endurance swimming performance and gait transition strategies using laboratory experiments and detailed morphometric analyses using rigorous phylogenetic comparative methods (Chapter 2). This study reveals that trigger and filefishes generally follow the widespread trend of increasing fin aspect ratios facilitating increased endurance swimming performance across their range of median fin kinematics. However, this research also uncovers a variety of biomechanical gait transition strategies that balistoid fishes use to achieve high endurance swimming performance. Balistiform specialists possess long, large median fins capable of meeting the large power requirements of high-speed locomotion using the median fins alone, which they use to power balistiform locomotion over a wide range of swimming speeds. Conversely, body/caudal fin specialists possess short, small median fins, ill-suited for high-speed balistiform locomotion, but narrow caudal peduncles capable of facilitating efficient, high-speed caudal fin-powered locomotion. Ultimately, median fin size (area) is the best predictor of endurance swimming performance using the balistiform gait alone, while median fin aspect ratios were the best predictors of overall endurance swimming performance. The wide range in endurance swimming performance observed in this chapter indicated that some balistoid species may be better biomechanically suited for life in high flow and open water environments, inspiring the study of balistoid habitat and feeding mode ecomorphology in chapter three.

The third chapter of this thesis employs evolutionary analyses of 80 balistoid species to test hypotheses about the relationships between balistoid morphologies and ecologies based on

the functional morphology patterns revealed in chapter two. Additionally, chapter three utilizes ancestral state estimations and phylogenetic comparative methods to explore patterns of balistoid fin and body shape evolution, including detailed examination of median fin aspect ratios and asymmetries. Endurance performance-linked variations in MPF swimmer fin shapes have been found to correlate with habitat use in other ecologically diverse fish families (C.J Fulton, Bellwood, and Wainwright 2001), suggesting a similar trend may be found within the Balistoidea. As predicted, the pelagic and planktivorous species, which spend the most time swimming in open water, tend to possess high aspect ratio dorsal and anal fins, well-suited for providing the high endurance swimming performance demanded by these lifestyles. However, balistoid fishes with low aspect ratio dorsal and anal fins occupy nearly every habitat and feeding group studied, suggesting that the likely maneuverability (Blake 1978; Marcoux and Korsmeyer 2019) and burst swimming (Weihs 1973; Paul W. Webb 1982) performance advantages associated with these low aspect ratio fins are beneficial for fishes in a wide array of habitat and feeding groups.

Ancestral state estimations reveal an early morphological divergence event between balistoid families with the filefish common ancestor exhibiting low dorsal, anal, and caudal fin aspect ratios and the triggerfish common ancestor possessing high aspect ratio median fins. This early median fin aspect ratio divergence event was followed by widespread dorsal and anal fin convergence, with extant members of both families possessing high, medium and low aspect ratio fins. Caudal fin aspect ratio appears to exhibit a more conserved evolutionary trajectory with the triggerfish common ancestor almost certainly possessing a high aspect ratio caudal fin and only one extant triggerfish possessing a low aspect ratio caudal fin. Conversely, the filefish common ancestor likely possessed either a low or medium aspect ratio caudal fin, and all extant

filefish species display one of these two caudal fin states. Furthermore, the results of this study revealed widespread dorsal and anal fin shape and positioning asymmetries, raising questions about the long-assumed biomechanical symmetry of dorsal and anal fins during balistiform locomotion.

Chapter four of this thesis uses detailed high-speed video analyses of gilded triggerfish, *Xanthichthys auromarginatus*, dorsal and anal fins to test hypotheses about the biomechanical consequences of the morphological median fin asymmetries revealed in chapter three. Most paired locomotor appendages are symmetrical about the sagittal (left-right) body axis, allowing organisms to move their appendages in biomechanically symmetrical fashions to power straight, forward locomotion. This condition is found in a variety of locomotor modes including terrestrial tetrapod locomotion (Biewener 2003), bird (Savile 1957), bat (Norberg 1981), and insect (Dudley 2000) flight, as well as fish pectoral fin-powered locomotion (Rosenberger 2001; Walker and Westneat 2002). The pairing of the asymmetrical balistiform locomotor appendages across the transverse (dorsal-ventral) axis presents balistoid fishes with an unusual biomechanical challenge in terms of fin coordination and stability, suggesting that these fishes may use asymmetrical median fin kinematics in order to achieve steady, forward swimming. Although balistiform dorsal fin kinematics have been studies in a number of species (Blake 1978; Wright 2000; Loofbourrow 2009; Korsmeyer, Steffensen, and Herskin 2002; J. Lighthill 1990), prior to this thesis, anal fin biomechanics had only been described in a single balistoid species (Blake 1978), and were otherwise assumed to mirror the dorsal fin biomechanics.

The discovery that *X. auromarginatus* do indeed use asymmetrical median fin kinematics during steady balistiform locomotion is a central finding of this thesis. Both the dorsal and anal fins display fin ray kinematics and wave property differences along their anterior-posterior

lengths, and the dorsal fin ultimately contributes greater propulsive effort than the anal fin. This chapter also includes a discussion of the anatomy of the large dorsal and anal fin erector and depressor muscles that power and control the described balistiform kinematics.

The final chapter of this thesis reviews and discusses the implications of these central findings for the evolution of the balistiform swimming mode. Suggested future directions and preliminary observations from ongoing field and lab based balistoid maneuverability and muscular anatomy studies are described.

A Review and Critique of Fin and Wing Aspect Ratio Calculations

As discussed above, the aspect ratio of an organismal aero- or hydrofoil can have key implications for the locomotor biomechanics of the appendage (Bushnell and Moore 1991; Vogel 1994). Consequentially, researchers have calculated and studied the aspect ratios of fish fins and animal wings involved in locomotor thrust production across a number of species. The mechanical interest in airfoil aspect ratios appears to have originated in aeronautical and nautical engineering, and subsequently been applied to organismal flight and swimming biomechanics. Organismal aspect ratios have been studied since as early as 1957, when Savile (1957) described an adaptation of the traditional aeronautic rectangular wing aspect ratio equation (span / chord) to suit the more complex shapes of bird wings. Savile's solution to account for the complex bird wing shape was to replace the chord measurement with the "mean aerodynamic chord" of the wing, measured as "total wing area/ span," thus making the new aspect ratio equation: $span^2$ / area. As Savile (1957) was interested in aerodynamic lift, and the portion of a bird's body between the wings effects the total lift, bird wing span was defined as the total length from wing tip to wing tip, and wing area also included the portion of the body between the wings. The

equation for calculating the aspect ratio of irregularly shaped organismal appendages across a wide range of organisms has largely remained the same: span^2 / area. However, the definitions of span and area vary between studies based on the specific anatomies and biomechanics of interest, complicating direct comparison of appendage aspect ratios between species and studies.

Fishes have a particularly large number of and high diversity of locomotor appendages, as fin shapes, positions, and even presence/ absence vary greatly among species (Larouche, Zelditch, and Cloutier 2017). Among the first papers to explore fish fin aspect ratios was a broad comparison of caudal fin aspect ratios across actinopterygian species including the bowfin, *Amia calva*, lake trout, *Salvelinus namaycush*, little tuna, *Euthynnus alletteratus*, and white marlin, *Makaira albida* (Nursall 1958). As the caudal fin is a single structure, rather than a set of paired appendages, the question of including the body is irrelevant. However, calculating the aspect ratio of a tuna would require a span measurement that includes the negative space between the tips of the forked caudal fin, while the span of a bowfin caudal fin would not include this negative space. Fierstine and Walters (1968) next calculated the caudal fin aspect ratios of 58 additional scombrid fish species. Once again their span measurements included the negative space between the caudal fin forks. Here they calculated area by tracing the fins and both measuring the area directly and using a gravimetric technique that required weighing cut-out paper tracings of each fin. These methods both accounted for the full surface area of the caudal fin and yielded similar results.

The first study to measure the pectoral fin aspect ratios of fishes appears to be a study of flying fish pectoral fins by Fish (1990). In this study, Fish (1990) was interested in flight performance, so he followed the methods used by ornithologists, and included the body in pectoral fin span and area measurements. Specifically, the span and area of a single pectoral fin

was measured (measurements extended through the midline of the body), and these values were doubled to calculate the full span and area measurements used in aspect ratio calculations. Vogel (1994) then appears to have slightly altered the definitions of wing span and area to involve each wing independently, thus removing the body width from the equation and allowing for aspect ratio comparisons between paired appendages of a single organism. Following this adjustment, ichthyologists have calculated the aspect ratios of paired fins in a number of different ways. A few researcher have chosen to continue to include the body in pectoral fin aspect ratio measurements, as in the case of the some batoid locomotion studies, in which the body between the fins is very slender (Fontanella et al. 2013).

However, the majority of studies concerning pectoral fin locomotion have typically only measured span and area for a single pectoral fin, assumed that the other pectoral fin was identical in morphology, and left the body out of the equation. Some of these studies calculated the aspect ratio of just the one measured fin (Christopher J. Fulton and Bellwood 2002; C. J. Fulton and Bellwood 2004; Binning and Fulton 2011; Gerry, Wang, and Ellerby 2011), while others doubled the span and area measurements in order to calculate one aspect ratio that encompasses both pectoral fins, and thus the whole biomechanical system (Walker and Westneat 2002; Wainwright, Bellwood, and Westneat 2002; Denny 2005; Martinez, Rohlf, and Frisk 2016). Other than the few cases in which body measurements were included, the subtle differences in pectoral fin aspect ratio calculation do not preclude comparison across studies. One could simply divide the doubled aspect ratios in half in order to re-calculate the aspect ratio of a single pectoral fin. The major issue with the removal of the body from fish pectoral fin aspect ratio measurements coupled with the continuation of calculating a single aspect ratio to represent both paired propulsors combined, is that the resulting aspect ratios are no longer directly comparable

to the aspect ratios of bird or bat wings, nor are they representative of individual fin morphologies.

The trend of doubling the span and area measurements from a single fin in order to calculate an aspect ratio of a full paired propulsor biomechanical system can be especially troubling when applied to asymmetrical paired fins, as in the case of the dorsal and anal fins powering balistiform locomotion. Wright (2000) appears to be among the first studies to calculate aspect ratios of paired median fins (the dorsal and anal fins) that do not lie across the symmetrical sagittal plane of the body. In this study Wright (2000) measured the spans and areas of the dorsal and anal fins separately. As Wright (2000) focused his biomechanical analyses on the dorsal fin alone, the dorsal fin span measurements were then simply doubled and used to represent the combined dorsal and anal fin span. The dorsal and anal fin area measurements were added together to calculate one total fin area value. The doubled dorsal fin span measurements and the combined dorsal and anal fin area measurements were then used to calculate a single aspect ratio for each fish that combines the dorsal and anal fin morphologies into one measurement. This method allowed for direct comparison of combined balistoid median fin aspect ratios to combined pectoral fin aspect ratios that were calculated without including the body between the fins. However, calculating a single aspect ratio to represent the morphologies of two asymmetrical balistoid fins is not ideal, especially because these fins do not generally even attach to the body with the same angles. To further complicate the comparative study of balistoid dorsal and anal fins, the next study to examine fin aspect ratios in this group (Dornburg et al. 2011) appears to have been confused by Wright's method, and used his equation to calculate aspect ratios for *individual fins*, resulting in unusually high single fin aspect ratios. Consequentially, Dornburg et al. (2011) ended up calculating aspect ratios for each fin using two

separate equations, and averaging the results. This resulted in aspect ratio calculations somewhere in between what would be expected for a single fin and what would be expected for two fins combined.

Ultimately, in this thesis, I argue that the asymmetrical dorsal and anal fins of balistoid fishes should be treated as independent morphological and biomechanical structures, and should thus each have their aspect ratios calculated independently. By doing so in this thesis, I was able to measure the degree of morphological and biomechanical asymmetry in the median fins of these fishes in order to elucidate a clearer understanding of balistiform locomotion. Furthermore, due to these asymmetries in some fin groups, I argue that aspect ratios should be calculated independently for all fish fins, regardless of presumed symmetry between paired fins in order to facilitate a simpler comparison between the aspect ratios of dorsal, anal, caudal, pelvic, and pectoral fins across fishes.

CHAPTER TWO: FUNCTIONAL MORPHOLOGY OF ENDURANCE SWIMMING PERFORMANCE AND GAIT TRANSITION STRATEGIES IN BALISTOID FISHES

Published as: Functional morphology of endurance swimming performance and gait transition strategies in balistoid fishes (George and Westneat 2019)

Abstract

Triggerfishes and filefishes (Balistoidea) use balistiform locomotion to power steady swimming with their dorsal and anal fins, and transition to a gait dominated by body and caudal fin (BCF) kinematics at high speeds. Fin and body shapes are predicted to be strong determinants of swimming performance and gait transitions. The goal of this study was to combine morphometrics and critical swimming tests to explore the relationships between fin and body shapes and swimming performance in a phylogenetic context in order to understand the evolution of balistiform swimming. Among 13 species of balistoid fishes, those with high aspect ratio fins tended to achieve higher critical swimming speeds than fishes with low aspect ratio fins. Species with long, large median fins and wide caudal peduncles used the balistiform gait alone for a larger percentage of their total critical swimming speed than fishes with short, small median fins and narrow caudal peduncles. Although analyses revealed overall positive relationships between median fin aspect ratios and gait transition speeds, fishes on both ends of the aspect ratio spectrum achieved higher swimming speeds using the balistiform gait alone than fishes with median fins of intermediate aspect ratios. Each species is specialized for taking advantage of one gait, with balistiform specialists possessing long, large median fins capable of the large power requirements of high-speed swimming using the median fins alone, while BCF specialists possess short, small

median fins, ill-suited for powering high-speed balistiform locomotion, but narrow caudal peduncles capable of efficient caudal fin oscillations to power high-speed locomotion.

Introduction

Fishes employ a wide variety of biomechanically distinct swimming modes to power aquatic locomotion, and this functional diversity is often reflected in the morphology of the fins and body. Accordingly, fish swimming modes are defined based on the parts of the body involved in thrust production during steady swimming (Breder 1926; P. W. Webb 1984; Sfakiotakis, Lane, and Davies 1999). The two major categories of classically defined swimming modes are body/caudal fin (BCF) and median/paired fin (MPF) locomotion. BCF swimmers undulate sinusoidal body bending waves along the body, or oscillate their caudal fins. Conversely, MPF swimmers rely on undulations or oscillations of their median or paired fins for propulsion, while holding their bodies and caudal fins steady at most speeds. The reliance of fishes on particular anatomical features for locomotion has led to extensive research aimed at understanding important trends among fin shape, body shape and swimming performance (Nursall 1958; Walker and Westneat 2002; Wainwright, Bellwood, and Westneat 2002; Rouleau, Glémet, and Magnan 2010; Xin and Wu 2013). These studies have revealed a widespread correlation between increasing aspect ratio (AR) of fins involved in propulsion and increasing steady swimming performance across a variety of swimming modes. AR is a measure of how 'wing-like' an airfoil is, and in the context of fish fins it is typically defined as the span of the fin squared, divided by the surface area of the fin (Nursall 1958; M. J. Lighthill 1970). The theory behind high AR fins leading to high-endurance swimming performance is based on hydrodynamic efficiency. High AR fins reduce the production of destabilizing tip vortices and experience decreased drag due to lift along their edges (Bushnell and

Moore 1991; Vogel 1994). However, relationships between fin ARs and fish swimming hydrodynamics and performance have generally been examined theoretically (M. J. Lighthill 1970; Karpouzian, Spedding, and Cheng 1990; Xin and Wu 2013) or experimentally (Drucker and Jensen 1996; Walker and Westneat 2002; Wainwright, Bellwood, and Westneat 2002; C. J. Fulton and Bellwood 2004) in fishes that power locomotion with oscillatory fin kinematics, leaving these relationships largely unexplored in the context of undulatory fins.

An important characteristic of MPF swimmers, and a central focus of this study, is the fact that they undergo a gait transition with increasing speed from their respective steady MPF gait to an unsteady burst-and-glide BCF gait (Whoriskey and Wootton 1987; Wright 2000; Korsmeyer, Steffensen, and Herskin 2002; Walker and Westneat 2002; Cannas et al. 2006; Hale et al. 2006; Svendsen et al. 2010; Feilich 2017). The gait transition from MPF to BCF propulsion requires recruitment of axial body musculature and caudal fin oscillations, suggesting that body and caudal fin shape might play an important role in determining swimming efficiency and performance of MPF swimmers. Despite extensive research on pectoral fin shape and gait transitions in fishes (Drucker and Jensen 1996; Walker and Westneat 2002), relationships among body and caudal fin morphometrics and endurance swimming performance of MPF swimmers have not previously been explored. Thus, a central goal of this study was to explore patterns of fish lateral profile morphometrics, including the dorsal, anal and caudal fins as well as body shape, and their associations with swimming performance and gait transitions.

Fishes in the superfamily Balistoidea are an ideal system in which to test hypotheses about morphology and swimming performance across a range of MPF kinematic patterns and gait transition strategies. This monophyletic superfamily is made up of 42 triggerfish species (Balistidae) and 107 filefish species (Monacanthidae), all of which power slow forward

locomotion using their dorsal and anal fins while holding their bodies and caudal fins steady in the balistiform swimming mode. Despite this shared swimming mode, balistoid fishes possess a wide range of morphologies from deep-bodied *Balistes* and *Brachaluteres* genera to elongate *Oxymonacanthus* and *Anacanthus* genera (Dornburg et al. 2011; Hutchins and Swainston 1985). Additionally, balistoid fishes possess median fins spanning a morphological continuum from high AR, posteriorly tapering fins of *Odonus niger* and *Canthidermis sufflamen* to low AR, rectangular fins of *Oxymonacanthus* and *Aluterus* species (Wright 2000; Dornburg et al. 2011). Coupled with this morphological diversity, balistoid fishes lie on a kinematic continuum from swimming powered by highly oscillatory, flapping median fin kinematics to highly undulatory, wave-like median fin kinematics (Wright 2000; J. Lighthill and Blake 1990). Balistoid fishes with high AR median fins use oscillatory fin kinematics, while fishes with low AR median fins utilize more undulatory fin kinematics (Wright 2000). Balistoid fishes undergo a gradual gait transition with increasing speed from balistiform locomotion alone at low speeds, to a gait involving both balistiform locomotion and a small BCF contribution at intermediate speeds, and finally to a gait dominated by burst-and-glide BCF locomotion at their fastest speeds (Wright 2000; Korsmeyer, Steffensen, and Herskin 2002). Wright (2000) examined relationships between morphology and swimming performance of balistoid fishes, and discovered that triggerfishes with higher AR median fins were capable of increased endurance swimming performance and higher gait transition speeds compared with triggerfishes with lower AR fins. To build on this prior work, a second major goal of the present study was to increase the sampling of triggerfishes, add a set of filefishes, and interpret morphometrics and swimming performance datasets within a well-resolved phylogeny of the Balistoidea. Recent advances in our understanding of balistoid phylogenetics (Dornburg, Santini, and Alfaro 2008; Dornburg et al. 2011; Santini, Sorenson, and Alfaro 2013;

McCord and Westneat 2016b) and the development of rigorous phylogenetic comparative methods have allowed us to account for phylogenetic structure in analyses of balistoid functional morphology. Additionally, the advancement of geometric morphometric techniques now allows for fine-scale analyses of morphological diversity (Dornburg et al. 2011; Feilich 2016) beyond linear measurements and ratio calculations (Wright 2000). Using these methods, we set out to quantify important axes of shape variation within balistoid fishes in a phylogenetic context.

The primary goals of this study were thus to use endurance swimming performance tests, geometric morphometrics and phylogenetic comparative methods to test functional hypotheses between balistoid fin and body shapes and swimming performance in order to better understand the evolution and subsequent functional diversification of the unique balistiform swimming mode.

Materials and methods

Species selection and care

Swimming performance data were analyzed for eight triggerfish and five filefish species (Figure 2.1). We combined swimming performance data for seven triggerfish species [*Balistapus undulatus* (Park 1797), *Balistoides conspicillum* (Bloch and Schneider 1801), *Melichthys vidua* (Richardson 1845), *Odonus niger* (Rüppell 1836), *Rhinecanthus aculeatus* (Linnaeus 1758), *Sufflamen chrysopterum* (Bloch and Schneider 1801) and *Xanthichthys auromarginatus* (Bennett 1832)] and one filefish species [*Cantherhines macrocerus* (Hollard 1853)] from Wright (2000), with new performance measures from one additional triggerfish species [*Sufflamen bursa* (Bloch and Schneider 1801)] and four additional filefish species [*Acreichthys tomentosus* (Linnaeus 1758), *Oxymonacanthus longirostris* (Bloch and Schneider 1801), *Paraluteres prionurus* (Bleeker 1851) and *Pervagor janthinosoma* (Bleeker 1854)]. Data from *Pseudobalistes fuscus* (Bloch and

Schneider 1801) (Wright 2000) were not included in our analyses, as swimming data were only available for two individuals. Swimming data from a total of 54 individuals were included in this study with an average of 4.2 individuals per species (range: 3–5). All individuals were post-juveniles with total lengths ranging from 6.04 to 12.31 cm (mean: 9.02 cm).

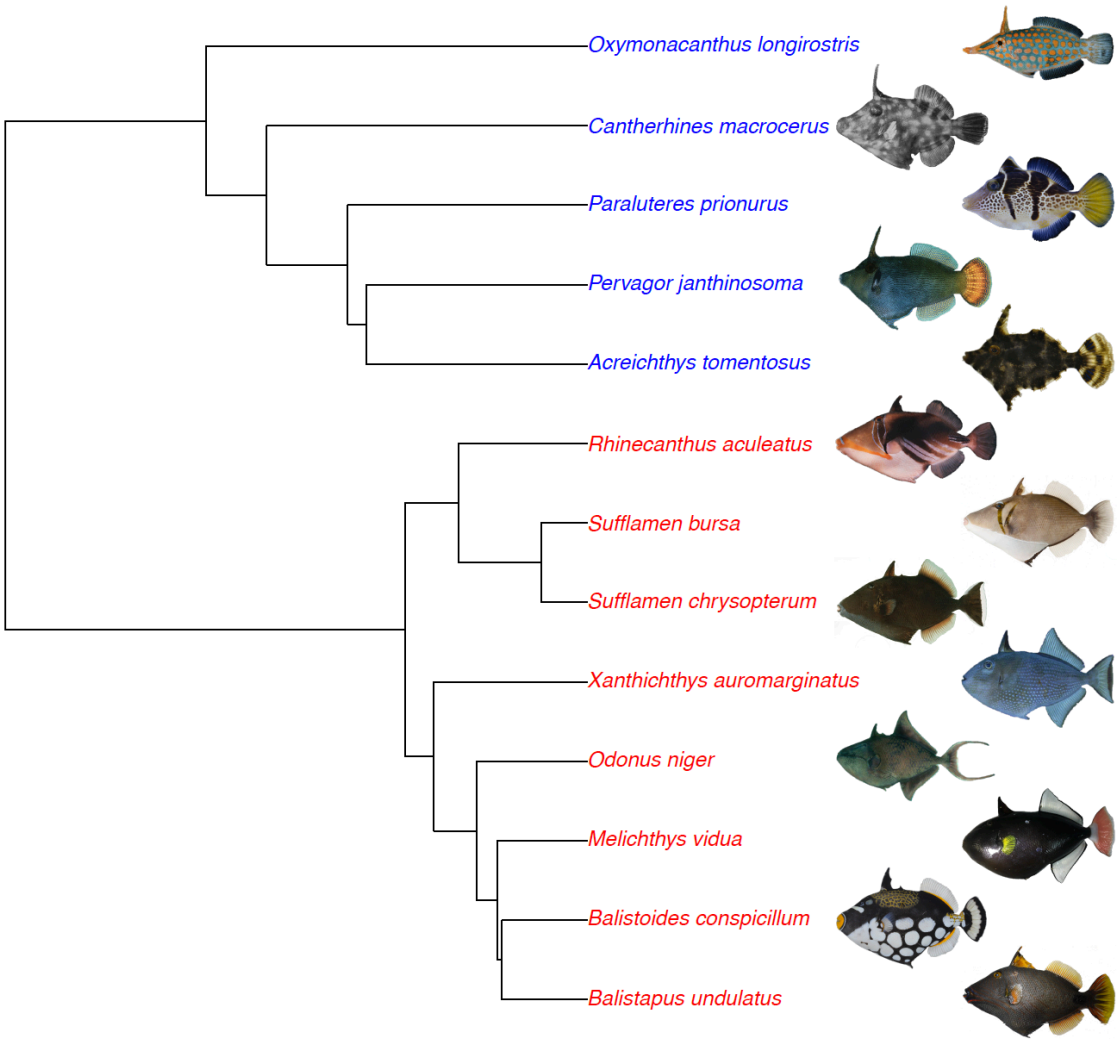

Figure 2.1. Phylogeny of the 13 balistoid species used in this study.
Species are color coded, with triggerfishes (Balistidae) in red and filefishes (Monacanthidae) in blue. Photo credits: *A. tomentosus*, *B. conspicillum*, *P. prionurus* (KPM-NR 53324, KPM-NR 45205, KPM-NR 57283; Hiroshi Senou); *B. undulatus*, *M. vidua* (A.B.G and M.W.W.); *C. macrocerus*, *O. longirostris*, *P. janthinosoma*, *R. aculeatus*, *S. chrysopterum* (John E. Randall); *O. niger* (Rick Winterbottom); *X. auromarginatus* (ROM 40935; Rick Winterbottom); *S. bursa* (USNM 439728; Jeffrey T. Williams. Copyright 2006 Moorea Biocode, Smithsonian Institute). Phylogeny trimmed from McCord and Westneat (2016).

Prior to swimming performance tests, all fishes were housed in separate tanks connected through a 1200 l saltwater flow-through system. The artificial seawater in this system was maintained at a temperature of 24±1°C and a specific gravity of 1.024±0.001. All fishes were fed freeze-dried krill, fish flakes and pellets with the exception of corallivorous *O. longirostris*, which were provided with live brown Acropora spp. coral. All fishes were deprived of food for 24 h before swimming tests in order to control for metabolism (Alsop and Wood 1997). All animal care protocols were approved by University of Chicago IACUC 72365.

Endurance swimming performance tests

Fish swimming performance is typically measured using a flow tank, in which fishes are forced to swim against a controlled flow. The standard metric for assessing a fish's endurance swimming performance is critical swimming speed (U_{crit}), defined as: $U_{crit} = u_i + ((t_i / t_{ii}) \times u_{ii})$, where u_i is the penultimate velocity (in cm s^{-1}) reached by the fish, t_i is the time (in minutes) that the fish swam at the highest reached velocity before exhaustion, t_{ii} is the length (in minutes) of each velocity increment, and u_{ii} is the prescribed velocity step increment (in cm s^{-1}) (Brett 1964). The results of critical swimming performance tests in fishes are dependent on the chosen magnitude and timing of the velocity step increment (u_{ii} and t_{ii}, respectively), complicating direct comparisons of critical swimming performance among studies (Farlinger and Beamish 1977; reviewed in Kolok 1999). In order to ensure reliable comparisons between balistoid U_{crit} data gathered from the literature (Wright 2000) and those measured in this study, we followed the critical swimming protocol of Wright (2000) exactly. Specifically, the length of each fish was quickly measured and recorded during transfer of the fish from their holding tanks to the flow tank. This measurement was used to calculate the length-specific velocity increments (u_{ii}) used in the swimming tests. All fishes then

performed a critical swimming test consisting of a 2 h acclimation period in which fishes swam in the flow tank at a low velocity of 0.5–1 total lengths (TL) s^{-1}, followed by a stepwise increase in flow velocity of approximately 0.5 TL s^{-1} (u_{ii}) (fork lengths for *O. niger*) every 15 min (t_{ii}) until the fishes were exhausted, as evidenced by their inability to remove themselves from the downstream grate for greater than 30 s (Wright 2000). All swimming tests were conducted in the same custom-made flow tank used by Wright (2000), with a working section with dimensions 25 cm×33 cm×104 cm. The working section was subdivided length-wise into three equal partitions (25 cm×33 cm×32 cm) using plastic 'egg-crate' barriers as collimators between partitions. A thin sheet of acrylic was bent into a half-pipe shape and inserted into each subdivision of the working section in order to prevent the fishes from avoiding swimming by wedging themselves into corners using their erectable dorsal spines and ventral keels. In a few cases, the critical swimming performance of two or three individuals was determined at the same time by restricting each individual to its own separate partition of the flow tank. In such cases, exhausted fish were quickly removed from their partition using a dipnet, and the remaining fish continued the swimming test uninterrupted. Wright (2000) calibrated the flow tank velocity before the swimming trials by filming and digitizing the downstream motion of suspended particles over a range of speeds. In this study, flow speed was measured and adjusted during each swimming trial in real-time using a Höntzsch Instruments flow sensing probe (HFA serial no: 843, Waiblingen, Germany).

U_{crit} provides a measure of the total sustained swimming performance limits regardless of the swimming gait used. In order to investigate the endurance swimming limits of balistiform locomotion alone (swimming powered by median fins only), gait transition data were recorded for each fish during the critical swimming trials. Because of the gradual nature of gait transitions from balistiform locomotion to BCF locomotion, Wright (2000) defined two gait transition speeds: $U_{t,low}$

and $U_{t,high}$. $U_{t,low}$ was defined as the speed interval during which the first signs of gait transition are evident, as indicated by occasional use of the caudal fin. This gait is characterized by steady balistiform locomotion plus occasional short BCF-powered bursts (balistiform+BCF). As $U_{t,low}$ is the speed at which fish no longer power locomotion using the median fins alone, this speed can be considered the upper limit of swimming speed accomplished using balistiform locomotion alone. $U_{t,high}$ is defined as the speed interval during which the fish is no longer able to maintain a steady position in the flow tank using the median fins alone, as evidenced by use of the caudal fin every 10 s or less. This gait is characterized by frequent, large BCF-powered bursts followed by unsteady median fin-powered locomotion as the fish glides downstream and prepares for the next BCF burst. Using this definition, it is possible for $U_{t,high}$ to be greater than U_{crit} if this gait transition occurs during the same velocity increment in which the fish becomes exhausted. Following swimming performance tests, U_{crit}, $U_{t,low}$ and $U_{t,high}$ were calculated for each individual. In order to control for the effect of fish size on swimming performance, these swimming performance metrics were expressed in terms of total lengths per second (TL s^{-1}) rather than raw speed (cm s^{-1}) for subsequent analyses. Because of the presence of elongate fin extensions at the dorsal and ventral margins of *O. niger* caudal fins, the total length of *O. niger* individuals was measured as the length from the anterior-most point of the head to the distal edge of the center of the caudal fin (similar to fork length). Finally, we calculated the percentage of the total critical swimming speed in which each fish swam using its median dorsal and anal fins only (percent balistiform locomotion) as:

% Balistiform locomotion = ($U_{t,low}$ / U_{crit}) x 100%.

Quantifying morphology

Following swimming experiments, fishes were killed with tricaine sulfonate salt (MS-222) and photographed for morphometric analyses. All specimens included in Wright's (2000) swimming performance study were fixed in formalin and stored in 70% ethanol at the Field Museum of Natural History (FMNH) in 2000. As a result of the fixation process, the fins of many of these specimens had become rigid in an unnatural position, but were otherwise in good condition. In order to spread the fins out to their natural positions for morphometric analyses, we soaked the preserved fish in a trypsin solution for 72 h. These fishes, along with the individuals tested in our swimming trials, were laid flat on their sides, pinned out with their fins fully extended and photographed with a ruler for morphometric analyses. In order to increase the sample size for morphometric analyses, photographs of museum and aquarium trade specimens within 25% of the length range of the individuals used in the swimming experiments were included, resulting in a total of 102 individuals included in morphometric analyses (see Table S2.1 for sample sizes of individual morphological datasets).

In order to quantify the morphological diversity of fin and body shapes, a total of 109 digital landmarks were placed along the fins and bodies of the fishes using the R package StereoMorph (Olsen and Westneat 2015) (Figure 2.2). Twenty-six landmarks were manually placed along the fins and bodies of each fish using the landmarks function in StereoMorph (white circles and blue triangles in Figure 2.2), and the dorsal, anal and caudal fins were outlined using the curves function in StereoMorph (blue lines in Figure 2.2). The curves function interprets and returns the position of landmarks along a digitized Bezier curve. Curves were digitized along the anterior, dorsal, posterior and ventral surface of each fin, resulting in four independent curves along each fin. Following digitization, landmarks placed along the fins using the curves function

were subsampled and evenly spaced, resulting in 34, 34 and 27 landmarks along the dorsal, anal and caudal fins, respectively (blue circles in Figure 2.2). If any structures of a specimen were visibly damaged, those structures were not digitized or included in subsequent analysis. A few dorsal and anal fins (n = 4 and 7, respectively) in otherwise good condition had preservation artifacts in the positions of one or more fin rays. In order to include these fins in subsequent analyses, we developed and utilized a Mac application FinRotate (https://github.com/mwestneat/FinRotate), capable of rotating individual fin rays about their base to digitally spread the fin membrane a small amount, while retaining the fin ray lengths and leaving the base positions unchanged. We ensured that the area of each fin changed less than 6.5% during these adjustments. These fins are indicated in Table S2.2 and the details of each fin adjustment are given in Table S2.3. Most balistoid fishes possess a mobile ventral keel that can be extended and retracted. For photographs in which the ventral keel was not positioned in its fully extended position (indicated with an asterisk in Table S2.2), the estimate.missing function in the R package geomorph (https://cran.r-project.org/package=geomorph) was used to estimate the position of the pelvic fin rudiment at the ventral tip of the extended ventral keel. The missing landmark positions were estimated for individuals of each species separately using all correctly positioned individuals of the same species as reference specimens. As all *C. macrocerus* individuals within the size range of the those included in the swimming trials were formalin fixed with the ventral keel depressed, a photograph of one slightly smaller, but correctly positioned, *C. macrocerus* individual was identified in the literature (John E. Randall 1964) and used to estimate the position of the extended ventral keel for this species. This reference specimen was not used in subsequent morphometric analyses.

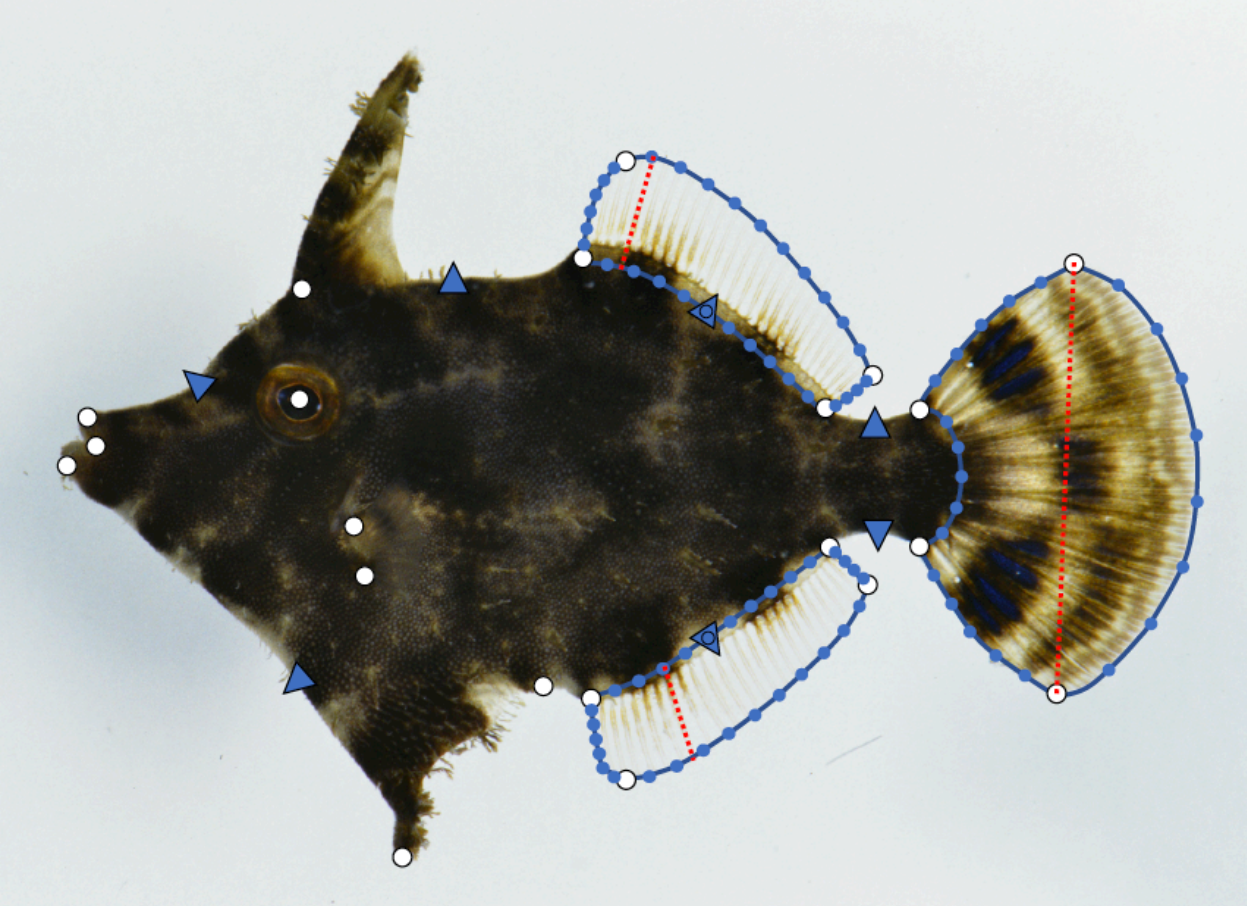

Figure 2.2. Geometric morphometrics digitization scheme demonstrated for the filefish *Acreichthys tomentosus* (KPM-NR 53324).
White circles represent functionally homologous non-sliding landmarks. Blue triangles represent sliding semi-landmarks included in only the full-shape and body-only datasets. Blue curves outlining the dorsal, anal and caudal fins were used for area calculations, and points along these curves (blue circles) were subsampled and treated as sliding semi-landmarks in geometric morphometric analyses. Red dotted lines represent the span measurements used for aspect ratio (AR) calculations. Photo credit: Hiroshi Senou.

The digitized landmark data were subdivided into five separate datasets for geometric morphometric analyses: full shape (all landmarks), body only, dorsal fin only, anal fin only and caudal fin only. Next, each landmark was designated as either a functionally homologous 'landmark' (white circles in Figure 2.2) or a geometrically relative 'semi-landmark' (blue shapes in Figure 2.2). The landmarks and semi-landmarks included in each morphological dataset were then projected into tangent space using generalized Procrustes analysis (GPA) in order to remove

variation in landmark position due only to rotation, translation and scaling using the gpagen function in geomorph. During Procrustes superimposition, each semi-landmark was allowed to slide relative to neighboring static landmarks using a method that minimizes the bending energy among specimens. In addition to translating, rotating and scaling the relative landmark positions of each specimen while preserving the important shape information, the gpagen function also calculates the centroid size (a measure of relative size) for each specimen. Each morphological dataset (full shape, body shape, dorsal fin shape, anal fin shape and caudal fin shape) underwent GPA independently, so that Procrustes-transformed shapes and centroid sizes of each morphological unit could be analyzed separately.

Following GPA, we calculated species means of Procrustes-transformed landmark coordinates and centroid sizes for each morphological dataset. Principal components analyses (PCA) were then performed on the species-averaged, Procrustes-aligned landmark coordinates of each morphological dataset in order to identify, describe and quantify major axes of shape variation within the 13 species examined in this study using the PlotTangentSpace function in geomorph.

The shape changes described by the two most significant axes of morphological variation [principal component (PC)1 and 2] of each dataset were then visualized using backtransform morphospaces (MacLeod 2009; Olsen 2017). We used this backtransformation method to visualize the theoretical fin and body shapes of each species as described only by morphological characteristics relevant to the two most significant axes of shape variation. We then plotted these shapes in their relative positions of morphospace for each morphological dataset. In order to visualize the full range of theoretical shapes in this PC1–PC2 morphospace, we generated evenly spaced PC scores along the observed ranges of the first two axes of shape variation (PC1 and 2) for each dataset and plotted the corresponding shapes in their respective position in each

morphospace. Finally, we projected a phylogeny (McCord and Westneat 2016b) into each morphospace using the phylomorphospace function in the R package phytools (Revell 2012) in order to assess evolutionary directionality of shape changes within and between each family. In addition to the geometric–morphometric datasets described above, five morphological ratios were calculated for each species. First, we calculated the ARs of the dorsal, anal and caudal fins. AR was calculated as: AR = (b^2 / A), where b is the maximum span of the fin perpendicular to the direction of forward motion (dotted red lines in Figure 2.2) and A is the surface area of the fin. For the dorsal and anal fins, span was measured as the Euclidian distance from base to tip of the longest fin ray of each fin independently. Caudal fin span was measured as the Euclidian distance from the dorsal-most point of the fin to the ventral-most point of the fin when the caudal fin was fully spread open. Span and area measurements were calculated using the photos digitized in StereoMorph. Finally, in order to assess variation in relative fin sizes among species, we calculated two area ratios. The first area ratio (median fin:BCF area ratio) provides a measure of relative combined dorsal and anal fin area compared with the combined body and caudal fin area. The second area ratio (caudal fin:body area) provides a measure of relative caudal fin size.

Statistical analyses

All statistical analyses were carried out in a phylogenetic context, using a pruned time-calibrated phylogeny based on four mitochondrial and five nuclear gene sequences from 80 balistoid species and six outgroup taxa from the families Diodontidae, Ostraciidae and Tetraodontidae (McCord and Westneat 2016b). In order to account for numerical imprecision due to small rounding errors when reading this phylogeny into R, we used the nnls method in the force.ultrametric function within phytools (Revell 2012) to force the tree to conform to the strict ultrametric requirements of

R packages used in downstream analyses. In order to assess relationships between fish size and size-adjusted swimming metrics (in TL s^{-1}), univariate phylogenetic generalized least squared (PGLS) regressions were conducted between species-averaged fish total length and species-averaged, size-adjusted swimming performance metrics (U_{crit}, $U_{t,low}$, $U_{t,high}$ and percent balistiform locomotion) using the pgls function in the R package caper (https://CRAN.R-project.org/package=caper). PGLS regressions were also conducted among all swimming performance metrics in order to identify correlations between swimming metrics. PGLS regressions between species-averaged centroid sizes and GPA-transformed coordinates of each geometric–morphologic dataset were conducted in order to assess lingering allometric relationships between size and shape of each structure following GPA. Only the anal fin dataset exhibited a significant allometric correlation between centroid size and GPA-transformed shape (PGLS: P=0.015), so centroid size was used as a covariate in all subsequent geometric–morphometric functional morphology PGLS regressions for the anal fin. Spearman's rank correlations were used to assess correlations between geometric–morphometric PC scores and fin aspect and area ratios.

Functional morphology hypotheses were tested using univariate PGLS regressions between the species-averaged fin ratios and PC scores of the first two axes of shape variation for each geometric–morphometric dataset versus size-adjusted (TL s−1), species-averaged swimming performance metrics (U_{crit}, $U_{t,low}$, $U_{t,high}$ and percent balistiform locomotion). The multiple R^2 values for each relationship given by the pgls function in caper are provided below and in Table 2.1. In order to account for multiple statistical tests being conducted on the same dataset, all functional morphology P-values were adjusted to control for false-discovery rate using the Benjamini–Hochberg (BH) method (Benjamini and Hochberg 1995) with the P.adjust function in

the R package stats (http://www.R-project.org/). All functional morphology trends were nearly identical between $U_{t,low}$ and $U_{t,high}$ (see Table S2.4), so $U_{t,high}$ functional morphology relationships are not discussed below or included in the BH P.adjust method, resulting in a total of 45 functional morphology statistical tests input into the BH p-adjust function. The BH-adjusted P-values for functional morphology relationships are reported below, and raw P-values can be found in Table S2.4. Results were considered significant when the BH-adjusted P-values were less than 0.05. All other statistical tests (correlations between measured swimming variables, allometric relationships between size and shape, and correlations between fin ratios and geometric–morphometric PC scores) were undertaken prior to hypothesis testing in order to ensure that subsequent functional morphology analyses controlled for any confounding correlations between variables, and thus the P-values of these tests were not adjusted using the BH method. In order to further explore and account for any non-isometric relationships between fish length and swimming performance, residuals from linear regressions between species-averaged fish TL and species-averaged raw (cm s^{-1}) swimming performance metrics (U_{crit}, $U_{t,low}$ and $U_{t,high}$) were used in additional PGLS regressions of swimming performance metrics (residuals) against morphology datasets as recommended by (Kolok 1999). The P-values from these additional PGLS regressions were adjusted using the BH P.adjust method and subsequently compared with those of the original (swimming metrics expressed in TL s^{-1}) functional morphology tests. All statistical analyses were performed using R software version 3.3.2 (http://www.R-project.org/).

Results

Swimming performance

Critical swimming performance (U_{crit}) of the 13 balistoid species examined ranged from 3.58 TL s^{-1} in the triggerfish *B. conspicillum* to 6.41 TL s^{-1} in the triggerfish *O. niger* with an average of 4.67 TL s^{-1} (Table S2.5). Five individuals (one *O. niger*, two *R. aculeatus* and two *X. auromarginatus*) reached the maximum speed of the flow tank before exhaustion, so these species' U_{crit} values should be considered conservative estimates. The U_{crit} family averages were 5.04 and 4.09 TL s^{-1} for the triggerfishes and filefishes, respectively. The initial gait transition speed ($U_{t,low}$) ranged from 2.14 TL s^{-1} in *B. conspicillum* to 4.94 TL s^{-1} in *O. niger*, with an average of 3.40 TL s^{-1} (Table S2.5). The $U_{t,low}$ family averages were 3.28 and 3.59 TL s^{-1} for the triggerfishes and filefishes, respectively. Two filefishes, one *P. prionurus* and one *O. longirostris*, never fully transitioned to the unsteady BCF gait ($U_{t,high}$). Among fishes that did make the second gait transition, $U_{t,high}$ ranged from 2.94 TL s^{-1} in the triggerfish *R. aculeatus* to 5.56 TL s^{-1} in *O. niger* (Table S2.5), with an average of 3.99 TL s^{-1}. The $U_{t,high}$ family averages were 3.87 and 4.18 TL s^{-1} for the triggerfishes and filefishes, respectively. The percentage of the critical swimming trial in which the fishes swam using their median fins only (percent balistiform locomotion) ranged from 45.3% in *R. aculeatus* to 93.9% in *P. prionurus* (Table S2.5). All filefish species used balistiform locomotion exclusively (with no caudal fin contribution) for greater than 75% of their critical swimming tests, with a family average of 88%. Conversely, all triggerfish species used balistiform locomotion alone for less than 78% of their swimming tests, with a family average of 66%.

PGLS regressions revealed no significant relationships between size-adjusted (TL s^{-1}) swimming performance metrics and fish TL (U_{crit}: P=0.41, multiple R^2=0.0627; $U_{t,low}$: P=0.22,

multiple R^2=0.131; $U_{t,high}$: P=0.29, multiple R^2=0.102; percent balistiform locomotion: P=0.23, multiple R^2=0.126). U_{crit} was significantly correlated with $U_{t,low}$ (P=0.00064, multiple R^2=0.668) and $U_{t,high}$ (P=0.0037, multiple R^2=0.550), but not with percent balistiform locomotion (P=0.46, multiple R^2=0.050). Percent balistiform locomotion was significantly correlated with $U_{t,low}$ (P=0.0043, multiple R^2=0.538) and $U_{t,high}$ (P=0.0085, multiple R^2=0.482). Finally, a PGLS regression revealed a highly significant correlation between $U_{t,low}$ and $U_{t,high}$ (P=$1.0e^{-6}$, multiple R^2=0.895). Nearly all trends between morphology and gait transition speeds were the same regardless of which gait transition speed was used (Table S2.4), so subsequent results include only $U_{t,low}$, U_{crit} and percent balistiform locomotion.

Fin ratios

Anal fin ARs ranged from 0.32 in *O. longirostris* to 1.24 in *O. niger*, with an average of 0.62. Triggerfishes tend to have higher anal fin ARs (range 0.52–1.24, mean 0.73) than filefishes (range 0.32–0.62, mean 0.43). Dorsal fin AR ranged from 0.31 in *O. longirostris* to 1.16 in *O. niger*, with an average of 0.60. Triggerfishes also tend to have higher dorsal fin ARs (range 0.46–1.16, mean 0.72) than filefishes (range 0.31–0.53, mean 0.41). Caudal fin AR ranged from 1.57 in *C. macrocerus* to 3.05 in *X. auromarginatus* with an average of 2.51. Triggerfishes tend to have higher caudal fin ARs (range 2.46–3.05, mean 2.73) than filefishes (range 1.57–2.70, mean 2.16). Median fin: BCF area ratio ranged from 0.15 in *R. aculeatus* and *A. tomentosus* to 0.32 in *O. niger*, with an average of 0.21. There was no difference between triggerfish and filefish family means for this metric. Caudal fin:body area ratio ranged from 0.13 in *B. conspicillum* to 0.32 in *P. prionurus* with an average of 0.18. Filefishes have larger caudal fins relative to their bodies (range 0.20–0.32, mean 0.25) than triggerfishes (range 0.13–0.16, mean 0.14).

Geometric morphometrics

Full shape. The primary axis of variation (PC1: 46%) for this dataset, including all parts of the fish, describes the length and position of the dorsal and anal fins and caudal peduncle depth (Figure 2.3A). High PC1 scores are associated with narrow caudal peduncles, deep bodies and short, posteriorly positioned dorsal and anal fins. The second axis of variation (PC2: 24%) differentiates fishes primarily based on fin shape. High PC2 morphospace is occupied by fishes with concave or truncated caudal fins and high AR median fins with long leading edges and short trailing edges. Conversely, low PC2 morphospace is occupied by fishes with highly convex caudal fins and low AR median fins with leading and trailing edges of similar lengths. Filefishes cluster in the area of morphospace defined by shallow bodies, wide caudal peduncles and long median fins (low PC1) as well as convex caudal fins and low AR median fins (low PC2). Triggerfishes occupy the area of morphospace defined by deep bodies, narrow caudal peduncles and short median fins (high PC1) as well as convex or truncate caudal fins and mid to low AR median fins (low to mid PC2), with the exception of *O. niger*, which sits in a largely unoccupied area of morphospace (low PC1 and high PC2).

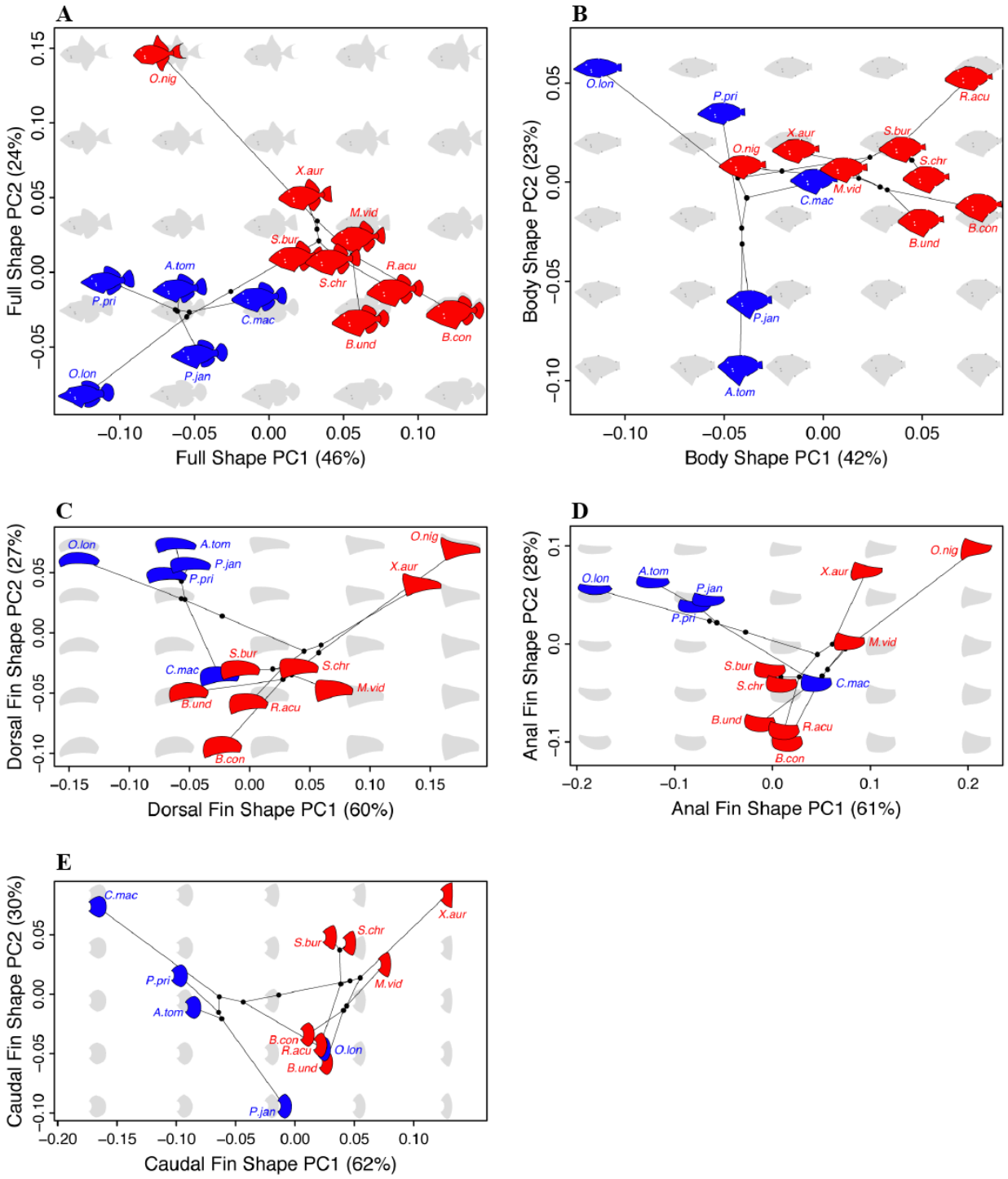

Figure 2.3. continued on page 35.

Figure 2.3. Phylomorphospaces depicting backtransformed shapes along the two most significant axes of shape variation for each morphological dataset.
Red (Balistidae) and blue (Monacanthidae) shapes represent the backtransformed shapes of each species included in this study. Gray shapes represent theoretical backtransformed shapes corresponding to each location in morphospace. Black lines represent the phylogeny from Figure 2.1 transformed into each morphospace. Black dots along these lines represent theoretical positions of each ancestral node. (A) Full shape. (B) Body shape. (C) Dorsal fin shape. (D) Anal fin shape. (E) Caudal fin shape. Sample sizes for each morphometric dataset are reported in Table S2.1.

Body only. The primary axis of variation (PC1: 42%) describes the ratio of anterior body depth to posterior body depth, the slope of the head profile and median fin length (Figure 2.3B). Fishes with high PC1 scores are deep-bodied anteriorly with narrow caudal peduncles, short median fins and convex forehead profiles. Conversely, fishes with low PC1 scores are shallow-bodied anteriorly with wide caudal peduncles, long median fins and concave forehead profiles. PC2 (23%) describes ventral keel depth. Fishes with deep ventral keels occupy areas of low PC2 morphospace. Most triggerfishes cluster in areas of morphospace defined by deep bodies, narrow caudal peduncles, convex forehead profiles (mid to high PC1) and ventral keels of moderate to shallow depth (mid to high PC2). Filefishes generally occupy areas of morphospace defined by narrow bodies, wide caudal peduncles and concave forehead profiles (mid to low PC1) and span the full range of PC2 morphospace. The filefish *C. macrocerus* appears to have converged upon an area of body morphospace primarily occupied by triggerfishes.

Dorsal fin. The primary axis of variation (PC1: 60%) describes the length ratio of the leading edge to the trailing edge of the fin (Figure 2.3C). Low PC1 regions of morphospace are occupied by fins with leading and trailing edges of similar lengths, while high PC1 regions are occupied by fins with long leading edges and short trailing edges. Dorsal fin PC1 scores are positively correlated with dorsal fin ARs (Spearman's rank correlation $\rho=0.97$, $P<0.0001$). PC2 (27%) describes overall

length–depth ratio, with long, shallow fins occupying areas of higher PC2 morphospace, and short, deep fins occupying areas of low PC2 morphospace. Dorsal fin PC2 is not correlated with dorsal fin AR (Spearman's rank correlation $\rho=-0.30$, $P=0.32$). Filefishes cluster in morphospace defined by low AR, shallow and elongate fins (low PC1, high PC2) with the exception of C. macrocerus, which groups with most triggerfishes in the area of morphospace defined by short, deep dorsal fins of intermediate AR (mid PC1, low PC2). *Odonus niger* and *X. auromarginatus* diverged from the rest of the Balistidae to occupy the area of morphospace defined by high AR, elongate dorsal fins (high PC1 and high PC2).

Anal fin. The primary axis of variation (PC1: 61%) describes the overall length–depth ratio of the fin as well as the orientation and length ratio of the leading edge to the trailing edge of the fin (Figure 2.3D). Low PC1 regions of morphospace are occupied by elongate, shallow fins, with leading and trailing edges of nearly equal length. Conversely, high PC1 morphospace is occupied by short, deep anal fins with anteriorly oriented leading edges that are significantly longer than their trailing edges. Anal fin PC1 scores are positively correlated with anal fin ARs (Spearman's rank correlation $\rho=0.97$, $P<0.0001$). PC2 (28%) differentiates anal fins primarily by the length of the leading edge and shape of the distal edge. Anal fins with high PC2 scores have anteriorly oriented, straight leading edges with posteriorly tapering distal edges, while fins with low PC2 scores have posteriorly curved leading edges and deep, convexly rounded distal edges. Anal fin PC2 is not correlated with anal fin AR (Spearman's rank correlation $\rho=0.011$, $P=0.98$). Filefishes cluster in morphospace defined by shallow, elongate anal fins (low PC1) with anteriorly oriented leading edges and slightly tapering distal edges (high PC2), with the exception of *C. macrocerus*, which groups with most triggerfishes in the area of morphospace defined by deep, rounded anal

fins (low PC2) of intermediate length and AR (mid PC1). *Odonus niger* and *X. auromarginatus* occupy the area defined by elongate, posteriorly tapering, high AR anal fins (high PC1 and high PC2).

Caudal fin. The forked caudal fin of *O. niger* is a major outlier along caudal fin PC1 according to a Rosner's generalized extreme studentized deviate test conducted with the rosnerTest function in R (Millard, 2013), so this species was removed from all caudal fin geometric– morphometric analyses and the caudal fin PCA was rerun without *O. niger*. Among the remaining 12 species, the primary axis of variation (PC1: 62%) describes changes in overall length:depth ratios and the shape of the posterior edge of the caudal fin (Figure 2.3E). Caudal fins occupying areas of low PC1 morphospace are elongate and narrow with highly convex posterior edges, while caudal fins occupying areas of high PC1 morphospace are short and deep with truncate posterior edges. Caudal fin PC1 is positively correlated with caudal fin AR (Spearman's rank correlation $\rho=0.94$, $P<0.0001$). Caudal fin PC2 describes the length of the dorsal and ventral edges of the fin. Fins with low PC2 scores have short dorsal and ventral edges, while fins with high PC2 scores have long dorsal and ventral edges. Triggerfishes possess fairly deep caudal fins with slightly convex or truncate distal edges (mid to high PC1). Most filefishes possess fairly narrow caudal fins with more convex distal edges (mid to low PC1). Fishes from both families span the entirety of PC2.

Functional morphology

Analyses revealed significant relationships among several aspects of balistoid fin and body shape variation, endurance swimming performance and gait transition strategies. As expected, median fin size and many aspects of median fin shape were found to be strong predictors of critical

swimming performance and gait transition speeds. Several aspects of body and caudal fin shape were also found to be significantly correlated with swimming performance. Functional morphology results were quite similar between the two size-adjustment methods (Table S2.4), so subsequent statistics, results and discussion are based on performance metrics measured in TL s^{-1} only.

Fin ratios and performance. Univariate PGLS regressions revealed significant positive correlations between U_{crit} and dorsal, anal and caudal fin ARs (see Table 2.1 for statistical significance) (Figure 2.4A–C). Additionally, increasing the area ratio of the median fins to the body and caudal fin (median fins:BCF area ratio) is associated with increased U_{crit} (PGLS: P=0.0268) (Figure 2.4D). Higher dorsal, anal and caudal fin ARs and increased median fins:BCF area ratio are also associated with increased gait transition speed ($U_{t,low}$) (Table 2.1) (Figure 2.5). Although not detected as outliers in these relationships by Rosner's generalized extreme studentized deviate tests, three triggerfish species with median fins of especially high ARs, *O. niger*, *X. auromarginatus* and *M. vidua*, clearly contribute substantially to the observed trends between fin ARs and both U_{crit} and $U_{t,low}$. Finally, median fin:BCF area ratio is positively correlated with percent balistiform locomotion (PGLS: P=0.0240) (Figure 2.6).

Table 2.1. Results of functional morphology phylogenetic generalized least squared (PGLS) regressions

		Multiple R^2	Benjamini-Hochberg-adjusted P-Value		
PGLS Relationship	Directionality	Balistoidea	Balistoidea	Balistidae	Monacanthidae
Dorsal AR vs U_{crit}	Positive	**0.591**	**0.0107**	**0.0478**	0.975
Anal AR vs U_{crit}	Positive	**0.605**	**0.0107**	**0.0416**	0.975
Caudal AR vs U_{crit}	Positive	**0.488**	**0.0240**	**0.0416**	0.553
Median Fins: BCF area ratio vs U_{crit}	Positive	**0.461**	**0.0268**	0.0833	0.975
Dorsal AR vs $U_{t\ low}$	Positive	**0.653**	**0.00746**	**0.0202**	0.994
Anal AR vs $U_{t\ low}$	Positive	**0.657**	**0.00746**	**0.0202**	0.994
Caudal AR vs $U_{t\ low}$	Positive	**0.421**	**0.0351**	**0.0400**	0.713
Median Fins: BCF area ratio vs $U_{t\ low}$	Positive	**0.797**	**0.00179**	**0.0202**	0.925
Median Fins: BCF area ratio vs % Bal	Positive	**0.487**	**0.0240**	0.0833	0.465
Full Shape PC2 vs U_{crit}	Positive	**0.444**	**0.0307**	0.0638	0.465
Body PC1 vs U_{crit}	Negative	**0.423**	**0.0351**	0.0521	0.975
Dorsal PC1 vs U_{crit}	Positive	**0.548**	**0.0162**	0.0521	0.975
Dorsal PC2 vs U_{crit}	Positive	**0.532**	**0.0162**	**0.0416**	0.975
Caudal PC1 vs U_{crit}	Positive	**0.497**	**0.0268**	0.351	0.540
Full Shape PC1 vs $U_{t\ low}$	Negative	**0.604**	**0.0107**	**0.0322**	0.975
Full Shape PC2 vs $U_{t\ low}$	Positive	**0.543**	**0.0162**	**0.0202**	0.540
Body PC1 vs $U_{t\ low}$	Negative	**0.692**	**0.00746**	**0.0202**	0.975
Dorsal PC1 vs $U_{t\ low}$	Positive	**0.592**	**0.0107**	**0.0202**	0.975
Dorsal PC2 vs $U_{t\ low}$	Positive	**0.668**	**0.00746**	**0.0202**	0.975
Anal PC2 vs $U_{t\ low}$	Positive	**0.717**	**0.0162**	**0.0416**	0.925
Caudal PC1 vs $U_{t\ low}$	Positive	**0.507**	**0.0265**	0.0833	0.811
Full Shape PC1 vs % Bal	Negative	**0.414**	**0.0358**	0.134	0.975
Body PC1 vs % Bal	Negative	**0.411**	**0.0358**	0.125	0.975

Results correspond to PGLS regressions using U_{crit} and $U_{t\ low}$ values measured in total length per second. AR = aspect ratio, % Bal = percent balistiform locomotion. Bold values indicate statistically significant trends ($p < 0.05$).

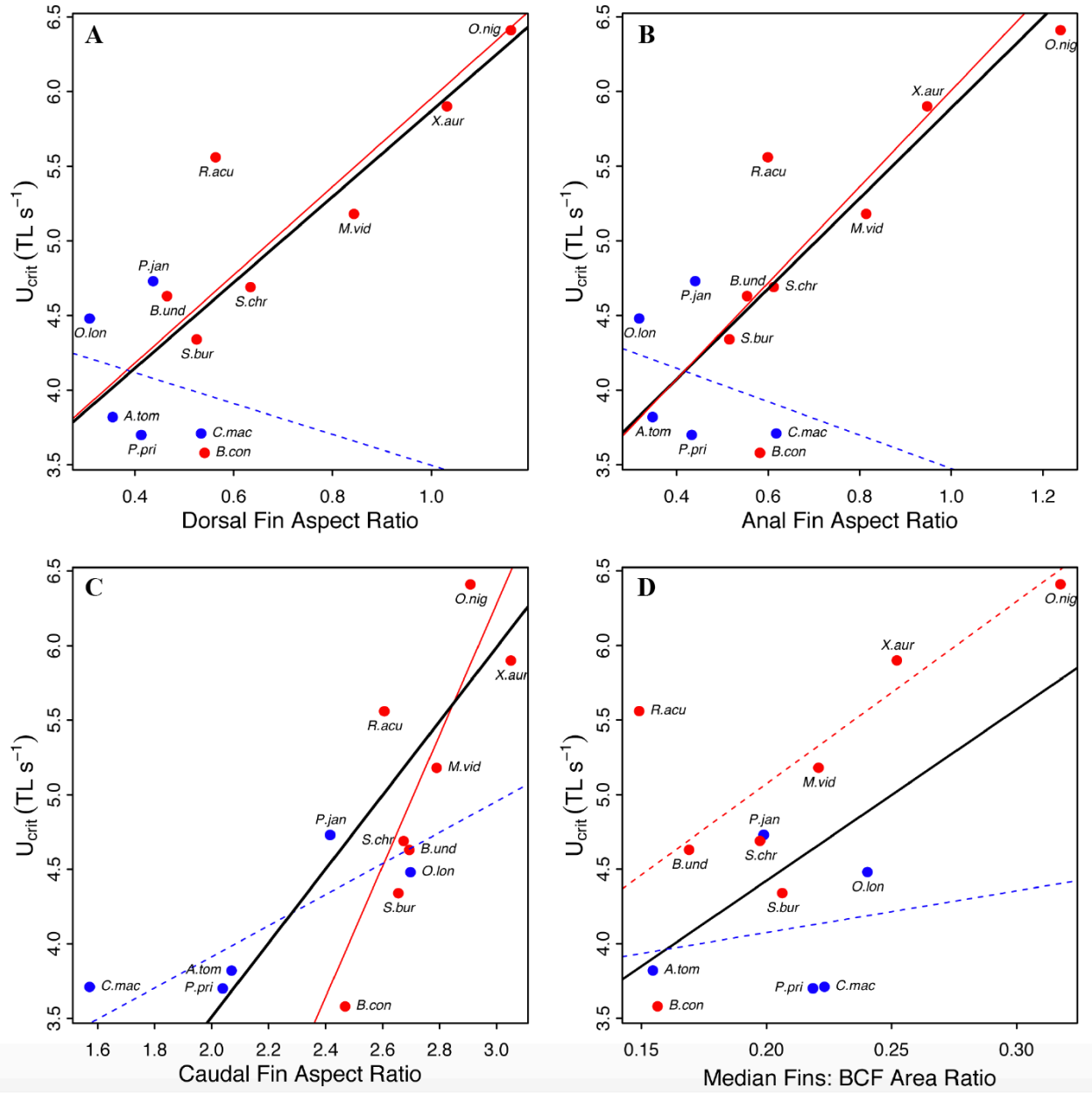

Figure 2.4. Relationships between fin ratios and critical swimming performance (U_{crit}). U_{crit} data are given in total lengths per second (TL s^{-1}). (A) Dorsal fin AR. (B) Anal fin AR. (C) Caudal fin AR. (D) Ratio of median fins area to combined body and caudal fin (BCF) area. All points represent species means. Red and blue points indicate triggerfishes and filefishes, respectively. Black lines depict the phylogenetic generalized least squared (PGLS) regression lines for all 13 balistoid species included in this study. Red and blue lines depict independent PGLS regression lines for the triggerfishes and filefishes, respectively. Solid and dashed lines indicate significant ($P<0.05$) and non-significant ($P>0.05$) trends, respectively. Sample sizes for U_{crit} and morphometric datasets are reported in Tables S2.5 and S2.1, respectively.

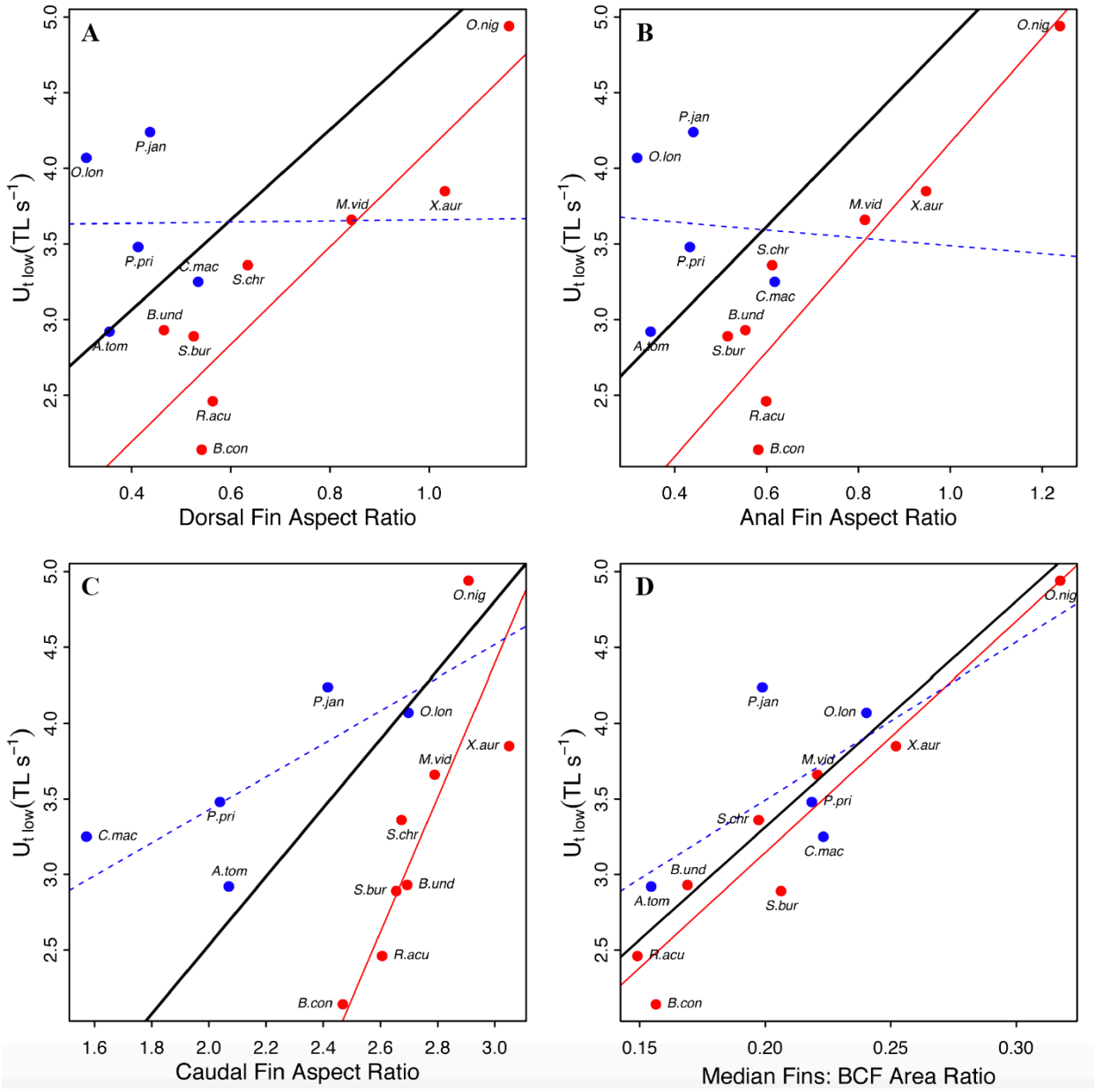

Figure 2.5. Relationships between fin ratios and the first gait transition speed ($U_{t,low}$). $U_{t,low}$ data are given in total lengths per second (TL s^{-1}). (A) Dorsal fin AR. (B) Anal fin AR. (C) Caudal fin AR. (D) Ratio of median fins area to combined BCF area. All points represent species means. Family association and statistical significance are indicated by color and line type, respectively, as in Figure 2.4. Sample sizes for $U_{t,low}$ and morphometric datasets are reported in Tables S2.5 and S2.1, respectively.

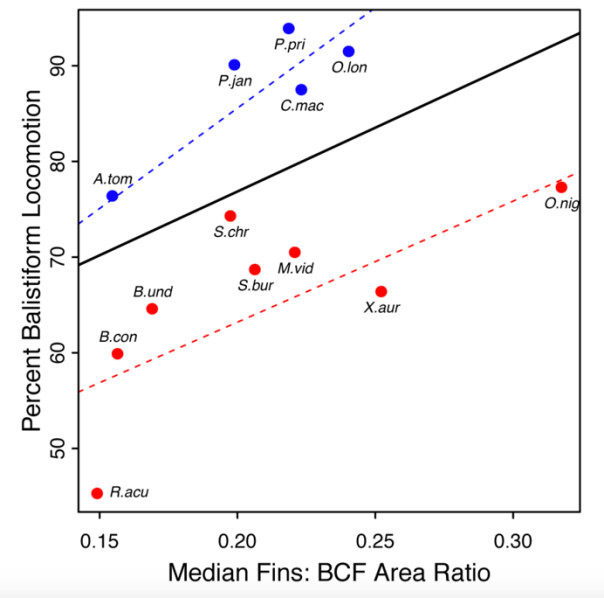

Figure 2.6. Relationship between median fins:BCF area ratio and the percentage of U_{crit} achieved using the balistiform gait alone. All points represent species means. Family association and statistical significance are indicated by color and line type, respectively, as in Figure 2.4. Sample sizes for percent balistiform locomotion and median fins:BCF area ratio are reported in Tables S2.5 and S2.1, respectively.

Geometric morphometrics and performance. Univariate PGLS regressions of PC scores against swimming performance metrics revealed 14 significant functional morphology trends within the superfamily Balistoidea (Table 2.1). Fishes with deeper bodies and less convex caudal fins (high full shape PC2, high caudal fin PC1) and fishes with elongate (high dorsal fin PC2), posteriorly tapering (high dorsal fin PC1) dorsal fins are associated with increased U_{crit} (Figure 2.7). Many aspects of balistoid fin and body shape are also associated with $U_{t,low}$ (Figure 2.8) (Table 2.1). Interestingly, the most significant axes of median fin shape correlated with $U_{t,low}$ are not correlated with fin ARs. Specifically, elongate dorsal and anal fins, regardless of AR (high dorsal and anal fin PC2s) are associated with higher $U_{t,low}$ (Figure 2.8C,D). Balistoid fishes with narrow caudal peduncles (high full shape PC1) and highly convex caudal fins (low full shape PC2, low caudal fin PC1) tend to recruit the caudal fin at slower speeds (lower $U_{t,low}$) than fishes with wide caudal peduncles and less convex caudal fins (Figure 2.8A). Finally, fishes with elongate median fins and wide caudal peduncles (low full shape and body PC1s) use balistiform locomotion alone for a

higher percentage of their overall U_{crit} (high percent balistiform locomotion) than fishes with short median fins and narrow caudal peduncles (high full shape and body PC1s) (Figure 2.9).

Family trends. Many of the trends in functional morphology remain significant when assessed among the eight triggerfish species alone, but many filefish species do not follow the overall balistoid functional morphology trends (Table 2.1). In fact, among the five filefish species examined in this study alone, no axes of body or fin shape variation are associated with U_{crit}, $U_{t,low}$ or percent balistiform locomotion (Table 2.1; Table S2.4).

Discussion

Triggerfishes and filefishes are capable of relatively high critical swimming performance compared with median and paired fin locomotor specialists from other fish families. The hypotheses that high fin ARs are associated with higher endurance swimming performance and higher gait transition speeds were strongly supported in our analysis. However, triggerfishes and filefishes showed different endurance swimming strategies and gait transition behaviors, with filefishes showing a strikingly high performance using pure balistiform locomotion. The central conclusions of this study are (1) fin and body shapes are good predictors of overall critical swimming performance in balistoid fishes, (2) balistoid fishes exhibit a variety of gait transition strategies to achieve high-speed endurance swimming performance and (3) each species appears to be morphologically specialized to take advantage of one of these gait transition strategies.

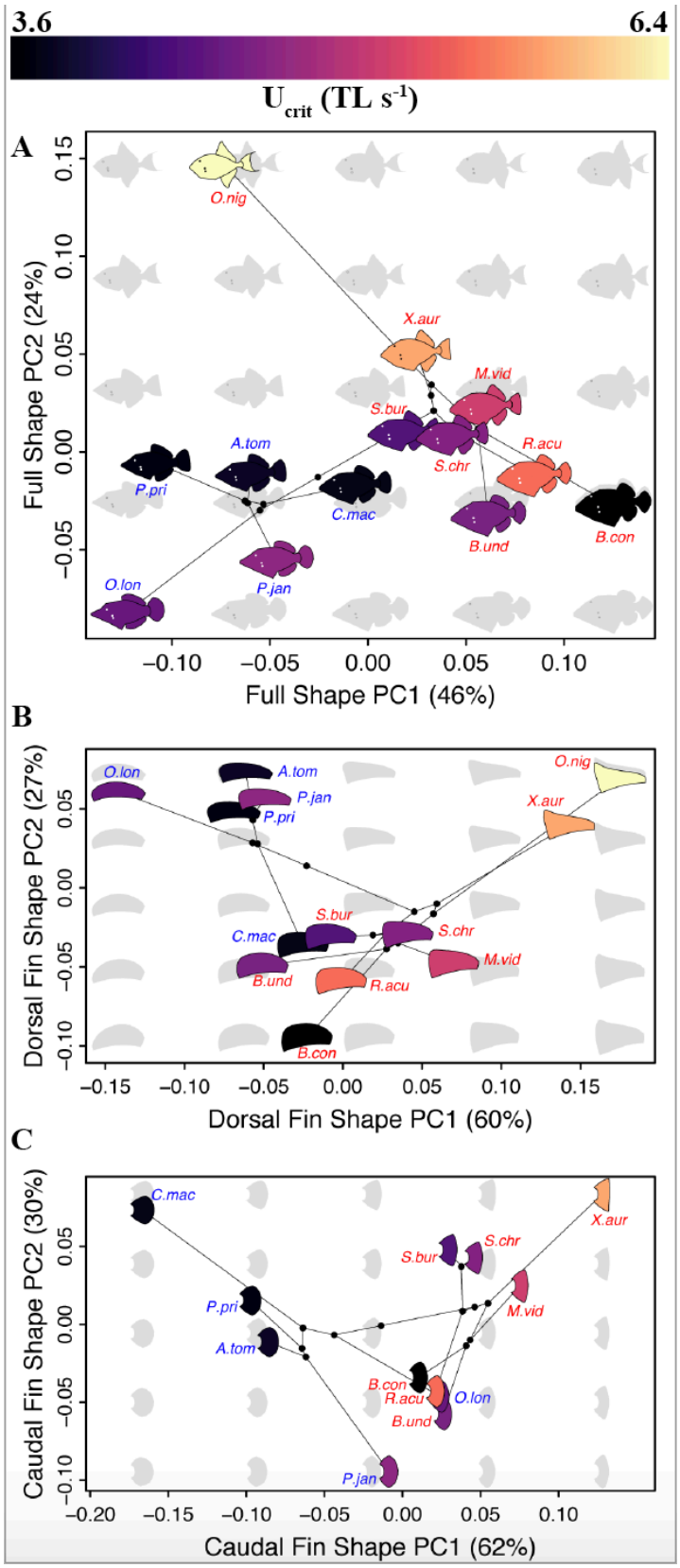

Figure 2.7. continued on page 45.

Figure 2.7. Backtransformation phylomorphospace plots color coded for U_{crit}.
See Figure 2.3 for a description of backtransformation phylomorphospace plots. Shapes affiliated with each species are color coded according to mean U_{crit} measured in TL s^{-1}, as indicated by the color bar. (A) Full shape. (B) Dorsal fin shape. (C) Caudal fin shape. Species abbreviations are color coded by family, with triggerfishes in red and filefishes in blue. Sample sizes for U_{crit} and morphometric datasets are reported in Tables S2.5 and S2.1, respectively.

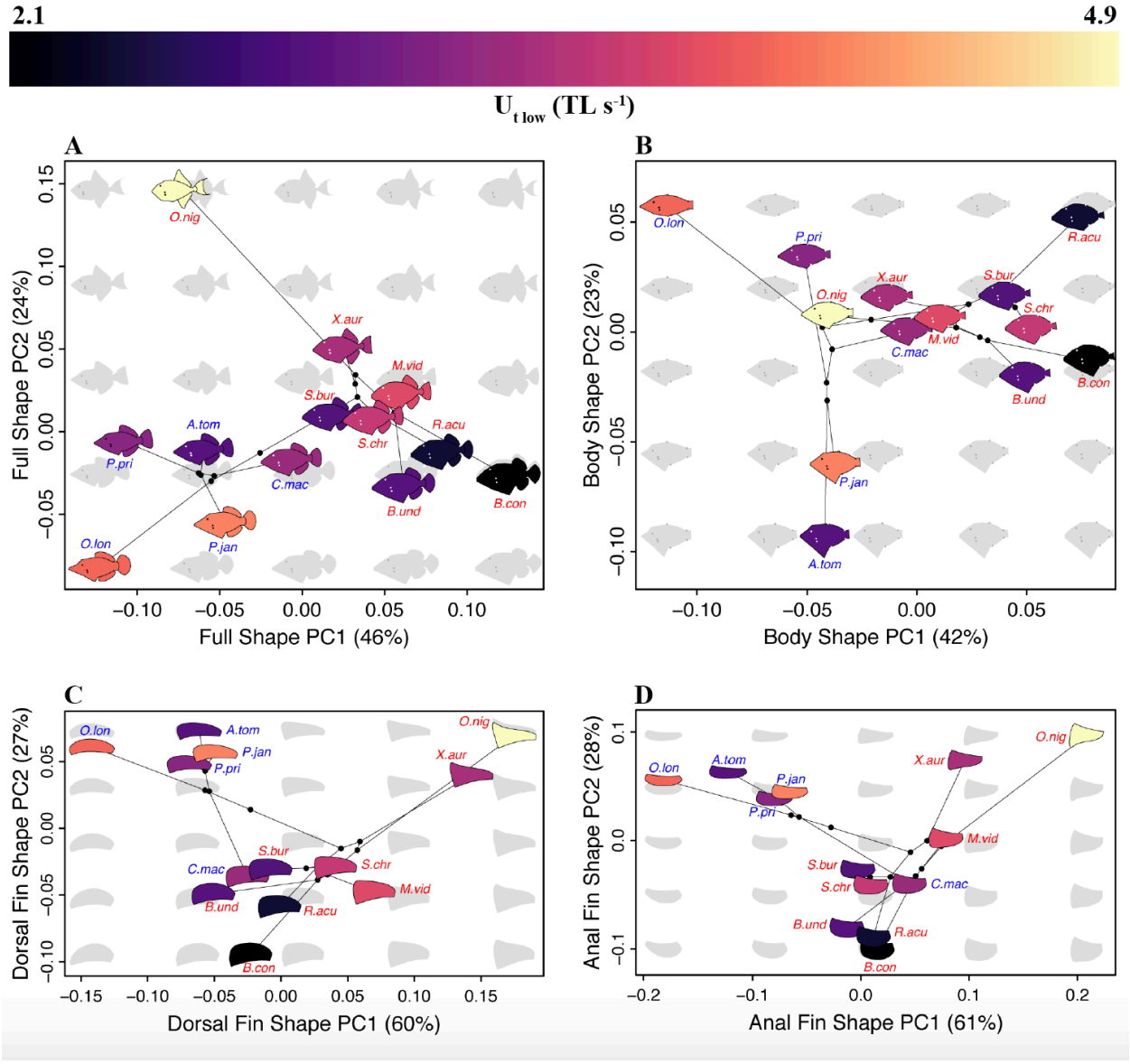

Figure 2.8. continued on page 46.

Figure 2.8. Backtransformation phylomorphospace plots color coded for the first gait transition speed ($U_{t,low}$).
See Figure 2.3 for a description of backtransformation phylomorphospace plots. Shapes affiliated with each species are color coded according to the mean speed at which the first gait transition occurred ($U_{t,low}$) measured in TL s^{-1}, as indicated by the color bar. (A) Full shape. (B) Body shape. (C) Dorsal fin shape. (D) Anal fin shape. Species abbreviations are color coded by family, with triggerfishes in red and filefishes in blue. Sample sizes for $U_{t,low}$ and morphometric datasets are reported in Tables S2.5 and S2.1, respectively.

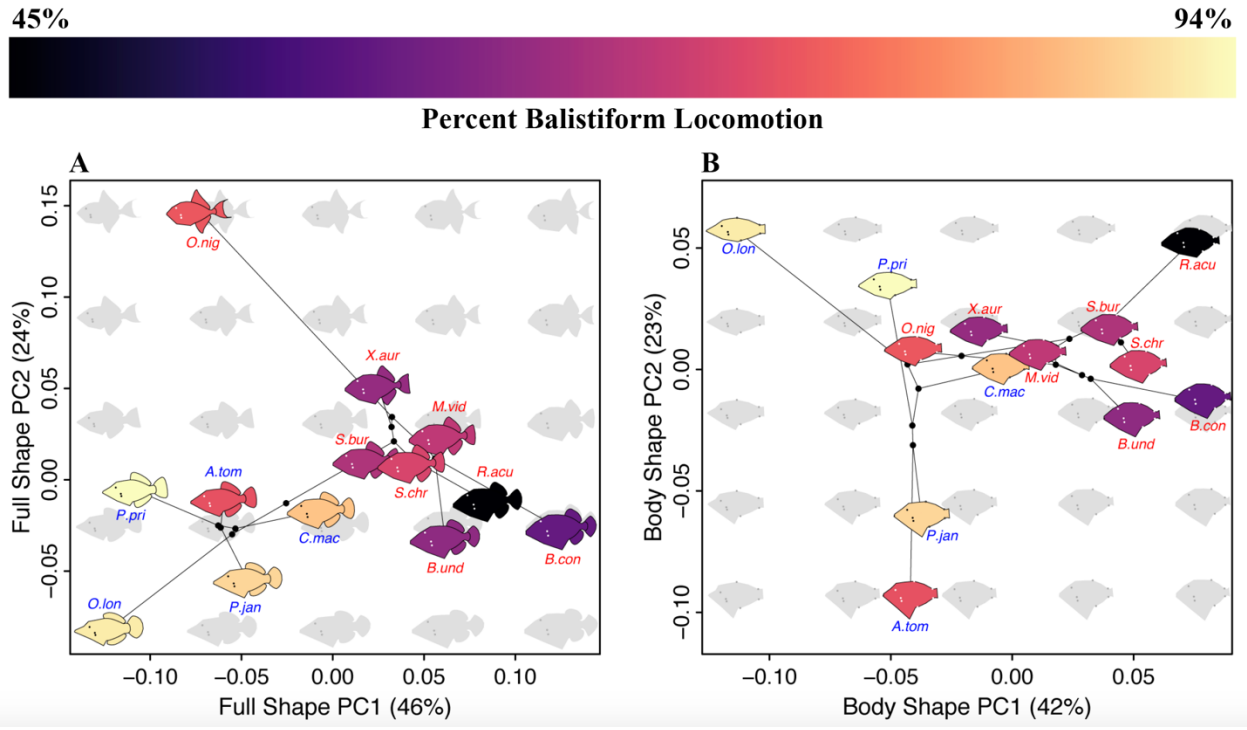

Figure 2.9. Backtransformation phylomorphospace plots color coded for the percentage of U_{crit} achieved using the balistiform gait alone.
See Figure 2.3 for a description of backtransformation phylomorphospace plots. Shapes affiliated with each species are color coded according to mean percent balistiform locomotion, as indicated by the color bar. (A) Full shape. (B) Body shape. Species abbreviations are color coded by family, with triggerfishes in red and filefishes in blue. Sample sizes for percent balistiform locomotion and morphometric datasets are reported in Tables S2.5 and S2.1, respectively.

Swimming performance

The results of this study indicate that balistoid fishes are capable of strong endurance swimming performance. All 13 balistoid species in this study achieved U_{crit} values above 3.5 TL s^{-1}. The nine fastest species achieved U_{crit} values above 4 TL s^{-1}, indicating that balistoid fishes are capable of

higher critical swimming performance than other MPF swimmers such as the knifefish *Gymnotus carapo* (mean U_{crit}=2.1 TL s^{-1}; McKenzie et al. 2012), parrotfish *Scarus schlegeli* (mean U_{crit}=3.2 TL s−1; Korsmeyer, Steffensen, and Herskin 2002), pufferfish *Takifugu rubripes* (mean U_{crit}=3.22 body lengths s^{-1}; Yu et al., 2015), burrfish *Diodon holocanthus* (mean U_{crit}=3.6 TL s^{-1}; Wiktorowicz, Lauritzen, and Gordon 2010) and boxfish *Ostracion meleagris* (mean U_{crit}=3.8 TL s^{-1}; Gordon et al. 2000). The fastest species in this study, *O. niger*, achieved an average U_{crit} of 6.41 TL s^{-1}, comparable to high-performance MPF endurance swimmers of similar length such as the wrasses *Gomphosus varius* and *Cirrhilabrus rubripinnis* (mean U_{crit}=5.26 and 6.05 TL s^{-1}, respectively; Walker and Westneat 2002). Previously reported MPF-to-BCF gait transition speeds range from 1.75 fork lengths (FL) s^{-1} (Cannas et al. 2006) and 2.3 FL s^{-1} (Svendsen et al. 2010) in the surfperch labriform swimmer *Embiotoca lateralis* to 3.5 TL s^{-1} in the parrotfish labriform swimmer *Scarus schlegeli* (Korsmeyer, Steffensen, and Herskin 2002) and over 5 TL s^{-1} in the boxfish ostraciiform swimmer *Ostracion meleagris* (Hove et al. 2001). Thus, the triggerfishes and filefishes in this study achieved fairly high swimming speeds using their MPF gait alone ($U_{t,low}$ range 2.14–4.94 TL s^{-1}, mean 3.40 TL s^{-1}) compared with MPF swimmers from other fish families.

The swimming performance results from this study also reveal interesting trends between balistoid families. Triggerfishes tend to achieve faster overall U_{crit} than filefishes (5.04 and 4.09 TL s^{-1}, respectively). However, triggerfishes recruit body and caudal fin musculature ($U_{t,low}$) at lower speeds than do filefishes (3.28 and 3.59 TL s^{-1}, respectively) and power swimming with balistiform locomotion alone for a lower percentage of their overall endurance swimming performance than do filefishes (66% and 88%, respectively). This means that, on average, filefishes achieved faster swimming speeds than triggerfishes using balistiform locomotion alone (higher $U_{t,low}$). Furthermore, this suggests that although nearly all past studies concerning the

evolution (Dornburg et al. 2011), biomechanics (Blake 1978; Wright 2000; Korsmeyer, Steffensen, and Herskin 2002; Hu et al. 2006; Loofbourrow 2009), energetics (Korsmeyer, Steffensen, and Herskin 2002) and performance (Wright 2000; Korsmeyer, Steffensen, and Herskin 2002) of balistiform locomotion have used triggerfishes as their balistiform swimming models, filefishes are likely a better system for studying high-speed balistiform locomotion because of their heavy reliance on the balistiform gait alone throughout much of their swimming speed range. Many past studies concerning balistiform locomotion (Korsmeyer, Steffensen, and Herskin 2002; Hu et al. 2006; Loofbourrow 2009) focused solely on *R. aculeatus*, the species that used balistiform locomotion for the smallest percentage of its U_{crit} in this study (45%), so the biomechanical and energetic trends observed in these studies may not be broadly applicable to all balistoid fishes. Keeping this in mind, it is important to note that previous research has indicated that R. aculeatus actually incurs a significant energetic cost when transitioning from balistiform locomotion to a combined balistiform plus BCF gait ($U_{t,low}$), suggesting that balistoid fishes might undergo gait transitions in order to meet the power requirements of swimming faster in a highly viscous aquatic environment (Korsmeyer, Steffensen, and Herskin 2002). This is in stark contrast to gait transitions of terrestrial animals, which are typically undergone to maximize mechanical efficiency at each speed (reviewed in Alexander 1989). This power-requirement, rather than mechanical efficiency, energetics pattern described in *R. aculeatus* suggests that our $U_{t,low}$ measurement may be a good estimate of the upper speed limit of the balistiform gait for each species. However, this energetics pattern might not apply to all balistoid species, especially those with different morphologies and fin kinematics. Either way, it is clear from our results and those of Korsmeyer, Steffensen, and Herskin (2002) and Wright (2000) that not all balistoid fishes power

aerobic endurance swimming using the balistiform gait alone; rather, they are capable of long-term aerobic locomotion using the combined balistiform and BCF gait.

Functional morphology

Critical swimming performance of balistoid fishes is highly correlated with fin ARs and area ratios. Fishes with high AR dorsal, anal and caudal fins and fishes with relatively large median fins tend to achieve higher U_{crit}. These trends support previous findings that balistoid fishes benefit from hydrodynamically efficient (high AR) and powerful (relatively large) dorsal and anal fins during endurance swimming (Wright 2000). By expanding the scope of performance measures and fin metrics to additional species, this trend is expanded to include filefishes. The relationships between increasing median fin ARs and increasing U_{crit} are not surprising, given the hydrodynamic benefits of high AR fins (M. J. Lighthill 1970; Bushnell and Moore 1991) and the fact that the median fins are significantly involved in thrust production throughout the majority of the critical swimming tests (through $U_{t,high}$). The relationship between caudal fin AR and overall critical swimming performance reflects the fact that, on average, these balistoid fishes started recruiting occasional caudal fin oscillations ($U_{t,low}$) at speeds only 74% of the way to their respective critical swimming limits. Triggerfishes were especially reliant on the caudal fin contribution, with a percent balistiform locomotion family average of only 66%. Theoretical work has demonstrated many hydrodynamic advantages of high AR fins, including decreased drag and decreased production of destabilizing tip vortices (Bushnell and Moore 1991; M. J. Lighthill 1970; Xin and Wu 2013). These hydrodynamic advantages likely make balistoid fishes with high AR median and caudal fins capable of more energetically efficient propulsion using the balistiform and BCF gaits, respectively.

The strongest trends between morphology and swimming performance measured in this study were associated with gait transition speed ($U_{t,low}$), rather than overall critical swimming performance. Specifically, fishes with large median fins, high AR median fins, long median fins (regardless of AR) and wide caudal peduncles recruited axial musculature and the caudal fin ($U_{t,low}$) at higher speeds than fishes with small, short and rounded median fins and narrow caudal peduncles. It is important to note that the filefishes in this study do not conform to the trends between increasing median fin ARs and increasing $U_{t,low}$. In fact, close examination of these trends (Figures 2.5 A,B and 2.8 C,D) actually suggests that possessing median fins at either extreme of the AR continuum or median fin PC1 range (significantly associated with AR) results in improved swimming performance while using the balistiform gait alone ($U_{t,low}$) compared with median fins of intermediate ARs. Specifically, the species with the second and third fastest $U_{t,low}$ speeds (*P. janthinosoma* and *O. longirostris*) actually possess some of the lowest AR median fins measured in this study. In other words, it appears that two optima may exist between median fin AR and swimming performance powered by the balistiform gait alone ($U_{t,low}$), with the fastest balistiform locomotion speeds ($U_{t,low}$) achieved by fishes with the highest and lowest AR median fins, and the slowest maximum balistiform swimming speeds ($U_{t,low}$) achieved by fishes with median fins of intermediate ARs.

The multiple optima discovered between median fin ARs and $U_{t,low}$ can likely be explained by the fin kinematics used to achieve these balistiform locomotion speeds. Kinematics research has shown that high AR median fins are associated with oscillatory, flapping balistiform fin kinematics, while low AR median fins are associated with more wave-like, undulatory median fin kinematics (Wright 2000). All filefishes added to this study (*A. tomentosus*, *O. longirostris*, *P. prionurus* and *P. janthinosoma*) have lower AR median fins than the fishes included in the Wright

(2000) study, suggesting that these filefishes may possess even more undulatory fin kinematics than previously described for the group, although fin kinematics must be experimentally confirmed. The different median fin kinematics used by balistiform swimmers at either end of the median fin AR spectrum likely place different hydrodynamic pressures on the fishes (Wright 2000; Sprinkle et al. 2017), and each fin shape may be hydrodynamically optimized for its respective kinematics. Specifically, low AR filefish fins may be optimized for high-speed endurance swimming using undulatory median fin kinematics, while the high AR fins of our three most influential species (*O. niger*, *X. auromarginatus* and *M. vidua*)may be optimized for high-speed endurance swimming using oscillatory median fin kinematics. The short, intermediate AR fins of species exhibiting the slowest $U_{t,low}$ speeds might not be optimized for high-speed endurance swimming using undulatory or oscillatory median fin kinematics, but these species appear to have evolved body and caudal fin shapes better suited for high-speed BCF swimming. Detailed research regarding dorsal, anal and caudal fin kinematics of morphologically diverse balistiform swimmers across multiple speeds and gait transitions could further clarify relationships between fin shapes and endurance swimming performance of balistoid fishes.

Associations among body and caudal fin shape and gait transition speed can also be explained by hydrodynamic principles. Balistoid fishes with high AR caudal fins and narrow caudal peduncles recruit their caudal fins ($U_{t,low}$) at lower speeds than do balistoid fishes with low AR caudal fins and wide caudal peduncles. These relationships are best understood by considering $U_{t,low}$ to represent the speed at which caudal fin recruitment is beneficial, rather than the limit of median fin propulsion. Modeling studies have shown that narrow caudal peduncles and high AR caudal fins are more hydrodynamically efficient than wide caudal peduncles and convex caudal fins (M. J. Lighthill 1969; 1970; reviewed in Webb 1982). Triggerfishes, on average, were aided

by caudal fin contribution during the upper 34% of their critical swimming performance, suggesting that caudal fin shape may be especially important for the endurance swimming performance of these triggerfishes at high speeds. Conversely, filefishes only recruited the caudal fin for an average of 12% of their critical swimming performance, suggesting that caudal fin shape is unlikely to be evolutionarily specialized for efficient endurance swimming performance in filefishes. This explains why triggerfishes tend to possess higher AR caudal fins than do filefishes (AR of 2.73 and 2.16, respectively). The low AR filefish caudal fins are likely to be more useful for short bursts of speed than for sustained swimming bouts (Weihs 1973; Paul W. Webb 1982). These body, median fin and caudal fin traits come together in the full shape dataset, where we find strong correlations between $U_{t,low}$ and full shape PC1 and PC2. Fishes with long median fins and wide caudal peduncles (low PC1) and fishes with concave, high AR caudal fins (high PC2) exhibited higher gait transition speeds than did fishes with short median fins and narrow caudal peduncles (high PC1) and highly convex caudal fins (low PC2) (Figure 2.8A).

Finally, some swimming performance trends are best explained by the percent balistiform locomotion data. Fishes with long and large median fins (regardless of their shape) and fishes with wide caudal peduncles used the balistiform gait alone for a larger percentage of their U_{crit} tests. This trend can be explained by the higher maximum power output made possible by large median fins (regardless of fin kinematics) while using the balistiform gait versus increased hydrodynamic efficiency of caudal fin oscillations provided by narrow caudal peduncles. Each species appears to be fairly specialized for taking advantage of one of these gaits, with balistiform specialists possessing elongate, large median fins, capable of overcoming the large power requirements of swimming at high speeds using the median fins alone, while BCF specialists possess short, small median fins, incapable of powering high-speed balistiform locomotion, but narrow caudal

peduncles capable of facilitating efficient caudal fin oscillations to power high-speed endurance swimming. In order to better understand these functional morphology trends, more work is needed on the energetics and kinematics of each swimming gait across a broad taxonomic balistoid sample.

Ecomorphology

The wide range of endurance swimming abilities and gait transition strategies observed among the balistoid species in this study likely has implications for the ecologies of these fishes. All species in this study are reef associated (John E Randall, Allen, and Steene 1997), but they do not all use the reef in the same way. As noted by Wright (2000), *O. niger* and *X. auromarginatus* are largely planktivorous (Fricke 1980; J. Randall, Matsuura, and Zama 1978) and spend large amounts of time swimming well above the reef while picking plankton from the water column (Fricke 1980; Meyers 1991), which explains why these two species have evolved fin and body morphologies suited for providing the highest critical swimming speeds measured in this study. The remaining 11 species can be classified as benthic grazers, as a large portion of their diet is composed of sessile or slow-moving benthic organisms (Peristiwady and Geistdoerfer 1991; John E. Randall 1955; 2007; J. E. Randall and Hartman 1968; Hiatt and Strasburg 1960; Meyer 1985). Most of these species remain close to the shelter of the reef as they nip at algae, crustaceans, sponges, bivalves or the coral itself. All filefishes in the present study fall into this category, and this lifestyle likely does not require high endurance swimming performance. However, these fishes probably do require large bursts of speed to escape predation into nearby holes in the reef, a behavior likely facilitated by their wide caudal peduncles and large, low AR caudal fins (Weihs 1973; Paul W. Webb 1982). Other benthic grazing species (*B. undulatus*, *B. conspicillum*, *R. aculeatus*, *S. bursa*

and *S. chrysopterum*) spend much of their time farther from the cover of the reef as they swim along open coral rubble lagoons and feed on more evasive prey such as crabs and even small fishes (Hiatt and Strasburg 1960; Meyers 1991; Sano, Shimizu, and Nose 1984; John E. Randall 1985; John E Randall, Allen, and Steene 1997; Vijay Anand and Pillai 2005). These species likely require some combination of fast, aerobic bursts of speed to catch prey and escape predators over long distances on open sandy bottoms as well as efficient slow swimming performance to sustain long bouts of searching for benthic prey. These species group in body morphospace defined by narrow caudal peduncles and short median fins and exhibit some of the slowest gait transition speeds ($U_{t,low}$) measured in this study (Figure 2.8), indicating that they rely heavily on caudal fin contribution to achieve high-speed locomotion. Furthermore, research has shown (Korsmeyer, Steffensen, and Herskin 2002) that one species with this body type and lifestyle, *R. aculeatus*, is capable of highly efficient slow swimming using the balistiform gait, as well as sustainable, aerobic BCF-supplemented locomotion at higher speeds. Combined, these trends suggest that the small, short median fins of *R. aculeatus* are sufficient for slow grazing using balistiform locomotion, while the narrow caudal peduncle facilitates efficient, high-speed, aerobic BCF swimming used to escape predators and chase down elusive prey over expansive sandy lagoons. In order to determine how well these ecomorphological trends apply to balistoid fishes as a whole, more research is required on the morphometrics and ecologies of a larger, phylogenetically informed sample of the superfamily Balistoidea.

CHAPTER THREE: FIN SHAPE, ASYMMETRY, AND THE INFLUENCE OF SWIMMING PERFORMANCE ON PATTERNS OF EVOLUTIONARY ECOMORPHOLOGY IN TRIGGERFISHES AND FILEFISHES (SUPERFAMILY: BALISTOIDEA)

Abstract

Triggerfishes and filefishes in the superfamily Balistoidea exhibit a wide range of fin and body morphologies, inhabit many distinct marine habitats, and feed on a variety of benthic and pelagic organisms. Particular combinations of fin and body shapes as well as levels of dorsoventral asymmetry, are predicted to provide functional advantages for swimming behaviors that facilitate life in diverse habitats and feeding guilds. Morphological diversity of 80 balistoid species was quantified using geometric morphometrics and used to examine patterns of evolutionary morphological integration between fin and body regions. Evolutionary integration was detected between all fin and body regions examined. Results revealed strong evidence for coordinated evolution and convergence of high and low aspect ratio dorsal and anal fins, the fins that power steady locomotion in these fishes. However, dorsal and anal fin shapes and positions were found to be asymmetrical across the dorsal-ventral body axis within most species, presenting balistoid fishes with an unusual paired propulsor biomechanical system that may be prone to asymmetrical force production and pitch. Balistoid species were grouped by primary habitat use and feeding mode based on data from published literature. High aspect ratio, posteriorly tapering dorsal and anal fins were found to be associated with fishes that live in offshore pelagic habitats and planktivorous species. These high aspect ratio fins provide efficient, high performance endurance swimming required for life in the open ocean and feeding on pelagic plankton. Conversely, low aspect ratio fins were found in nearly every habitat and feeding group, suggesting that the increased

maneuverability and burst performance provided by low aspect ratio fins are beneficial for fishes in all habitat and feeding groups.

Introduction

Fishes inhabit nearly every aquatic ecosystem on earth from the open ocean, structurally complex coral reefs and wave-swept shorelines to freshwater systems including fast flowing rivers, murky lakes and dark, isolated caves. Understanding patterns of association between organismal traits that allow fishes to successfully inhabit these ecosystems is a general goal of many evolutionary ichthyologists because these patterns can help explain both clade-specific evolutionary trajectories and larger trends between functional traits and ecology. Studies exploring relationships between organismal ecology and morphology, termed ecomorphology, have been especially useful for large taxonomic groups because detailed morphological data can be quickly gathered for a large number of species, allowing researchers to explore hypotheses on large evolutionary scales. However, to fully understand ecomorphological relationships, the morphological characters examined must have well established associations with organismal function or performance, often provided by biomechanical experiments. Consequently, many ecomorphology studies have focused on relationships between cranial morphology and diet (Evans et al. 2019; Friedman et al. 2016; Klaczko, Sherratt, and Setz 2016; McCord and Westneat 2016a; Olsen 2017) and locomotor morphology and habitat (C.J Fulton, Bellwood, and Wainwright 2001; Yuan, Wake, and Wang 2019). Although most fishes rely on swimming performance for nearly all aspects of their lives (including prey capture), few studies (but see Wainwright, Bellwood, & Westneat, 2002) have examined ecomorphological relationships between fish locomotor morphologies and feeding modes.

Triggerfishes (Balistidae) and filefishes (Monacanthidae) in the superfamily Balistoidea provide an exciting opportunity to explore relationships between locomotor fin and body morphologies and ecologies due to their wide range of morphological diversity, feeding modes and marine habitats. Balistoid fishes range in body shape from deep bodied, rounded forms to shallow bodied, elongate shapes and possess a wide range of dorsal, anal and caudal fin shapes, which they use to power steady swimming in the balistiform swimming mode (Blake, 1978; Wright, 2000). Dorsal and anal fin shapes range from wing-like, posteriorly-tapering, high aspect ratio forms to elongate and rectangular or rounded, low aspect ratio forms (Dornburg et al. 2011), and caudal fins range from deeply forked to highly convex (George and Westneat 2019). Laboratory experiments have revealed that balistoid species with high aspect ratio dorsal, anal and caudal fins are associated with increased endurance swimming performance (George and Westneat 2019; Wright 2000).

Past research on balistoid evolution has revealed that the common ancestor to the superfamily Balistoidea was likely reef associated (Santini, Sorenson, and Alfaro 2013), but many species have since evolved to occupy a variety of different marine habitats including seagrass beds, bare coastal shores and even the open ocean. Balistoid fishes also exhibit a variety of feeding modes including benthic grazing on slow moving or sessile organisms, planktivory in the water column, and predation on elusive prey such as cephalopods and other fishes. Triggerfish cranial morphology is tightly correlated with feeding mode (McCord and Westneat 2016a), and the diet and habitat differences between species are predicted to be tightly associated with swimming-related morphological differences as well.

Balistoid fin and body geometric morphometrics are used in this study to examine patterns of morphological integration of functionally informative traits as well as feeding mode and habitat

use ecomorphology in an evolutionary context. Triggerfish dorsal and anal fins exhibit high degrees of morphological integration across species (Dornburg et al. 2011), but broad observations of balistoid body plans suggest that dorsal and anal fin shapes and positions are not symmetrical across the dorsal-ventral body axis in many balistoid species. Phylogenetic analysis of morphometric data allows testing of the hypothesis that planktivorous and pelagic balistoid fishes possess higher aspect ratio fins than fishes in other feeding mode and habitat categories. This prediction is based on the high percentage of time these groups spend swimming in the water column, thus benefitting from the performance (George and Westneat 2019) and hydrodynamic (Wright 2000) advantages provided by high aspect ratio fins. Conversely, low aspect ratio fins are expected to be associated with species that feed on elusive prey and live in structured reef environments because low aspect ratio fins are often associated with high performance burst swimming and maneuverability (Walker and Westneat, 2002). Finally, deep ventral keels and long dorsal spines, also captured by a morphometric approach, were expected to be associated with fishes living in structured reef environments because these mobile elements could be used to avoid predation by safely locking fishes into reef crevices.

Materials and methods

Species Selection

In order to explore ecomorphological relationships of balistoid fishes in an phylogenetic context, I examined the 80 balistoid species in the most recent molecular phylogeny of the superfamily (McCord and Westneat 2016b). The 80 species in this tree include 32 triggerfish (Balistidae) species and 48 filefish (Monacanthidae) species and represent about 54% of the 150 described balistoid species with especially high triggerfish coverage (76%) compared to filefish coverage

(45%). This time-calibrated phylogeny was used for all phylogenetically-informed statistical analyses in this study.

Habitat Use and Feeding Mode Characters

The 80 balistoid species were grouped by primary habitat use and feeding mode based on published literature. A literature survey of 99 articles, books and encyclopedias (see Table S3.1) was performed to assign balistoid species into 6 habitat categories (coastal bare bottom, structured reef, open reef, open ocean pelagic, open ocean demersal, and seagrass/ weedy) and 4 feeding mode categories (benthic grazers, fishes that include elusive prey in their diets, planktivores, and a group comprised of fishes that exhibit even levels of benthic grazing and planktivory). When habitat and feeding data were not available from primary sources, the online database *FishBase* (Froese and Pauly 2019) was used to classify remaining species into habitat (n = 4 species) and feeding groups (n = 1 species).

Habitat category assignments were based on descriptive data and/or catch records, with quantitative data (timed behavioral studies) available for a few species. Quantitative diet data (based on stomach contents or timed feeding behavior studies) were available for 46 of the 80 species, allowing for easy placement of these species into primary feeding groups. When quantitative diet data was not available (n = 34 species), feeding mode classifications were based on detailed published descriptions of feeding behaviors, usually confirmed by multiple sources for each species. Habitat classifications were made for all 80 balistoid species in this study, and feeding mode classifications were made for 70 species.

Fin and Body Shape Quantification

Morphological diversity of fin and body shapes among the 80 balistoid species was quantified using photos of 569 fish specimens acquired through online museum databases, publications, online fish blogs, and physical museum specimens (see Table S3.2 for photograph sources). Each species was represented by an average of 6.6 specimens (range = 1-20). As morphometric quality of photos was prioritized over quantity, 4 rare species (*Eubalichthys mosaicus*, *Paramonacanthus filicauda*, *Paramonacanthus oblongus*, and *Thamnaconus arenaceus*) were represented by 1 specimen and 7 species were represented by 2 specimens. All other species were represented by 3 or more specimens. All specimens included in this study were scaled (using a ruler in the photograph or specimen-specific length information) with the exception of 6 visibly adult specimens due to the lack of accessible, scaled specimens for these species (see Table S3.2). For the 6 cases in which specimen-specific scale data were not available, and considering that shape and not size scaling is explored here, each specimen was assigned the mean adult standard length reported for their species on *FishBase* (Froese and Pauly 2019).

A total of 110 landmarks were digitally placed on each photo using the R package *StereoMorph* (Olsen and Westneat 2015) for detailed geometric morphometric analyses, following the methods of George & Westneat (2019) with the exception of the inclusion of an additional landmark on the distal tip of the first dorsal spine in the present study (Figure 3.1). If any structures of a specimen were visibly damaged, those structures were not digitized or included in subsequent analyses. Some dorsal and anal fins (n=94/336 and 82/329, respectively) in otherwise good condition had preservation artifacts leading to inconsistent fin positions between specimens. These preservation artifacts were corrected using the Mac App *FinRotate* (https://github.com/mwestneat/FinRotate) as described in George & Westneat (2019). All dorsal

spine tip landmarks were rotated with *FinRotate* so that a consistent 45 degree angle was formed between the dorsal spines and the anterior-posterior body axis. Similarly, the positions of un-extended ventral keel landmarks were estimated using the *estimate.missing* function in *geomorph* R package (Adams et al., 2017) following the methods of George & Westneat (2019).

Landmarks were subdivided into five separate morphometric datasets for independent geometric morphometric analyses: full shape (all landmarks), body only, dorsal fin only, anal fin only, and caudal fin only following the methods of George & Westneat (2019). The additional dorsal spine landmark in the present study was treated as a static landmark and included in the full shape dataset only. Following Procrustes-alignment, species average shapes for each morphological dataset were calculated, and allometric relationships between species centroid size and shape was assessed for each geometric morphometric dataset using the *procD.pgls* function in the R package *geomorph* (Adams et al. 2017) based on 1,000 permutations. As no significant allometric effects were detected in any of the morphological datasets ($F = 2.574$, $P = 0.492$; $F = 3.232$, $P = 0.602$; $F = 2.382$ $P = 0.2142$; $F = 2.781$, $P = 0.6854$; $F = 1.288$, $P = 0.634$; for full shape, body, dorsal fin, anal fin, and caudal fin shape data, respectively), no adjustments to the morphometric data were required, and principal components analysis (PCA) were conducted on each species-averaged, GPA-aligned geometric morphometric dataset. Resulting principal component (PC) scores along the two most significant axes of inter-specific variance (PCs 1 and 2) were extracted for each species for use in backtransform morphospace visualization (see Olsen, 2017) and subsequent statistical analyses. Final sample sizes (species, specimens) for each morphological unit are: body (80, 529), dorsal fin (76, 336), anal fin (77, 329), caudal fin (76, 253), full shape (74, 175).

Finally, dorsal, anal, and caudal fin aspect ratios were calculated for each specimen using the rotated fin landmarks and the equation

$$AR = \frac{b^2}{A}$$

where *b* is the maximum span of each fin perpendicular to anterior-posterior axis of the fish (red dotted lines in Figure 3.1) and *A* is the surface are of the fin (blue lines in Figure 3.1) (George and Westneat 2019). Species-average dorsal, anal, and caudal fin aspect ratios were then calculated.

Figure 3.1. Morphometrics digitization scheme demonstrated on the triggerfish *Balistapus undulatus*.
A total of 110 landmarks were placed along the fins and bodies of each fish. White circles represent static landmarks. Blue shapes represent sliding semi-landmarks, with triangles representing landmarks in the body dataset and circles representing subsampled fin landmarks from digitized Bezier curves. Fin area measurements are outlined in blue and span measurements were made along the dotted red lines.

Evolutionary Morphological Integration

In order to analyze the evolutionary ecomorphology of balistoid fishes, two methods of pair-wise morphological integration tests were conducted between each geometric morphometric dataset (body, dorsal fin, anal fin, and caudal fin) using a similar approach to that used by Dornburg et al. (2011). First, pair-wise phylogenetic integration tests were conducted between geometric morphometric datasets using the *phylo.integration* function in the *geomorph* R package. In a pair-wise context, the *phylo.integration* test uses two-block partial least squares (PLS) analysis to quantify the degree of morphological covariation (integration) among species in a phylogenetic context. Pairwise linear regressions were used to assess significance of correlation between primary phylogenetic partial least squared (pPLS) axes of each morphological unit. Second, separate pair-wise phylogenetic generalized least squares (PGLS) regressions were conducted between all combinations of the first two principal component (PC) axes of each geometric morphometric dataset using *pgls* function in the *caper* R package (Orme et al. 2013).

Morphological PLS analysis differs from morphological PCA in that the primary PLS axes correspond to the axes of maximum morphological *covariation* between two selected morphological units (such as dorsal and anal fins), termed blocks, while the primary PCA axes correspond to the axes encompassing the maximum morphological variance between species within a single morphological unit (ie. dorsal fin only). Thus, primary PLS axes represent the axis of morphological variation in one morphological subunit (ie. the dorsal fin) that is most-correlated with variation in the other morphological subunit (ie. the anal fin). This makes PLS analysis a powerful tool for identifying significant integration between morphological subunits along *any* axes of variation, while PGLS correlations between the primary or secondary PC axes (PCs 1 and

2) of two morphological units goes one step further by demonstrating that the two subunits display evolutionary integration along their *most significant* axes of morphological variation.

Evolutionary Ecomorphology

In order to assess relationships between balistoid morphology and ecology, phylogenetic ANOVA tests were conducted between fin aspect ratios and significant PC axes (PCs 1 and 2) of each morphological dataset (full shape, body, dorsal fin, anal fin, and caudal fin geometric morphometrics datasets) and the habitat and feeding mode categories using the *phylANOVA* function in the R package *phytools* (Revell 2012). Statistical significance of phylogenetic ANOVA tests were based on 10,000 simulations. For all cases in which the F statistic for the phylogenetic ANOVA test was found to be significant ($P < 0.05$), pair-wise t-tests were conducted to identify ecotypes (habitat or feeding groups) exhibiting significantly different morphologies from one another.

Dorsal and Anal Fin Symmetry

Dorsal and anal fin symmetry was assessed in all 175 specimens included in the full shape dataset, representing 74 species. Median fin shape symmetry was quantified using three separate morphological ratios: 1) Dorsal fin aspect ratio: Anal fin aspect ratio, 2) Dorsal fin area: Anal fin area, and 3) Dorsal fin base length: Anal fin base length. Median fin position and orientation symmetry was assessed by comparing the position of the first dorsal and anal fin rays along the anterior-posterior axis and by comparing the angles of dorsal and anal fin attachment.

Additionally, the *bilat.symmetry* function in the R package *geomorph* was used to comprehensively measure symmetry/ asymmetry using ANOVA tests between the dorsal and anal

fin landmarks. Two separate *bilat.symmetry* tests were conducted to assess the level of directional symmetry/ asymmetry, or the average difference between dorsal and anal fin shapes (Klingenberg, Barluenga, and Meyer 2002). First the null hypothesis of matching symmetry [symmetry between two separate shapes (dorsal and anal fins)] was tested. Matching symmetry analysis was performed by flipping the anal fin coordinates over the body axis (to remove the mirror-image effect) and Procrustes aligning the dorsal and anal fin landmarks together. This process removes information about translation, rotation and scaling between dorsal and anal fins, and thus only tests for symmetry/ asymmetry of the shapes themselves. Next, the null hypothesis of object symmetry (symmetry across a "midline" axis) was tested. Object symmetry takes the position, size and orientation of the dorsal and anal fins into account while assessing the level of symmetry between the two fins (Klingenberg, Barluenga, and Meyer 2002). The final fin asymmetry test involved calculating the Procrustes distance (the square root of the sum of squared differences in the positions of the landmarks of two shapes) between Procrustes-aligned dorsal fins and flipped anal fins in order to measure the total spatial transformation shape differences between dorsal and anal fins without taking size or orientation along the body axis into account.

Fin Ancestral State Estimations

Each species was binned into one of four categorical aspect ratio groups (low, medium, high and very high) using a modified gap coding method to allow for relatively even group sizes while ensuring large gaps between species at the inter-group boundaries. Individual aspect ratio ancestral state estimations were then conducted for each fin using the *ace* function in the R package *APE* (Paradis, Claude, and Strimmer 2004) using an equal rates, maximum likelihood model. The evolution of fin asymmetry was also explored by conducting an ancestral state estimation of the

Procrustes distances between dorsal and anal fin shapes. Procrustes distance was treated as a continuous trait and ancestral states were estimated using the *contMap* function in the *phytools* R package.

Statistical Analyses

All statistical analyses were carried out in R version 3.3.2 (R Core Team 2016). Prior to running all statistical tests described above, data and residuals were examined for alignment with the assumptions of each test. Phylogenetic generalized least squares (PGLS) and phylogenetic ANOVA analyses both assume that the residuals of the analyses are normally distributed. This assumption was assessed by visualizing the distribution of residuals from each test, and performing Lilliefors (Kolmogorov-Smirnov) tests using the *lillie.test* function in the *nortest* R package (Gross and Ligges 2015). The phylogenetic ANOVA tests also assume homogeneity of variance (equal variance across groups), which was tested using Levene's tests with the *leveneTest* function in the *car* R package (Fox and Weisberg 2011). Log transformations were effective for correcting most cases in which raw morphological data violated these assumptions. Three variables (Full Shape PC1, Body PC1, and Anal PC2) could not be transformed to exhibit homogeneity of variance across habitat groups, so these variables were not included in phylogenetic ANOVA testing. All p-values resulting from phylogenetic ANOVA post-hoc pair-wise t-tests conducted with the *phylANOVA* function were adjusted for multiple tests using the "holm" method (Holm 1979). Statistical significance was determined as $p < 0.05$.

RESULTS

Evolution of Fin Aspect Ratios

The balistoid fishes included in this study exhibit a wide range of fin and body shapes. Dorsal fin aspect ratio (AR) ranged by nearly an order of magnitude from 0.277 in the filefish *Meuschenia freycineti* to 2.49 in the triggerfish *Canthidermis sufflamen*. Similarly, anal fin AR ranged from 0.250 in the filefish *Aluterus scriptus* to 2.45 in the triggerfish *C. sufflamen.* Balistoid fishes also exhibited a wide range of caudal fin AR from 0.742 in the filefish *Aluterus heudeloti* to 4.29 in the triggerfish *Abalistes stellatus*. Triggerfishes tend to have higher dorsal fin AR (range = 0.365 – 2.486, mean = 0.852) and anal fin AR (range = 0.379 – 2.453, mean = 0.786) than filefishes (dorsal fin range = 0.277 – 1.35, mean = 0.483; anal fin range = 0.250 – 1.16, mean = 0.473) ($t = 3.67$, $df = 39.6$, $p = 0.000717$; $t = 3.72$, $df = 38.7$, $p = 0.000625$ for dorsal and anal fins respectively). Balistoid fishes exhibit even larger differences in caudal fin AR between families ($t = 9.74$, $df = 63.62$, $p = 3.13e\text{-}14$) with triggerfishes generally exhibiting much higher caudal fin AR (range = 2.07 – 4.29, mean = 2.99) than filefishes (range = 0.74 – 2.75, mean = 2.01).

Ancestral state estimations of dorsal, anal and caudal fin AR revealed multiple convergent events on high, medium, and low AR in all three fin groups as well as interesting differences in the evolution of these traits between families (Figures 2 and 3). Despite these convergence events, closely related taxa tend to exhibit similar fin AR, and all three fin aspect ratios showed high levels of phylogenetic signal (kmult = 0.18, P = 1e-04, kmult = 0.17, P = 1e-04; and kmult = 0.36, P = 1e-04, for dorsal, anal and caudal fins, respectively). Dorsal and anal fin AR are highly correlated (PGLS: P = 2.2e-16, multiple $R^2 = 0.774$), but caudal fin AR is not correlated with dorsal or anal fin AR (PGLS: P = 0.0789, multiple $R^2 = 0.0417$; P = 0.149, multiple $R^2 = 0.0283$, respectively).

The triggerfish common ancestor likely possessed high AR dorsal, anal and caudal fins, and most extant triggerfishes possess high or medium aspect AR (Figures 3.2 and 3.3**)**. The highest aspect ratio dorsal, anal and caudal fins were found within the Balistidae. These very high AR dorsal fins likely evolved once in *Balistes vetula* and once in the common ancestor to the *Canthidermis* genus, and very high AR caudal fins likely evolved once in *B. vetula* and once in *Abalistes stellatus*. Medium AR anal fins exhibit the highest degree of convergent evolution within the Balistidae, likely evolving 5 times independently (Figure 3.2 B). These convergence events include the common ancestor of the *Sufflamen* + *Rhinecanthus* clade, and four individual species *Balistapus undulatus, Melichthys vidua, Xanthichthys ringens* and *Balistes punctatus*.

A few triggerfish species also possess low AR dorsal, anal and caudal fins. Low AR dorsal and anal fins likely convergently evolved a few times each within the Balistidae (Figure 3.2). Specifically, low AR dorsal fins likely evolved in the common ancestor of the species pair *Balistoides conspicillum* and *Balistapus undulatus*, in the common ancestor of the *Abalistes* genus, and in *Rhinecanthus abyssus*. Low AR anal fins likely evolved twice within Balistidae, once in the *Abalistes* common ancestor, and once in *B. conspicillum*. Only one triggerfish species, *Pseudobalistes naufragium*, possesses a low AR caudal fin.

The common ancestor of the Monacanthidae, on the other hand, shows a maximum likelihood estimation of low AR dorsal and anal fins and a low to medium AR caudal fin. Most extant filefishes possess low AR dorsal and anal fins. As in the Balistidae, medium AR dorsal and anal fins evolved independently many times in the filefishes. Interestingly, 9 filefish species exhibit medium AR dorsal fins and 11 filefish species possess medium AR anal fins, and in both cases none of the species with medium AR fins are sister species. Consequently, it appears that medium AR dorsal and anal fins have evolved independently up to 9 times each. High AR dorsal

and anal fins also appear in multiple areas of the monacanthid tree and likely independently evolved 4 times each, once in the common ancestor to the *Paramonacanthus* genus, twice within the *Thamnaconus* genus, and once in *Nelusetta ayraudi*. Caudal fin evolutionary trends are a bit more complicated in the Monacanthidae due to a lack of clarity in the ancestral state, with similar likelihoods of low and medium AR caudal fins. If the ancestral state was a medium AR caudal fin, then low AR fins convergently evolved up to 8 times, and if the ancestral state was a low AR caudal fin, then medium AR fins evolved at up to 6 times independently. However, none of the extant filefishes examined in this study exhibited high or very high AR caudal fins, making it highly likely that filefishes evolved from an ancestor possessing low or medium aspect ratio fins.

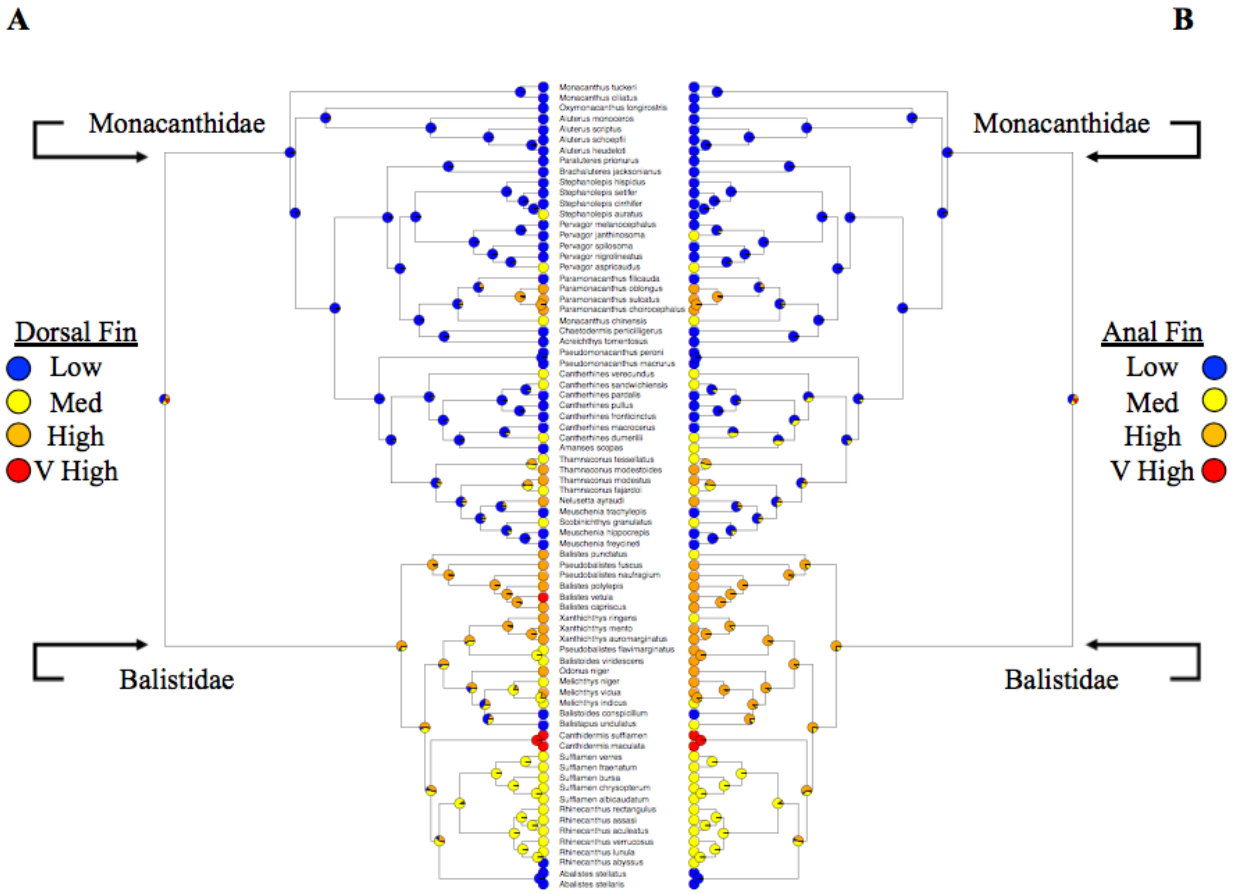

Figure 3.2. continued on page 70.

Figure 3.2. Dorsal and anal fin aspect ratio ancestral state estimations.
(A) Dorsal fin. Low = 0.28 – 0.45, Med = 0.47 – 0.67, High = 0.76 – 1.35, Very High = 2.08 – 2.49. (B) Anal fin. Low = 0.25 – 0.44, Med = 0.46 – 0.66, High = 0.68 – 1.20, Very High = 2.07 – 2.45. Colored pie charts represent the likelihood of each fin aspect ratio state at each ancestral node based. Tip colors depict the measured states of extant species.

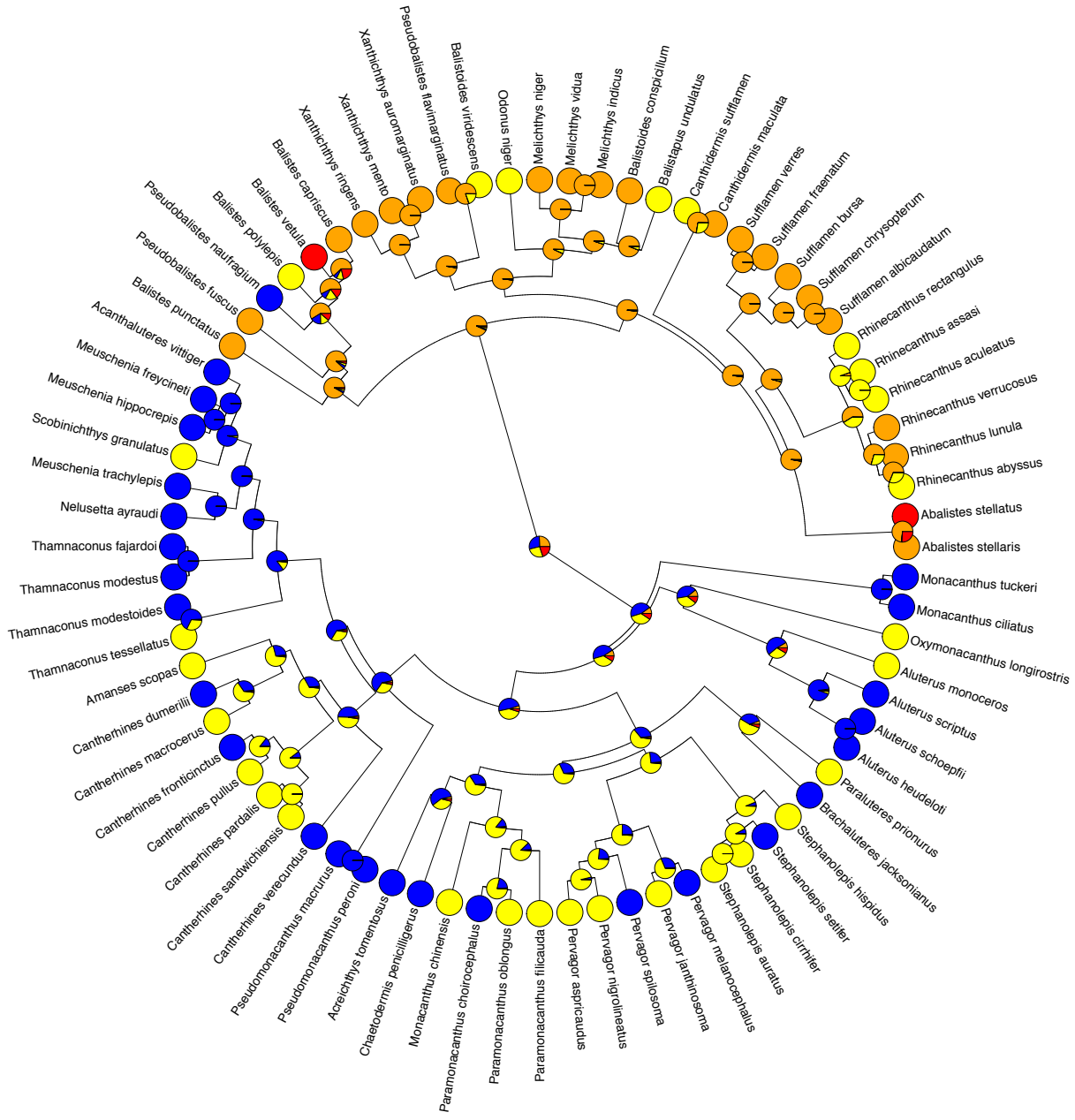

Figure 3.3. Caudal fin aspect ratio ancestral state estimation.
Colored pie charts represent the likelihood of each caudal fin aspect ratio state at each ancestral node. Tip colors depict the measured states of extant species. Low (blue) = 0.74 – 2.09, Med (yellow) = 2.14 – 2.75, High (orange) = 2.81 – 3.61, Very High (red) = 4.14 – 4.29.

Overall, these results suggest that the common ancestor of balistoid fishes possessed low aspect ratio dorsal and anal fins, and that low, medium and high AR dorsal and anal fins have all convergently evolved multiple times within the superfamily (Figure 3.2). The ancestral state of the Balistoid caudal fin was not clearly resolved, however it is likely that triggerfishes and filefishes diverged in caudal fin shape shortly following the split between the families with the triggerfish common ancestor very likely possessing a high AR caudal fin and the filefish common ancestor likely possessing a low or medium AR caudal fin.

Dorsal and Anal Fin Symmetry

Balistoid dorsal and anal fins exhibited asymmetry along multiple shape and position axes. Although dorsal and anal fin aspect ratios are highly correlated across species, a linear regression between dorsal and anal fin aspect ratios for all 175 individuals in which both dorsal and anal fin aspect ratio data were available revealed that dorsal and anal fin aspect ratios are not symmetrical within individuals (slope = 0.85). Nine species possess dorsal and anal fin aspect ratios binned into different aspect ratio groups (Figure 3.2) and only 43% of individuals exhibit the same dorsal and anal fin aspect ratio when rounded to a single digit, demonstrating the widespread asymmetry of median fin aspect ratios. Furthermore, although exactly half the species exhibit higher aspect ratio dorsal fins than anal fins, while the other half show the reverse pattern, all species possess longer dorsal than anal fins except the *Aluterus* species, which all possess longer anal fins than dorsal fins. A two-sample t-test indicated that balistoid dorsal fin bases, on average, are significantly longer than balistoid anal fin bases ($t = 2.3081$, $df = 344.35$, $P = 0.02159$). Additionally, 97% of individuals exhibited anal fins that begin posteriorly to their dorsal fins. Anal fins begin an average of 4% of SL posterior to the dorsal fins (Fig. S1). A linear regression also revealed deviations from

symmetry in terms of fin angles of attachment (slope = 0.55). Dorsal and anal fins exhibit higher levels of symmetry in their areas (slope = 0.92346) than any other metric. The discovery of asymmetrical fin aspect ratios, fin base lengths and fin angles of attachment despite highly symmetrical fin areas, suggests that the dorsal and anal fin *shapes*, *positions* and *orientations*, but *not sizes* have evolved asymmetrically.

Full fin shape asymmetry was also assessed using the geometric morphometric fin data. Directional symmetry tests between dorsal and anal fin landmarks conducted with *bilat.symmetry* ANOVA revealed both significant matching asymmetry (asymmetry between the average dorsal and anal fin shapes that does not account for differences in size or orientation) ($F = 34.7204$, $P = 0.001$) and object asymmetry (asymmetry between the average dorsal and anal fin shapes that accounts for differences in size and orientation across the midline axis) ($F = 317.5782$, $P = 0.001$), providing strong evidence for asymmetry in both the shape (primarily fin length) and orientation (primarily angle of attachment) of balistoid dorsal and anal fins (Figure 3.4). Procrustes distance between aligned dorsal fins and flipped anal fins revealed that triggerfishes generally possess more asymmetrical fins than filefishes ($t = 5.1225$, $df = 170.3$, $P = 8.1e\text{-}07$). Furthermore, ancestral state estimations of these Procrustes distances revealed multiple convergence events towards highly asymmetrical median fins throughout the evolution of the superfamily Balistoidea with triggerfishes likely evolving from a common ancestor possessing moderately asymmetrical fins and filefishes likely evolving from a common ancestor with fairly symmetrical fins (Figure 3.5).

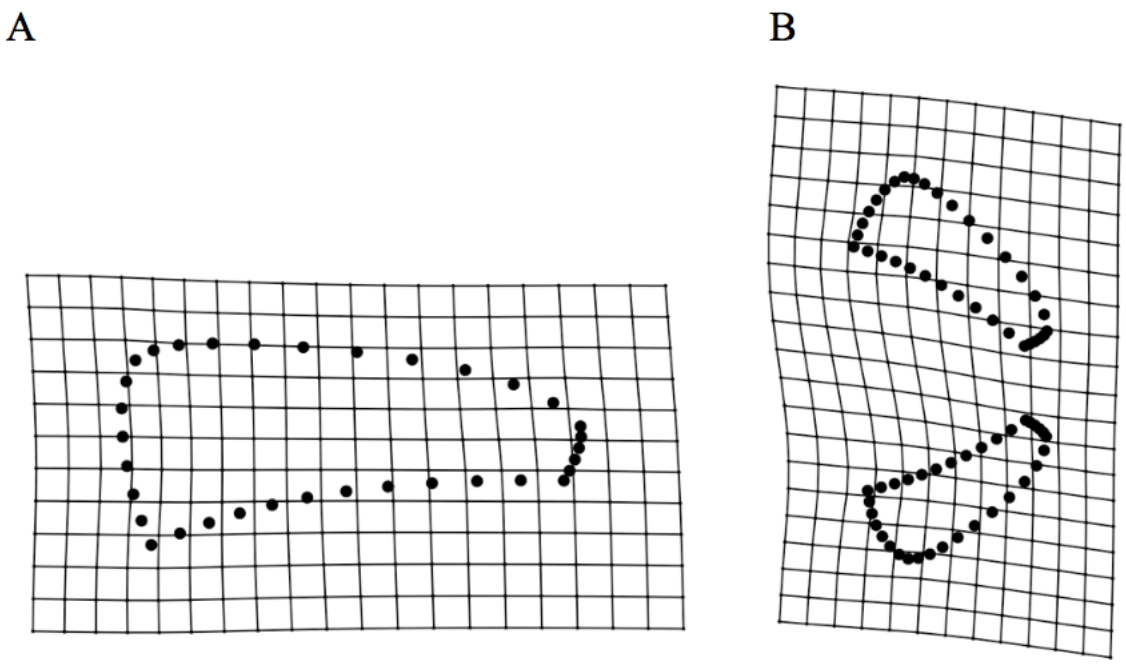

Figure 3.4. Balistoid dorsal and anal fin asymmetry.
(A) Mean directional matching asymmetry warp grid depicting that fin length is a major axis of asymmetry between dorsal and anal fins. (B) Mean directional object asymmetry warp grid depicting that fin angles of attachment are a major axis of asymmetry between dorsal and anal fins.

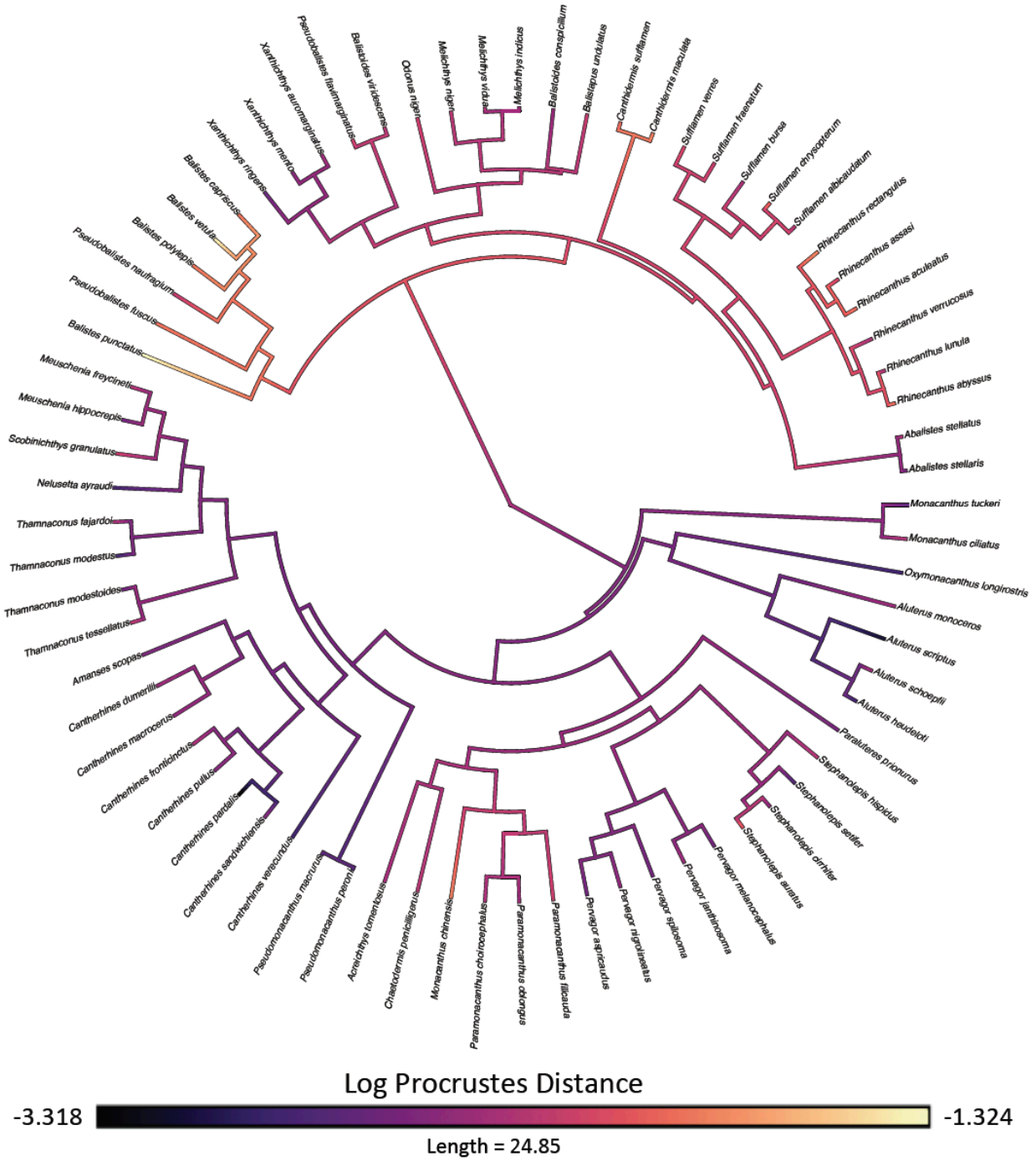

Figure 3.5. Ancestral state estimation of dorsal and anal fin asymmetry measured as log Procrustes distance.

Light and dark colors represent high and low levels of fin asymmetry, respectively. Tip colors tips represent measured fin asymmetry and nodes colors represent fin the most likely asymmetry states as determined by the ancestral state estimation model.

Geometric Morphometrics

The primary axis of variation in the full shape dataset (PC1: 37%) describes changes in the overall length-depth ratio of the fishes with long, thin fishes occupying areas of low PC1 morphospace and short, deep-bodied fishes occupying areas of high PC1 morphospace (Figure 3.6 A). The second axis of variation (PC2: 20%) encompasses differences in dorsal, anal and caudal fin aspect ratios as well as dorsal spine length. Fishes in areas of high PC2 morphospace have long dorsal spines and low aspect ratio fins (Spearman's rank correlation rho = -0.7905, P = 2.2e-16; rho = -0.7694, P = 2.2e-16; rho = -0.4466, P = 7.91e-05 for dorsal, anal and caudal fins respectively). Conversely, fishes occupying areas of low PC2 morphospace have high aspect ratio, posteriorly tapering dorsal and anal fins and high aspect ratio forked or concave caudal fins. Balistoid families exhibit considerable overlap in full shape morphospace, however monacanthid fishes tend to cluster towards high PC2 scores (low aspect ratio fins) with the exceptions of *Paramonacanthus oblongus*, *P. choirocephalus*, and *N. ayraudi* which exhibit lower PC2 scores (high aspect ratio fins) and group with many triggerfishes. Filefishes also span the full range of PC1 scores, while triggerfishes cluster in central PC1 space defined by intermediate body depths.

Species differ in caudal fin morphospace mostly by the shape of the distal edges of their fins (PC1: 53%) with convex caudal fins occupying areas of low PC1 morphospace and forked or concave caudal fins occupying areas of high PC1 (Figure 3.6 B). Both families tend towards low PC1 scores (convex fins), but a few members of both families exhibit high PC1 scores defined by concave caudal fins. Caudal fin PC2 (36%) describes the length-depth ratio of the fins and is associated with caudal fin aspect ratio (Spearman's rank correlation rho = 0.9584, P = 2.2e-16). Balistoid families exhibit little overlap in caudal fin PC2 morphospace, with filefishes exhibiting long, low AR caudal fins and triggerfishes almost exclusively exhibiting short, high AR fins.

The primary axis of dorsal fin variation (PC1: 69%) differentiates fishes by aspect ratio with posteriorly tapering, high AR fins occupying areas of low PC1 morphospace and low AR, more rectangular fins occupying areas of high PC1 morphospace (Spearman's rank correlation rho = -0.9593, P = 2.2e-16) (Figure 3.7 A). Dorsal fin PC2 (13%) primarily describes the angle between the leading edge of the fin and the body axis, with dorsal fins exhibiting anteriorly oriented leading edges possessing high PC2 scores and fins with posteriorly oriented leading edges possessing low PC2 scores. Filefishes tend to cluster in high PC1 morphospace defined by low AR dorsal fins, with the exceptions of *Paramonacanthus sulcatus* and *P. oblongus*, which lie in low PC1 morphospace (high AR fins) primarily occupied by triggerfishes. Both families span the full range of PC2 morphospace.

Anal fin morphospace is similar to that of the dorsal fin, with the primary axis of variation (PC1: 61%) significantly correlated with aspect ratio (Spearman's rank correlation rho = -0.9585, P = 2.2e-16) (Figure 3.7 B). Once again, high AR fins are associated with low PC1 scores. PC2 (17%) describes the angle of the leading edge of the fin as well as the distribution of area along the fin, with anteriorly-oriented leading edges and front-loaded area distributions found in areas of low PC2 morphospace, and posteriorly oriented leading edges and back-loaded area distributions found in high PC2 morphospace. Balistoid families show more separation in anal fin morphospace than in dorsal fin morphospace with filefishes almost exclusively exhibiting low AR fins (high PC1) and triggerfishes tending towards mid to high AR fins (mid to low PC1). Notably, two triggerfish species have diverged from all other balistoid fishes to occupy the top left corner of morphospace (low PC1, high PC2) described by very high AR, sharply posteriorly-tapering anal fins. Interestingly, the filefish *Paramonacanthus oblongus* is the next closest species to this region of anal fin morphospace.

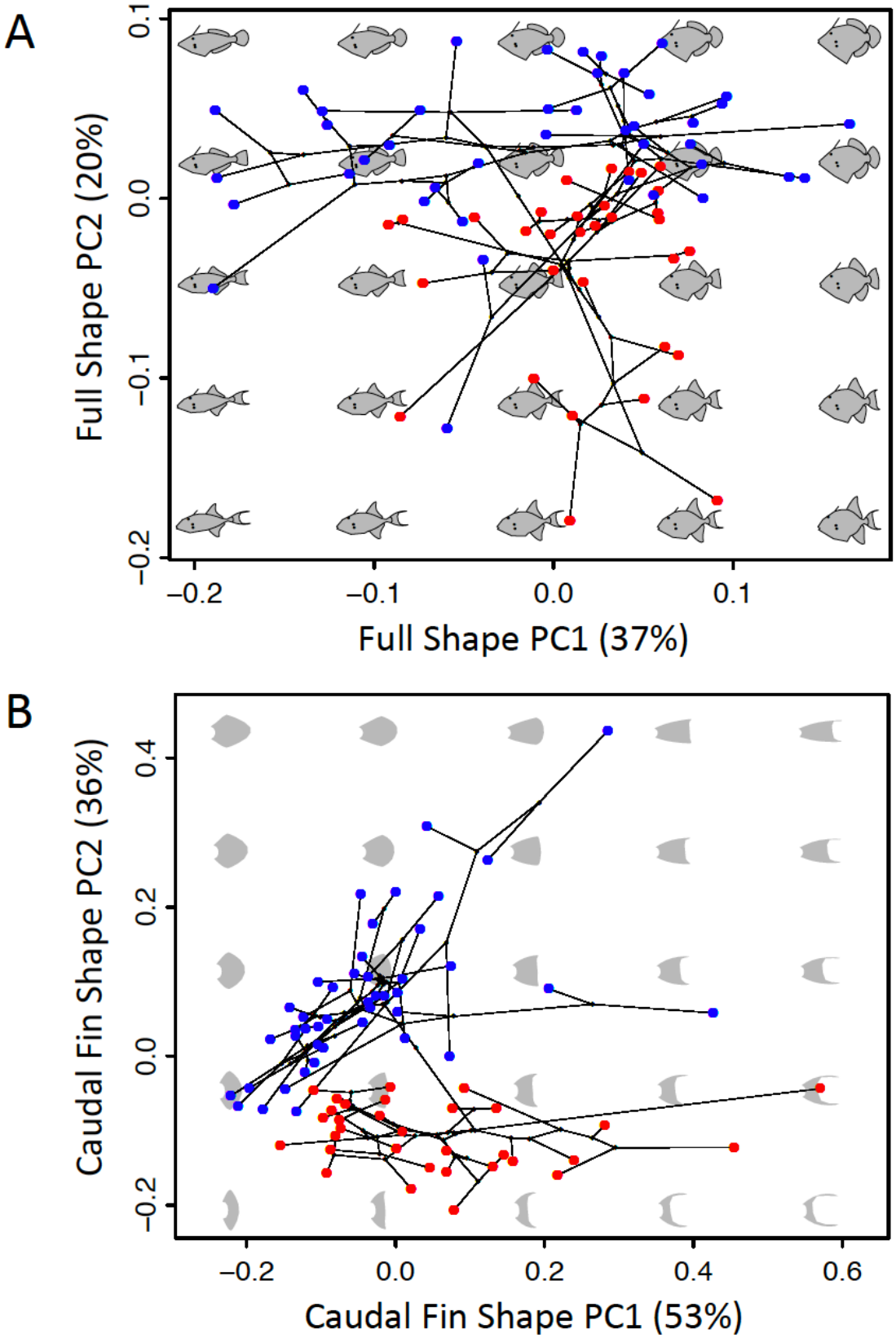

Figure 3.6 continued on page 78.

Figure 3.6 Balistoid full shape and caudal fin shape diversity.
(A) Full shape. (B) Caudal fin shape. Colored dots represent each species' position in morphospace with triggerfishes (Balistidae) in red and filefishes (Monacanthidae) in blue. Gray shapes represent theoretical backtransformed shapes corresponding to morphologies representative of each location in morphospace. Black lines depict the balistoid phylogeny transformed into each morphospace to facilitate inspection of evolutionary shape change trajectories. Bifurcation points along these lines represent theoretical positions (and morphologies) of each ancestral node.

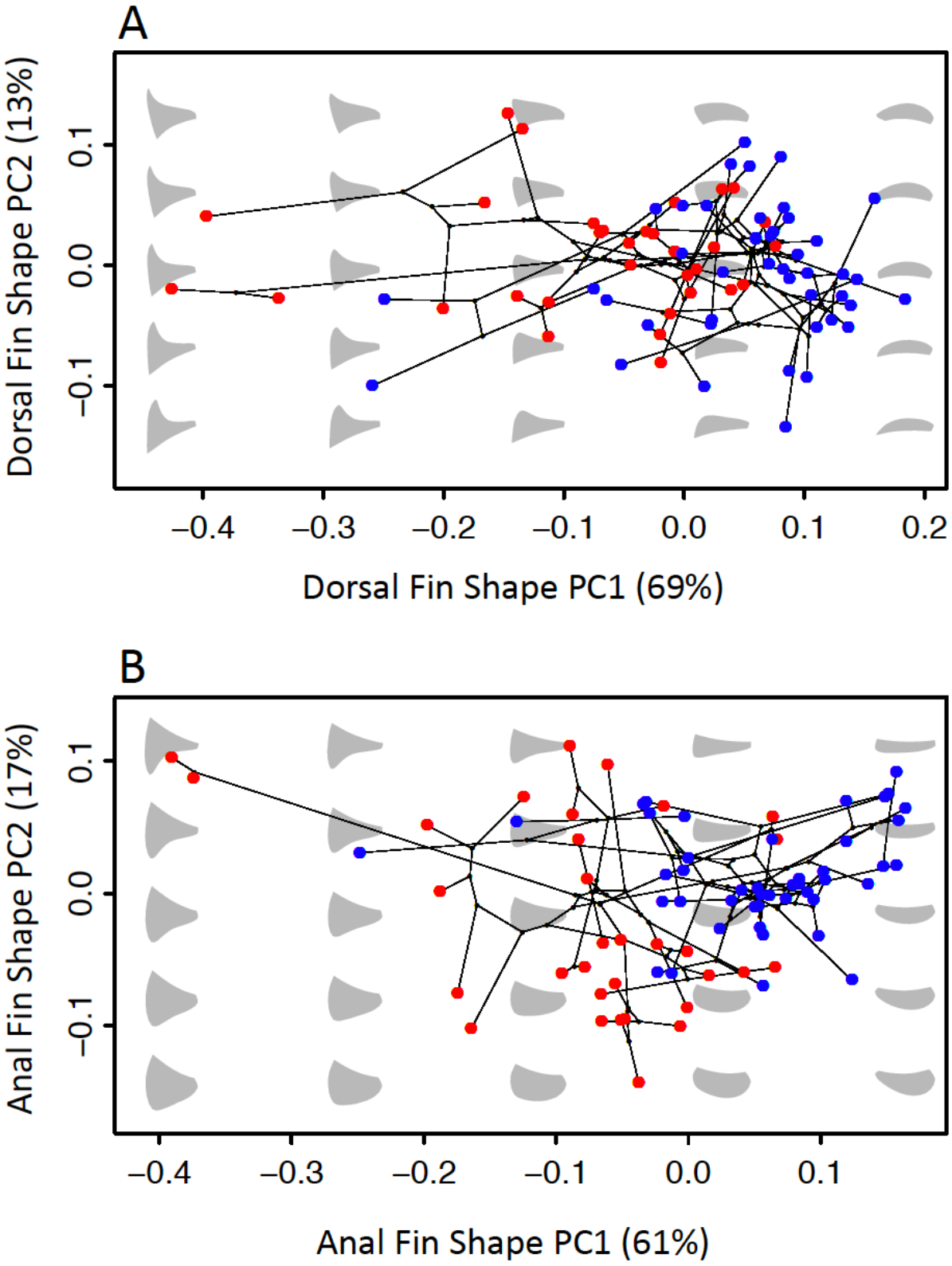

Figure 3.7 continued on page 80.

Figure 3.7. Balistoid dorsal and anal fin shape diversity.
(A) Dorsal fin shape. (B) Anal fin shape. Colored dots represent each species' position in morphospace with triggerfishes (Balistidae) in red and filefishes (Monacanthidae) in blue. Gray shapes represent theoretical backtransformed shapes corresponding to morphologies representative of each location in morphospace. Black lines depict the balistoid phylogeny transformed into each morphospace to facilitate inspection of evolutionary shape change trajectories. Bifurcation points along these lines represent theoretical positions (and morphologies) of each ancestral node.

Morphological Integration

Phylogenetic integration tests revealed high levels of morphological integration between all fin and body regions (Table 3.1) indicating that balistoid fin and body shapes have been tightly correlated throughout their evolutionary history. Pairwise PGLS regressions show that dorsal and anal fin PC1s are positively correlated ($P = 2.2e\text{-}16$, multiple $R^2 = 0.7183$) and bodies with narrow caudal peduncles and long faces (low body PC2) are correlated with anal fins that exhibit posteriorly-oriented leading edges and back-loaded area distributions (low anal fin PC2) ($P = 0.0001302$, multiple $R^2 = 0.1832$). Finally, high aspect ratio dorsal fins with long leading edges (low dorsal fin PC1) are correlated with convex caudal fins (low caudal fin PC1) ($P = 0.00237$, multiple $R^2 = 0.1196$). No significant correlations were found between the primary axes of body and caudal fin shapes, body and dorsal fin shapes, or caudal and anal fin shapes.

Table 3.1. Phylogenetic integration and pair-wise correlations between primary shape pPLS axes.

Shape Dataset (Block 1 vs Block 2)	Overall Phylogenetic Integration (r-PLS/ P value)	Block 1 pPLS1 vs Block 2 pPLS1 (Multiple R-squared/ P value)
Body vs Caudal Fin	0.6622/ 1e-04	0.4385/ 1.32e-10
Body vs Dorsal Fin	0.7772/ 1e-04	0.604/ 3.925e-16
Body vs Anal Fin	0.8015/ 1e-04	0.6424/ 2.2e-16
Dorsal Fin vs Anal Fin	0.8817/ 1e-04	0.7774/ 2.2e-16
Dorsal Fin vs Caudal Fin	0.8679/ 1e-04	0.7532/ 2.2e-16
Anal Fin vs Caudal Fin	0.8853/ 1e-04	0.7838/ 2.2e-16

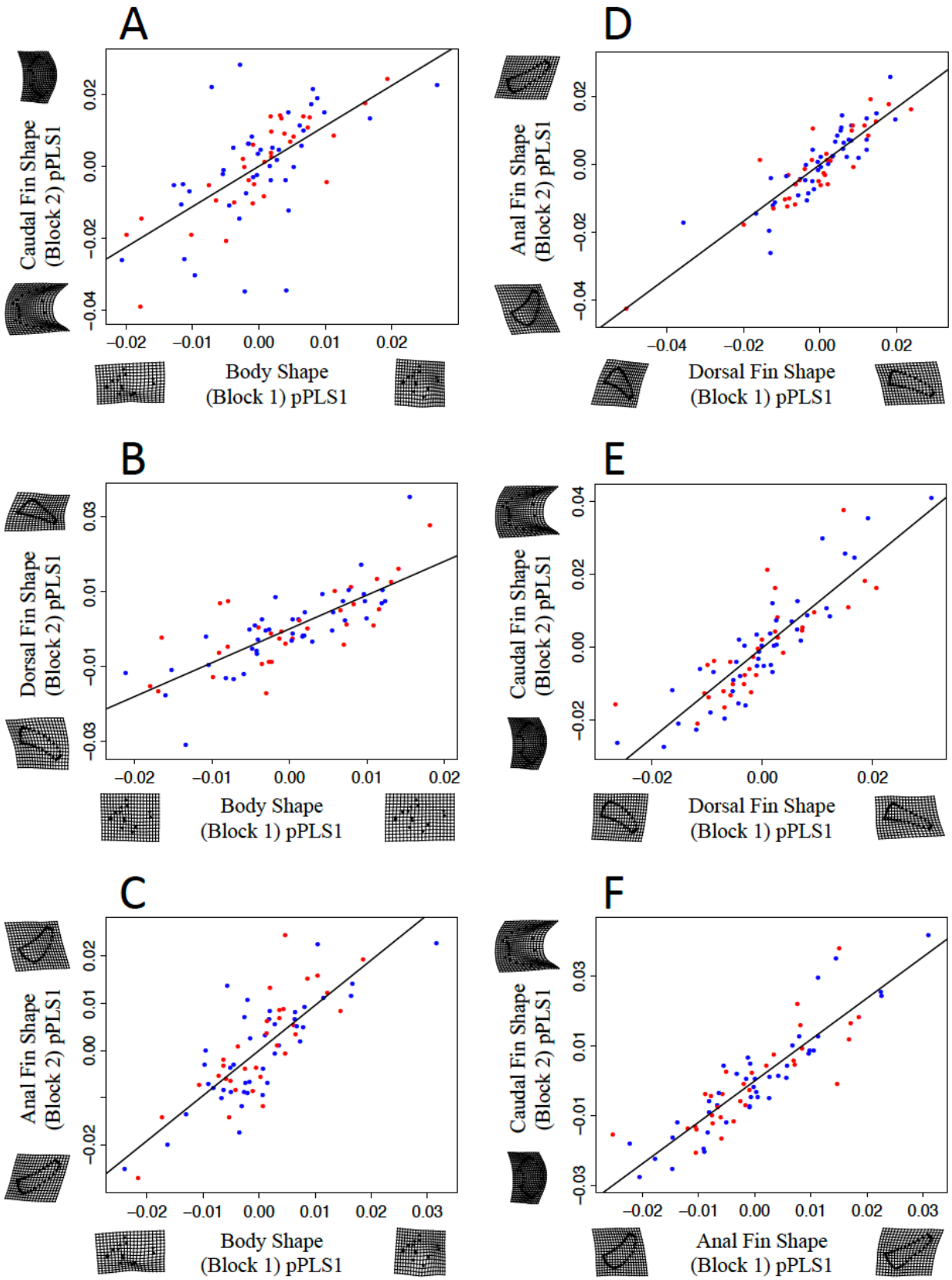

Figure 3.8 continued on page 82.

Figure 3.8. Evolutionary morphological integration.
Each panel depicts the relationship between the primary phylogenetic partial least squares (pPLS) axes of shape covariation between pairs of morphological subunits. (A) Body and caudal fin. (B) Body and dorsal fin. (C) Body and anal fin. (D) Dorsal and anal fin. (E) Dorsal and caudal fin. (F) Anal and caudal fin. Points represent species and are colored by family with triggerfishes in red and filefishes in blue.

Evolutionary Ecomorphology

Planktivorous balistoid species and species that live in open ocean pelagic habitats exhibit distinct dorsal fin, anal fin and full shape morphologies compared to the other balistoid fish ecotypes examined (Figures 3.9 - 3.11). All morphologies (PC scores and ratio measurements) that distinguished planktivorous and pelagic species from other ecotypes are associated with median fin aspect ratios (AR). Significant differences were found in the full shape geometric morphometric dataset for both the feeding mode and habitat group analyses ($F = 8.824$, $P = 0.0295$; $F = 10.072$, $P = 0.0357$, respectively). Planktivorous fishes exhibit more triangular, higher AR dorsal and anal fins and more forked, higher AR caudal fins (low full shape PC2) than benthic grazers ($p = 0.0288$). Open ocean pelagic species exhibit lower full shape PC2 scores than nearly all other habitat groups ($p = 0.0030$, 0.0377, and 0.0224 for structured reef, open reef, and seagrass/ weedy associated fishes, respectively).

Significant differences were also found in dorsal fin ARs (log transformed) for both the feeding mode and habitat categories ($F = 10.107$, $P = 0.0191$; $F = 9.881$, $P = 0.0493$, respectively). Planktivorous fishes exhibit significantly higher dorsal fin ARs than benthic grazers ($p = 0.0054$). Likewise, open ocean pelagic fishes possess higher AR dorsal fins than fishes inhabiting the structured reef, open reef and seagrass/ weedy habitat groups (see Table 3.2 for pair-wise p-values). The relationships between dorsal fin AR and feeding and habitat groups are further supported by significant relationships between log-transformed dorsal fin PC1 (highly correlated

with dorsal fin AR) and feeding and habitat groups (F= 8.578, P = 0.0531; F = 9.846, P = 0.0494, respectively) (Figures 3.9 B and 3.11 A). Dorsal fin geometric morphometric results provide more detail about the dorsal fin shapes associated with these ecotypes than the aspect ratio data alone. Specifically, fishes with long leading edges and posteriorly-tapering dorsal fins (low dorsal PC1) are associated with planktivorous and open ocean pelagic habitats.

Similar trends were found in regard to log-transformed anal fin aspect ratio with planktivorous fishes and open ocean pelagic fishes exhibiting significantly higher anal fin aspect ratios than all other feeding and habitat groups (F= 9.879; P = 0.0226; F = 11.712, P = 0.0253, respectively) (see Table 3.2 for pair-wise significance). Anal fin PC1 also showed significant between-habitat morphological differences (F = 12.112, P = 0.0206) with open ocean pelagic fishes exhibiting triangular, posteriorly-tapering anal fins (low PC1) and all other habitat groups possessing more rectangular or rounded anal fins (Figure 3.11 B; Table 3.2). Interestingly, no relationship was discovered between anal fin PC1 and feeding mode. No relationships were detected between fin asymmetry and ecology. Furthermore, no significant pair-wise morphological differences were discovered between any other feeding or habitat groups, indicating that benthic grazers, predators of elusive prey and fishes that combine benthic grazing and planktivory are morphologically indistinguishable from one another, as are fishes that live in structured reef, open reef, seagrass bed, coastal bare bottom and open ocean demersal habitats.

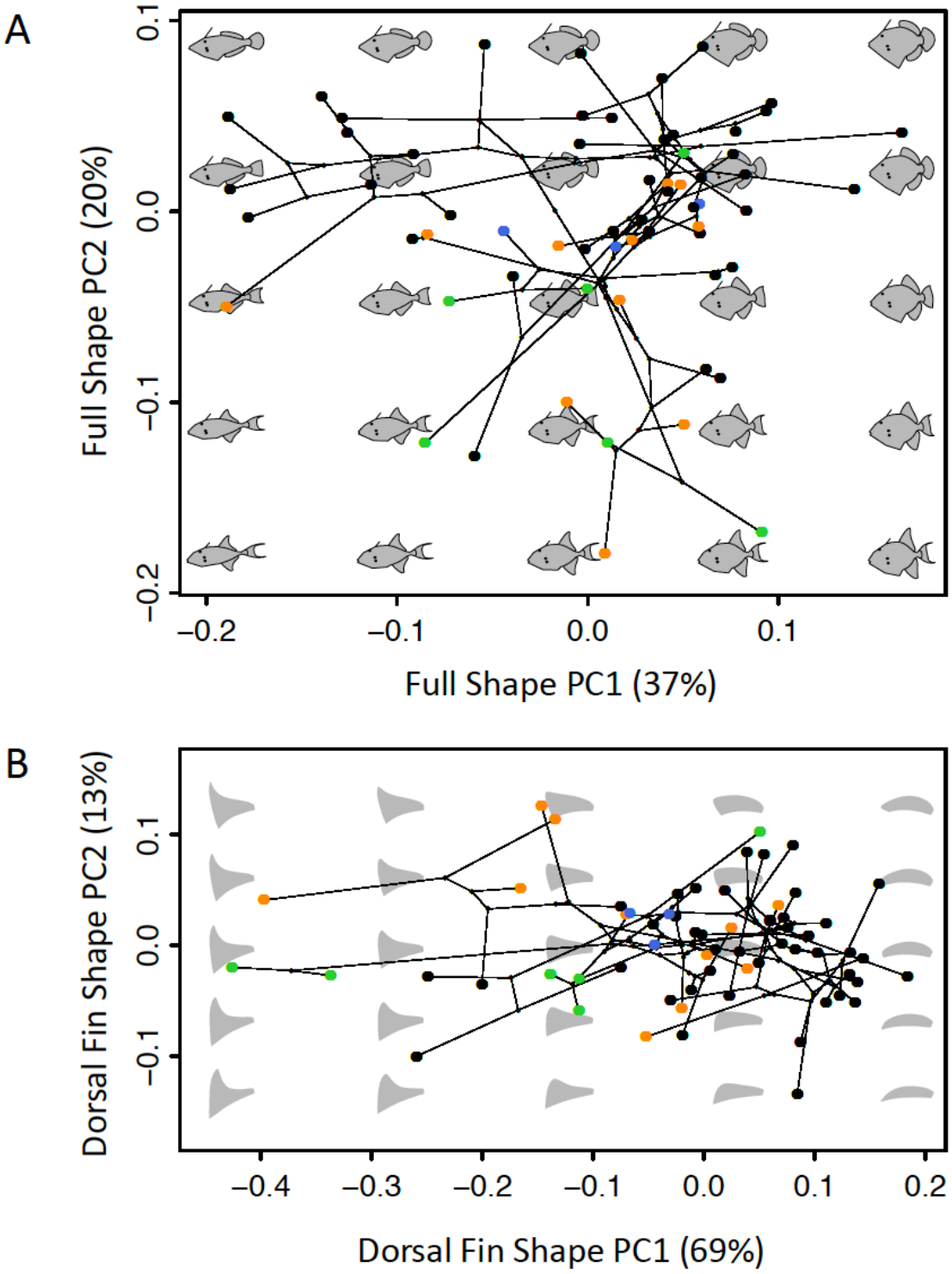

Figure 3.9. Relationships between balistoid morphology and feeding mode. Backtransformation phylomorphospace colored coded according to the feeding mode of each species with black indicating benthic grazers, orange indicating predators of elusive prey, blue representing mixed grazing and planktivory, and green representing planktivory. (A) Full shape. (B) Dorsal fin.

Table 3.2. Significant results of phylogenetic ANOVA ecomorphology pairwise t-test correlations.

Primary Ecology Group and Shape Axis	Significantly Different Ecology Groups	Significance (t/ P value)
Planktivory and Full Shape PC2	Benthic Grazers	-4.215/ 0.0288
Pelagic and Full Shape PC2	Structured Reef, Open Reef, Seagrass/ Weedy	-5.659/ 0.0030; -3.447/ 0.0377; -5.560 0.0224
Planktivory and log(Dorsal AR)	Benthic Grazer	4.771/ 0.0054
Pelagic and log(Dorsal AR)	Structured Reef, Open Reef, Seagrass/ Weedy	5.450/ 0.0015; 3.842/ 0.0091; 6.210/ 0.0015
Planktivory and log(Dorsal PC1)	Benthic Grazer	4.367/ 0.0246
Pelagic and log(Dorsal PC1)	Structured Reef, Open Reef, Seagrass/ Weedy	5.248/ 0.006; 3.727/ 0.0084; 6.121 / 0.0104
Planktivory and log(Anal Fin AR)	Benthic Grazer	5.039/ 0.0060
Pelagic and log(Anal Fin AR)	Coastal Bare Bottom, Demersal, Structured Reef, Open Reef, Seagrass/ Weedy	4.806/ 0.0198 5.579/ 0.0072 5.932/ 0.0015; 4.638/ 0.0026; 7.072/ 0.0015
Pelagic and Anal Fin PC1	Coastal Bare Bottom, Demersal, Structured Reef, Open Reef, Seagrass/ Weedy	-5.064/ 0.0143 -5.805/ 0.0048 -5.839/ 0.0015 -4.652/ 0.0015 -7.167/ 0.0026

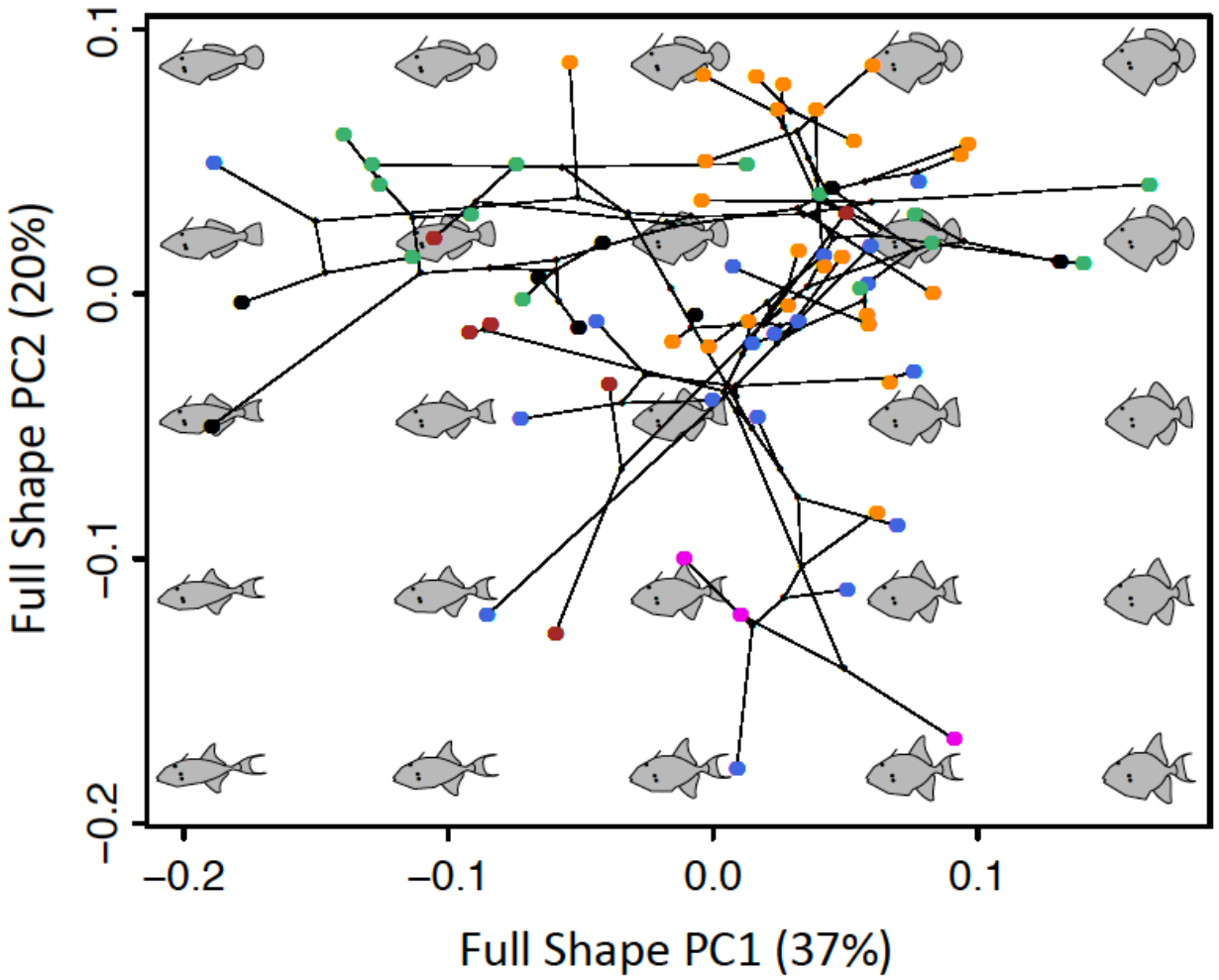

Figure 3.10. Relationships between balistoid full shape morphology and habitat use. Backtransformation phylomorphospace colored coded according to the primary habitat of each species with orange indicating structured reef, blue indicating open reef, green indicating seagrass/ weedy, black indicating open ocean demersal, brown indicating coastal bare bottom, and pink indicating open ocean pelagic.

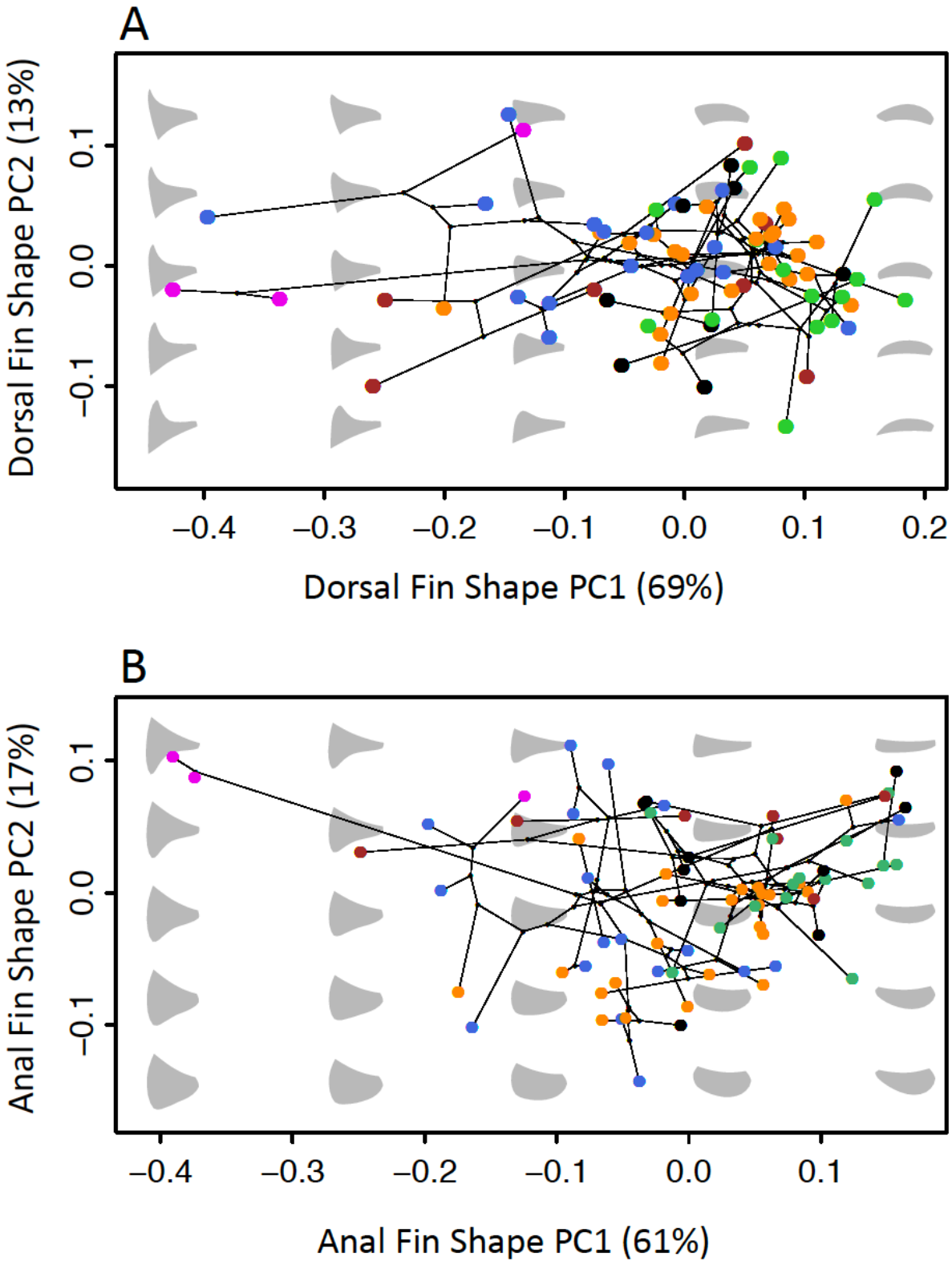

Figure 3.11 continued on page 88.

Figure 3.11. Relationships between balistoid median fin morphology and habitat use. Backtransformation phylomorphospace colored coded according to the primary habitat of each species with orange indicating structured reef, blue indicating open reef, green indicating seagrass/ weedy, black indicating open ocean demersal, brown indicating coastal bare bottom, and pink indicating open ocean pelagic. (A) Dorsal fin shape. (B) Anal fin shape.

Discussion

Balistoid fishes exhibit a wide range of body morphologies from deep bodied to elongate forms, possess dorsal and anal fins that vary in aspect ratio by nearly an order of magnitude, and caudal fins that range from shallow and convex to deep and forked. Every morphological unit tested (body, dorsal fin, anal fin, and caudal fin) displayed evolutionary integration with every other unit along primary pPLS covariation axes, and the dorsal and anal fins exhibited especially high integration. Despite this strong evolutionary integration, balistoid dorsal and anal fins are asymmetrical in most balistoid fishes, with triggerfishes, on average, displaying higher levels of fin asymmetry than filefishes. Species generally cluster by family in morphospace, however each morphological unit examined (full shape, body, dorsal fin, anal fin, and caudal fin) also exhibits regions of morphospace with substantial overlap of species from both families. Triggerfishes tend to have higher aspect ratio dorsal, anal and caudal fins than filefishes, but multiple species from both families exhibit high, medium and low aspect ratio dorsal and anal fins, demonstrating the high level of convergence in these traits.

The diversity of balistoid fin and body shapes is reflected in their habitat and feeding ecologies. Phylogenetic morphometric analysis supports the hypothesis that high aspect ratio dorsal and anal fins are associated with planktivorous diets and pelagic habitats. These ecomorphological relationships are congruent with biomechanical predictions from swimming tests in which high aspect ratio balistoid fins are shown to be associated with increased endurance

swimming performance (George and Westneat 2019). Both planktivory and pelagic habitats present these fishes with the challenge of spending large amounts of time swimming in the open water. These strong ecomorphological relationships are concluded to be a central driver of the multiple evolutionary convergence events towards high aspect ratio dorsal and anal fins in the superfamily Balistoidea. However, many species with different habitat and feeding ecologies also inhabit overlapping regions of morphospace, demonstrating that balistoid fishes are capable of using a range of fin and body morphologies to feed on benthic and pelagic prey and inhabit most marine habitats.

Patterns of Morphological Evolution

Fishes in the superfamily Balistoidea are quite morphologically diverse and exhibit high levels of evolutionary morphological integration among all measured fin and body regions, supporting the previously reported pattern of morphological integration among triggerfishes (Dornburg et al. 2011), and expanding this trend to include filefishes. The full shape dataset revealed that triggerfishes and filefishes appear to have diversified along different major axes of morphological variation, with filefishes (Monacanthidae) spanning the full range of length-depth ratios (PC1) and triggerfishes (Balistidae) spanning nearly the full range of fin aspect ratios (PC2), while exhibiting conserved, intermediate length-depth ratios. Balistoid families show the largest degree of dissimilarity in their caudal fin shapes, with triggerfishes possessing deep, high aspect ratio tail fins (low PC2) and filefishes possessing elongate, low aspect ratio tail fins. The majority of species in both families possess convex caudal fins (Low PC1), with only a few members of each family possessing truncate or forked tail fins. However, when examining a combined PC1-PC2 caudal fin morphospace, there is virtually no overlap between families. The differences in caudal fin shape

appear to be a result of a morphological divergence event very shortly after the Balistidae-Monacanthidae split followed by conserved caudal fin aspect ratio evolution within each family. The triggerfish common ancestor likely possessed a high AR caudal fin, and the majority of extant triggerfishes have maintained relatively high AR caudal fins, with only one species (*Pseudobalistes naufragium*) exhibiting a low AR. In contrast, the filefish common ancestor likely had a low or medium AR caudal fin, and all measured extant filefishes still exhibit one of these two states, with no high or very high AR tail fins found within the monacanthids.

Members of both families overlap considerably in dorsal and anal fin morphospace, with the majority of species possessing low to medium aspect ratio fins (mid to high PC1 scores). Although triggerfish species exhibit the highest AR dorsal and anal fins, a couple filefish species (*Paramonacanthus oblongus* and *Paramonacanthus sulcatus*) have diverged from their low AR relatives to occupy areas of high AR morphospace. Dorsal and anal fin shapes are highly integrated and tend to nearly mirror each other, yet perfect symmetry in both the positioning and shape of these median fins is rare within balistoid fishes. The highly integrated nature of the dorsal and anal fins is likely a result of their reliance on coordinated fin motions between the two fins to power steady balistiform swimming (Dornburg et al. 2011), and this biomechanical coupling makes their asymmetry unusual. Perfect symmetry is quite common in other paired propulsors, such as fish pectoral fins and vertebrate wings, largely because pectoral fins and wings lie across the evolutionarily conserved, bilaterally symmetrical left-right plane of these organisms. Deviations from symmetry of paired locomotor appendages cause uneven thrust generation and shifts in the centers of lift and drag away from the center of mass, resulting in increased roll and yaw around the body axis and reduced turning performance (Swaddle and Witter 1998; Thomas 1993). In fact, bilateral aspect ratio symmetry is thought to be so conserved in fishes that power locomotion with

paired pectoral fins that comparative morphology and performance studies can reliably measure the aspect ratio of one pectoral fin and confidently assume that the other pectoral fin displays the same aspect ratio (Denny 2005; C. J. Fulton and Bellwood 2004; Martinez, Rohlf, and Frisk 2016). Likewise, bird and bat wing aspect ratios are typically calculated using a single wing-tip to wing-tip span measurement to encompass both fins, highlighting the well-supported assumption of symmetry in these paired bilateral propulsors (Norberg and Lighthill 1981; Savile 1957).

The paired propulsors utilized by balistoid fishes, on the other hand, lie across the dorsal-ventral axis of the body, an axis much less likely to allow for perfect symmetry in these bilaterally symmetrical organisms. In this system, the anal fin is bounded anteriorly by the position of the anus, while the dorsal fin is free to move as far forward as the back of the head. Consequently, balistoid anal fins tend to possess fewer fin rays, be slightly shorter, and be positioned slightly posteriorly compared to the dorsal fins. Thus, the finding that only 43% of the 175 balistoid individuals examined exhibited equal dorsal and anal fin aspect ratios could be regarded as a high degree of symmetry when considered in the broader evolutionary context of dorsal-ventral asymmetry across vertebrate body plans. However, from a functional perspective, this paired-propulsor asymmetry places balistoid fishes in a hydrodynamic situation quite unlike the symmetrical pectoral fin system of labriform swimmers or the paired flight wing system of birds, bats and even insects. The asymmetry of positioning and shape of most balistoid dorsal and anal fins sets up a biomechanical paired-propulsor system that likely requires slightly different dorsal and anal fin kinematics to avoid constant pitch and roll about the center of mass. Interestingly, no relationships were detected between fin asymmetry and ecology, indicating that fin asymmetry does not appear to hinder or improve balistoid fishes' abilities to successfully occupy the full range of this superfamily's set of habitats and feeding modes. These findings suggest that future balistoid

swimming kinematics studies should focus on detailed examination and comparison of dorsal and anal fin kinematics to determine how balistoid fishes compensate for this asymmetry.

Ancestral state estimations also reveal high levels of convergence in dorsal and anal fin aspect ratios as well as widespread convergence on highly asymmetrical fins, both within and between families. Triggerfishes likely evolved from a common ancestor with moderately asymmetrical, high AR dorsal and anal fins and exhibit many independent convergence events towards medium and low AR fins, while filefishes likely evolved from a common ancestor with fairly symmetrical, low AR fins and exhibit multiple convergence events onto medium and high AR fins. These fin morphology transitions are likely accompanied by changes in fin kinematics during steady swimming, as balistoid fishes are known to lie on a kinematic continuum from highly undulatory, wave-like dorsal and anal fin kinematics in low AR fins to highly oscillatory, flapping dorsal and anal fin kinematics in high AR fins. The multiple evolutionary events towards highly asymmetrical fins in fishes possessing both high and low aspect ratio fins suggest that balistoid species are able to overcome instabilities introduced by fin asymmetries regardless of whether they use undulatory or oscillatory fin kinematic strategies. The combination of fin shape and fin kinematics is also likely to affect the maneuverability of balistoid fishes with low AR, undulatory fins providing a strong maneuverability advantage over high AR, flapping fins.

Evolutionary Ecomorphology

Many past studies have hypothesized ecomorphological relationships between balistoid fin shapes and ecology (Dornburg et al. 2011; George and Westneat 2019; Wright 2000), largely based on relationships between fin aspect ratios and swimming performance. In this study, comparative methods revealed that offshore, pelagic and planktivorous fishes have higher AR, more

posteriorly-tapering dorsal and anal fins than species with other habitat and feeding mode ecologies. Additionally, the full shape dataset revealed that these pelagic and planktivorous fishes tend to possess concave, high AR caudal fins, in addition to their high AR dorsal and anal fins. However, no significant relationships were discovered between habitat use or feeding mode and caudal fin shape alone. The relationships between high AR fins and pelagic and planktivorous fishes support the strong biomechanical correlation between high AR fins and increased balistoid endurance swimming performance required for successful occupation of these ecotypes. Finally, almost all fishes living in structured reef environments possess long dorsal spines (high full shape PC2) and deep ventral keels (low shape PC1), mobile elements that likely allow these fishes to safely lock themselves into cervices in their structurally complex habitats (Figure 3.10).

Other ecomorphological hypotheses were not supported by the results of this study. Reef-associated fishes that swim above or around the reefs (open reef habitat group) were predicted to exhibit high AR fins similar to pelagic fishes, but this hypothesis was not supported. In fact, these open reef fishes were statistically indistinguishable from the structured reef habitat group, or any other habitat groups for that matter. On the other end of the spectrum, it was predicted that fishes in the structured reef habitat group would exhibit lower AR median fins than fishes in other habitat groups, as low AR median fins would likely facilitate fast bursts of speed required to escape predators. Fishes that included elusive prey, such as cephalopods or other fishes, in their diets were also predicted to possess low AR caudal fins to facilitate quick bursts of speed to catch their prey. Neither of these hypotheses were supported by the data, largely because some species from nearly every habitat and feeding group possess low aspect ratio fins, with the exception of the offshore pelagic group.

Extensive morphological convergence towards low aspect ratio dorsal and anal fins suggests some functional and ecological advantage of low AR fins. Low AR fins may simply be uncorrelated with specific balistoid habitat or feeding groups. This explanation is supported by the fact that at least one member from every feeding and habitat group except for offshore pelagic fishes possesses low AR dorsal and anal fins. Even one planktivorous filefish species *Paramonacanthus filicauda* possesses low AR dorsal and anal fins. This trend suggests that low AR fins are highly versatile in a number of ecological contexts. Considering that low AR fins are often associated with increased maneuverability and likely improve the backwards swimming performance of balistoid fishes, these low AR fins could be beneficial for life in a variety of habitats and for successful capture of a variety of prey items. Furthermore, many balistoid fishes across a variety of habitats exhibit mating and parental care behaviors that involve a high degree of maneuverability such as swimming in tight circles with their competitors (Kawase and Nakazono 1996), constructing nests (Fricke 1980; Gladstone 1994) and physically guarding and tending to benthic eggs (Fricke 1980; Ishihara and Kuwamura 1996; Kawase 2003; Kawase and Nakazono 1995; Nakazono and Kawase 1993), behaviors likely facilitated by low AR fins. Notably, many open reef and planktivorous fishes exhibit some form of these mating and parental care behaviors, which may explain the low AR fins in these species despite their water column use. Although the kinematics of these behaviors have not been studied in detail, future research on relationships between morphology and mating and parental care behaviors may help elucidate the high number of convergence events on low AR dorsal and anal fins.

Alternatively, assigning each species to a single habitat and feeding group could overshadow more minute differences in the ecologies of these fishes. As more quantified diet data become available, future studies may be able to assess specific relationships between diet

composition and morphology using PLS methods (Olsen 2017; Wilson et al. 2020). For example, a quantitative habitat study revealed that wrasses with low aspect ratio pectoral fins are associated with sheltered reef areas, while high aspect ratio fins were associated with high wave energy areas (C.J Fulton, Bellwood, and Wainwright 2001). Finally, the present study is limited to 80 out of about 148 described balistoid species due to the current state of balistoid phylogenetic sampling. As new phylogenetic tools improve our ability to resolve phylogenetic relationships and increase taxonomic coverage, additional species can be added to these analyses to reveal new ecomorphological relationships among these fascinating and charismatic marine fishes.

CHAPTER FOUR: THREE-DIMENSIONAL KINEMATIC ANALYSES REVEAL ASYMMETRIES IN *XANTHICHTHYS AUROMARGINATUS* MEDIAN FIN BIOMECHANICS DURING STEADY BALISTIFORM SWIMMING

Abstract

Many animals achieve locomotion through highly coordinated, symmetrical biomechanical motions between pairs of morphologically symmetrical appendages. Other organisms, such as triggerfishes and filefishes in the superfamily Balistoidea, rely on coordination of multiple morphologically asymmetrical appendages to power locomotion, and the biomechanics of these asymmetrical paired-propulsor systems remain poorly understood. In this study, I use a three-camera high-speed video system to describe and contrast the biomechanics of gilded triggerfish, *Xanthichthys auromarginatus*, high aspect ratio dorsal and anal fin kinematics during steady balistiform swimming. I hypothesized that the morphological asymmetries observed between *X. auromarginatus* dorsal and anal fins would result in biomechanical asymmetries between these fins during steady swimming. Specifically, I predicted that the longer, higher aspect ratio dorsal fins would exhibit higher fin ray amplitudes and provide greater propulsive thrust than the shorter, lower aspect ratio anal fins. The results revealed that dorsal and anal fin rays exhibit coordinated, yet significantly different kinematics both along and between the median fins, with the leading edge fin rays providing nearly half of the total propulsive effort. All dorsal and anal fin rays oscillate from left to right with the same frequency, but nearly all other studied kinematic traits differ between fin rays. The morphologically larger dorsal fins exhibit higher amplitude fin ray undulations, lower wave speeds, lower wave lengths, and provide an overall greater percentage of total propulsive effort than the anal fins. Given that *X. auromarginatus* possess some of the most

morphologically symmetrical median fins among balistoid fishes, our results suggest that the dorsal and anal fin biomechanical asymmetries observed in this species are likely applicable across a wide range of balistoid fin morphologies, challenging the long-standing assumption of symmetrical median fin biomechanics in balistoid fishes.

Introduction

Animals have evolved a wide array of locomotor modes to traverse terrestrial, aerial, and aquatic environments. Many organisms achieve forward locomotion by passing lateral body bending waves along their bodies from anterior to posterior in undulatory locomotor modes. This type of locomotion is common in fishes and limbless organisms such as snakes, caecilians, and a variety of terrestrial and aquatic invertebrate species. Most other locomotor modes involve some degree of coordination between multiple locomotor appendages such as the fore- and hind- limbs of most tetrapods (reviewed in Biewener 2003), the wings of birds (Tobalske 2007; Savile 1957), bats (Norberg 1981) and insects (Dudley 2000), and the pectoral fins of batoids (Rosenberger 2001) and wrasses (Walker and Westneat 2002; Aiello et al. 2019). In most cases, the appendages involved in these types of locomotion are paired and symmetrical in morphology and positioning across the sagittal (left-right) body axis. The symmetry of these paired appendages allows, and typically even requires, symmetrical and coordinated movements in the left and right appendages in order to achieve straight, forward movement. In fact, when paired locomotor wings lack morphological symmetry, they tend to experience instabilities such as roll and yaw (Swaddle and Witter 1998; Thomas 1993). Most of our knowledge about biomechanical consequences of asymmetrical paired appendages is based on experimental studies focusing on developmental

abnormalities (Swaddle and Witter 1998) or experimentally induced asymmetries (Thomas 1993), while natural examples of asymmetrical paired locomotor appendages remain largely unexplored.

Fishes in the order Tetraodontiformes have evolved a number of biomechanically distinct swimming modes that rely on coordination between multiple asymmetrical appendages including balistiform (Blake 1978; George and Westneat 2019), diodontiform (Arreola and Westneat 1996; Wiktorowicz, Lauritzen, and Gordon 2010), tetraodontiform (Plaut and Chen 2003) and ostraciiform (Hove et al. 2001) locomotion. The dorsal and anal fin-powered balistiform locomotor mode presents a particularly exciting opportunity to study how organisms use morphologically asymmetrical locomotor appendages to achieve steady forward locomotion because the triggerfishes and filefishes that use balistiform locomotion possess dorsal and anal fins of various anatomical, morphological and positional asymmetries (George, Chapter 3). Only about 40% of balistoid species exhibit dorsal and anal fins of the same aspect ratio, and on average, balistoid fishes possess dorsal fins of longer lengths, lower angles of attachment and more anterior starting positions compared to their anal fins (George, Chapter 3).

Despite these morphological median fin disparities, only one study to date has compared dorsal and anal fin kinematics of triggerfish swimming (Blake 1978). This study found that dorsal fin power output was greater than anal fin power output and that wave speed (the speed at which the undulatory wave moves anterior to posterior along the fins) was faster along the dorsal fin than along the anal fin during steady swimming of the triggerfish *Rhinecanthus aculeatus*. *Rhinecanthus aculeatus* possesses fairly asymmetrical dorsal and anal fin morphologies compared to other balistoid fishes (George and Westneat 2019; Loofbourrow 2009), suggesting that asymmetries in balistoid dorsal and anal fin shapes may indeed lead to asymmetries in median fin biomechanics. However this study (Blake 1978) filmed with only one camera at 64 frames s^{-1}, so

it is unlikely that the dorsal and anal fin data were collected during the same swimming sequence simultaneously, and no statistical analyses were conducted, so it remains unclear if the described differences in dorsal and anal fin biomechanics are significant. Conversely, a field biomechanics study on ocean sunfish, *Mola mola*, swimming found that these fishes synchronously flap their morphologically symmetrical, very high aspect ratio (~2 - 4), stiff dorsal and anal fins at the same frequency to generate the lift that powers their steady forward swimming (Watanabe and Sato 2008). This study also found that despite morphological and positional asymmetries in the ocean sunfish dorsal and anal fin muscles, the muscles exhibit identical masses and likely produce equal power during steady swimming. All other balistiform locomotion biomechanics studies have focused on describing balistoid dorsal fin leading edge kinematics across multiple swimming speeds (Wright 2000; Korsmeyer, Steffensen, and Herskin 2002; Loofbourrow 2009), and have assumed that anal fins and posterior fin rays produce approximately equal thrust.

In this paper, I use three synchronized high-speed video cameras to conduct detailed three-dimensional kinematic analyses of the dorsal and anal fins of the gilded triggerfish, *Xanthichthys auromarginatus*, during steady swimming. The primary objectives of this study are (1) to describe the detailed undulatory dorsal and anal fin kinematics of steady balistiform locomotion including characterization of fin-ray-specific changes in kinematics and wave parameters along the anterior-posterior length of each fin, and (2) to determine how asymmetries in dorsal and anal fin anatomies, morphologies and positionings translate to differences in fin biomechanics and relative thrust contributions during steady swimming. The gilded triggerfish is an ideal species for this study due to its high endurance swimming performance, high gait transition speed, and high aspect ratio, posteriorly tapering dorsal and anal fins (George and Westneat 2019; Wright 2000). The high gait transition speed allows for analysis of steady balistiform swimming biomechanics at a relatively

fast swimming speed, and the vastly different lengths of anterior and posterior median fin rays allow for interesting comparisons of fin ray-specific kinematics along the lengths of the median fins. Furthermore, although *X. auromarginatus* actually possesses fairly symmetrical dorsal and anal fin shapes compared to other balistoid species, the dorsal fins of this species are longer, larger, higher in aspect ratio and contain more fin rays than the anal fins (George, Chapter 3), suggesting that dorsal and anal fin biomechanics are unlikely to be symmetrical. In this study, I test the hypotheses that (1) fin ray amplitude and thrust production decrease from anterior to posterior along both median fins due to their posteriorly tapering shapes, and (2) the dorsal fin contributes more propulsive effort (thrust) than the anal fin due to the larger size and higher aspect ratio of the dorsal fin. Alternatively, it is possible that the combination of size, shape, position and angle of attachment asymmetries between the dorsal and anal fins actually serve to cancel out any biomechanical inequalities and destabilizing forces produced around the center of mass that I would predict from any one of these metrics and ultimately allow for symmetrical and synchronous median fin kinematics during steady balistiform swimming.

Materials and Methods

Fish Specimen Selection, Care and Anatomical Preparation

Three gilded triggerfish, *Xanthichthys auromarginatus* (Bennett 1832), specimens were purchased through aquarium suppliers for steady swimming kinematics experiments. All specimens were post-juveniles and similar in size, ranging from 11.5 – 12.0 cm in total length (TL), allowing for direct comparisons between specimen-specific swimming kinematics. The specimens used in the present study are just slightly larger than *X. auromarginatus* specimens used in endurance

swimming performance studies (mean: 9.23 cm TL) (George and Westneat 2019), allowing for interpretation of swimming kinematics results in the context of endurance swimming performance.

All specimens were fed a diet of freeze-dried krill, frozen algae, and frozen shrimp and housed in separate tanks connected through a 1200 L saltwater flow-through system. The aquarium housing tanks were maintained on a 12 hour light-dark cycle. The artificial seawater in this system was maintained at a temperature of 24±1°C, specific gravity of 1.024±0.001 and pH of 8.3±0.1. All fishes were deprived of food for 24 h before swimming tests in order to control for metabolism (Alsop and Wood 1997) as in George and Westneat (2019). All animal care and use protocols were approved by University of Chicago IACUC 72365.

Several specimens were dissected after euthanasia for study of the dorsal and anal fin structures, and the muscles that serve the fins. Images were recorded of whole fresh specimens by Mark Westneat, using fin pinning, dilute preservation to set the fin positions, and water tank photography, using a Sony RX10 SLR digital camera as well as a Leica stereomicroscope with digital camera. The skin was removed from the posterior half of the body between the dorsal and anal fins to record the epaxial and hypaxial body musculature and the small, superficial, fin inclinator muscles. The deep dorsal and anal fin erector and depressor muscles were exposed by removing the overlying axial muscle and connective tissue and imaging the main actuators of the propulsive fins.

Swimming Kinematics Experiments

All swimming kinematics tests were conducted in a custom built flow tank with a working section of 25 cm x 33 cm x 104 cm. A plexiglass partition was constructed to further restrict the fishes to a 30.5 cm x 20 cm x 30.5 cm working section that served as the filming area. All water parameters

of the flow tank system were consistent with those to those of the housing tanks. In order to elicit natural swimming behaviors, the fish were acclimated to the flow tank for at least 2 hours prior to filming. During the acclimation period, the flow was set to 6 cm sec^{-1} (~ 0.5 TL s^{-1}). Following acclimation, the flow speed was gradually increased in 0.5 TL s^{-1} increments approximately every 15 - 25 min to a maximum of 4 TL s^{-1}. In the present study, only swimming kinematics at the 2 TL s^{-1} swimming speed are analyzed and described. Flow speed was controlled in real-time using a Höntzsch Instruments flow sensing probe (HFA serial no: 843, Waiblingen, Germany) as in George and Westneat (2019).

During these swimming experiments, the fish were filmed at 500 frames s^{-1} with three time-synchronized Photron high-speed video cameras (Models: FASTCAM APX-RS, FASTCAM SA7, and Mini UX 100; Photron, San Diego, CA, USA). The cameras were orientated with one camera capturing a lateral view directly, one camera capturing a dorsal (top-down) view through a 45 degree mirror above the flow tank, and one camera capturing a ventral view (bottom up) through a 45 degree mirror below the flow tank. The lateral view provided a view of the full left side of the body including the dorsal and anal fins, while the dorsal view provided a view of the dorsal fin, and the ventral view provided a view of the anal fin. In order to capture clear video from the dorsal view without interference of ripples at the surface of the water, a floating glass "boat" was constructed, placed in the water, and tightly wedged above the working section between the mirror and the fish. Each camera was connected to a laptop with Photron FastCam video software that allowed for real-time viewing of each camera angle. All cameras were endlessly recording and constantly storing 8 - 10 seconds of video internally, until simultaneously triggered using a wired trigger system to stop recording and save the previous 8 - 10 seconds of footage. The cameras were triggered and video sequences were saved when the fish was recorded swimming steadily away

from all lateral, top and bottom walls of the flow tank for at least 5 consecutive dorsal and anal fin undulations. Following swimming trials, each specimen was returned to its housing tank, and the cameras were calibrated for three-dimensional video analysis.

Swimming Kinematics Analysis

The cameras were calibrated after each swimming trial by filming a custom, laminated 7 x 5 checkerboard grid composed of 10.16 mm x 10.16 mm squares moving throughout the entire flow tank working section at various angles. Eight distinct shapes were drawn around the clear, laminated margins of this grid in order to calibrate the directly-opposing dorsal and ventral camera views. The three-dimensional working section space was then calibrated using the *calibrateCameras* function in the R package *StereoMoprh* (Olsen and Westneat 2015). This function automatically calibrates the 3-dimensional space between the lateral and dorsal views and the lateral and ventral views using the checkerboard, and the dorsal-ventral views are calibrated by manually digitizing dozens of shapes along the laminated margins of the checkerboard in the dorsal and ventral views. Videos were not analyzed unless the mean point-to-point error between each view was less than 0.5 mm (mean: 0.10 mm, range: 0.066 - 0.239 mm).

Following calibration, 1 steady swimming video segment containing 5 – 6 full, consecutive dorsal and anal fin beat cycles at a swimming speed of 2 TL s^{-1} (24 cm s^{-1}) was selected for each individual for kinematics analysis. Video sequences in which fish were maneuvering throughout the working section were not analyzed in this study, but a brief description of the variety of swimming behaviors observed is reported. Video frames were extracted as PNGs using the *extract_frames* function in the *DeepLabCut* Python package (Mathis et al. 2018). Next, one full fin beat for each individual was manually digitized in *StereoMorph* at 125 frames per second

(every 4th frames) for use as a training dataset in the *DeepLabCut* auto-digitization program. A total of 23 landmarks were placed along the fish fins and bodies at each frame in at least two camera views each. As the fish did not tend to swim at a perfectly vertically oriented angle to the bottom of the tank, it was important to establish a midline along the sagittal (left-right) body axis. This was accomplished by digitizing the bases of the following dorsal and anal fin rays: ray 1, ray 5, ray 10, ray 15, ray 20, and the last fin ray in addition to the base of dorsal fin ray 25. In order to comprehensively analyze and describe the fin kinematics of *X. auromarginatus* during steady swimming, the tips of the following dorsal and anal fin rays were also digitized: leading edge, ray 10, ray 15, and ray 20.

Following the manual training set digitization, *DeepLabCut* was used to auto-digitize the remaining 4 -5 fin beats of each specimen at 250 frames per second. Due to the high level of required digitization accuracy of this study, each auto-digitized landmark was then manually checked and corrected using *StereoMorph* if necessary. Once all landmarks were placed in each camera view, the 3D coordinates of each landmark were calculated using the *reconstructStereoSets* function in *StereoMorph*. Next, the *alignLandmarksToMidline StereoMorph* function was used to align the 3D landmark coordinates to each fish's sagittal plane (left-right body axis). Then the 3D coordinates from each frame were rotated around the aligned left-right axis in order to align the landmarks along the frontal (anterior-posterior) and transverse (dorsal-ventral) body axes. This rotation was accomplished by using custom R code to align the base of each third dorsal fin ray with the base of each first anal fin ray, based on morphometric data from chapter three of this thesis.

Once the 3D coordinates were aligned to each fish's body axes, the following kinematics parameters were extracted for each digitized dorsal and anal fin ray: left and right frequency, left

and right lateral excursion amplitude through time, lateral velocity through time, and lateral acceleration through time. Additionally, dorsal and anal fin wave speed was calculated at multiple points along the anterior-posterior axis using the equation:

$$wave\ speed = \frac{\Delta x}{\Delta t}$$

where *x* is the position of maximum amplitude along the anterior-posterior body axis (mm) and *t* is the time (ms) at which maximum amplitude is reached. Wavelength was also calculated at multiple points along the dorsal and anal fins using the equation:

$$wavelength = \frac{wave\ speed}{wave\ frequency}$$

where *wave speed* is the speed of the wave (m s^{-1}) along the fin and *wave frequency* (Hz) is the average fin ray frequency of all fin rays along the fin. Wave speed and wavelength were both calculated at the following positions along the dorsal and anal fins: leading edge ray to ray 10, ray 10 to ray 15, and leading edge ray to ray 15. The leading edge ray to ray 15 measurements (*full wavelength* and *full wave speed*) serves as a generalized measurement for the whole fin for these wave terms. Next, the number of waves along each fin at one time was calculated using the equation:

$$number\ of\ waves = \frac{fin\ length}{full\ wavelength}$$

where *fin length* is the length of each fin. Finally, in order to estimate the relative propulsive contribution of each fin ray, fin ray efforts were calculated for each fin beat using the equation:

$$Fin\ Ray\ Effort = Fin\ Ray\ Amplitude \times Fin\ Ray\ Frequency$$

following the methods of Feilich (2017). In order to calculate fin ray effort for every fin beat individually, fin ray frequency for each beat was set to the mean of the two frequency

measurements made immediately before and after the time of each amplitude measurement. Total fin efforts were calculated for each dorsal and anal fin beat by adding up the individual fin ray efforts for each fin. Relative fin ray and whole fin efforts were then calculated using these measurements. Fin ray effort was then doubled and divided by swimming speed to calculate the Strouhal number (Sr) of each fin ray. All of these kinematic metrics were calculated for the left and the right side of the dorsal and anal fin waves separately to examine any left-right biomechanical asymmetries, with subsequent analyses including both left and right values.

Fin Ray Trajectory Shape Analyses

By overlaying all of the positions in three-dimensional space that a fin ray occupies during each fin beat, a 3D shape can be constructed to represent the trajectory of that fin ray, and these shapes can be analyzed using geometric morphometric statistical analyses (Aiello et al. 2019) to compare the trajectories of each fin ray. The 3D trajectory shape of each dorsal and anal fin ray tip (rays 10, 15, 20 and leading edge) was traced as it made its way from the midline to the maximum left amplitude, to the maximum right amplitude, and back to the midline for 4 consecutive fin beats for each individual. The trajectory shapes of anal fin ray 20 for one specimen were detected as outliers, so the anal and dorsal fin ray 20 trajectories from that individual were not included in subsequent analyses. This resulted in 12 trajectory shapes each for the dorsal fin leading edge tip, the anal fin leading edge tip, dorsal fin ray 10, anal fin ray 10, dorsal fin ray 15, and anal fin ray 15, and 8 trajectory shapes each for dorsal fin ray 20 and anal fin ray 20, for a total of 88 shapes. As the frequency of each fin ray was not identical during every fin beat for every individual, the raw fin ray trajectory shapes contained differing numbers of landmarks and were subsampled down to each include 40 landmarks. Fin ray three-dimensional coordinates were

smoothed using a cubic spline function prior to subsampling. Coordinates along each axis (transverse, sagittal, and frontal planes) were smoothed independently. The smoothed anal fin trajectory shapes were then flipped over the dorsal-ventral body axis so that they could be accurately aligned with the dorsal fin trajectory shapes.

All fin ray trajectory shapes were then Procrustes aligned using the *gpagen* function in the R package *geomorph* (Adams et al. 2017) to remove the effects of translation, rotation and scaling. Principal components analyses (PCA) were then conducted on the Procrustes-aligned fin ray trajectory shapes using the *PlotTangentSpace* function in *geomorph* in order to determine the primary axes of variation between the shapes. The primary axes of shape variation (PCs 1 and 2) were visualized using three-dimensional warp grids and a series of two-dimensional backtransformation morphospace plots (MacLeod 2009; Olsen 2017).

Statistical Analyses

Biomechanical hypotheses were tested using pair-wise t-tests between pairs of fin kinematics variables. Prior to statistical hypothesis testing, suspected outliers in each dataset were evaluated using the *rosnerTest* function in the *EnvStats* R package (Millard 2013), and detected outliers were removed. First, differences in fin kinematic properties between individuals were tested. Then, the fin kinematics properties from the three individual specimens were combined for further statistical analyses. Differences between right and left fin ray frequencies, lateral amplitudes, lateral velocities, and phase lags as well as whole fin wavelengths and wave speeds were examined. Then, all left and right kinematic parameters were combined for subsequent statistical analyses. Next, differences in kinematics properties along the dorsal and anal fins were tested using pairwise t-tests between all pairs of fin ray on the same fin. Linear regressions were also conducted between

fin ray kinematic variables and the average anterior-posterior position of each fin ray of the dorsal and anal fins separately. Then differences between dorsal and anal fin kinematics were inspected using t-tests between complementary pairs of fin rays (ex: dorsal fin leading edge vs. anal fin leading edge) as well as between whole-fin metrics including wavelengths, wave speeds and the number of waves on each fin. Finally, pair-wise t-tests were conducted between the primary principal component scores (PCs 1 and 2) of the three-dimensional fin ray trajectory shapes, both along each fin and between the dorsal and anal fins. P-values were adjusted for use in multiple tests by controlling for false discover rate using the Benjamini–Hochberg (BH) method (Benjamini and Hochberg 1995) implemented through the *p.adjust* function in R. P-values from the kinematic variable statistical tests (n = 122) were adjusted separately from shape trajectory analyses p-values (n = 14). Results were considered significant when BH-adjusted p values were less than 0.05. All statistical analyses were performed using R software version 3.3.2 (R Core Team 2016).

Results

Fin Morphology

The dorsal and anal fins of *Xanthichthys auromarginatus* are quite morphologically symmetrical, with the base of the first fin rays positioned just posterior to the body midpoint, and the dorsal fin originating slightly forward of the anal fin (Figure 4.1 A). The aspect ratios of *Xanthichthys auromarginatus* dorsal and anal fins are relatively high (1.05 and 0.95, respectively) and the fins taper from long leading edge rays to shorter trailing edge rays. The superficial fin inclinator muscles are greatly reduced, and the epaxial and hypaxial body musculature is a predominantly pale whitish color with a pink central band of muscle fibers, faintly similar to bands of darker muscle along the midline found in other lineages of fishes (Figure 4.1 B). The main muscles

powering the dorsal and anal fins are the paired erector and depressor muscles, positioned deep to the epaxial and hypaxial musculature (Figure 4.1 C). Each fin ray is powered by 4 of these deep muscles, an anterior erector and posterior depressor on each side. These muscles originate centrally on the pterygiophores supporting the fins and on the vertical septum connecting the neural spines, and insert via tendons attaching to small, bony, lateral processes on the bases of each fin ray.

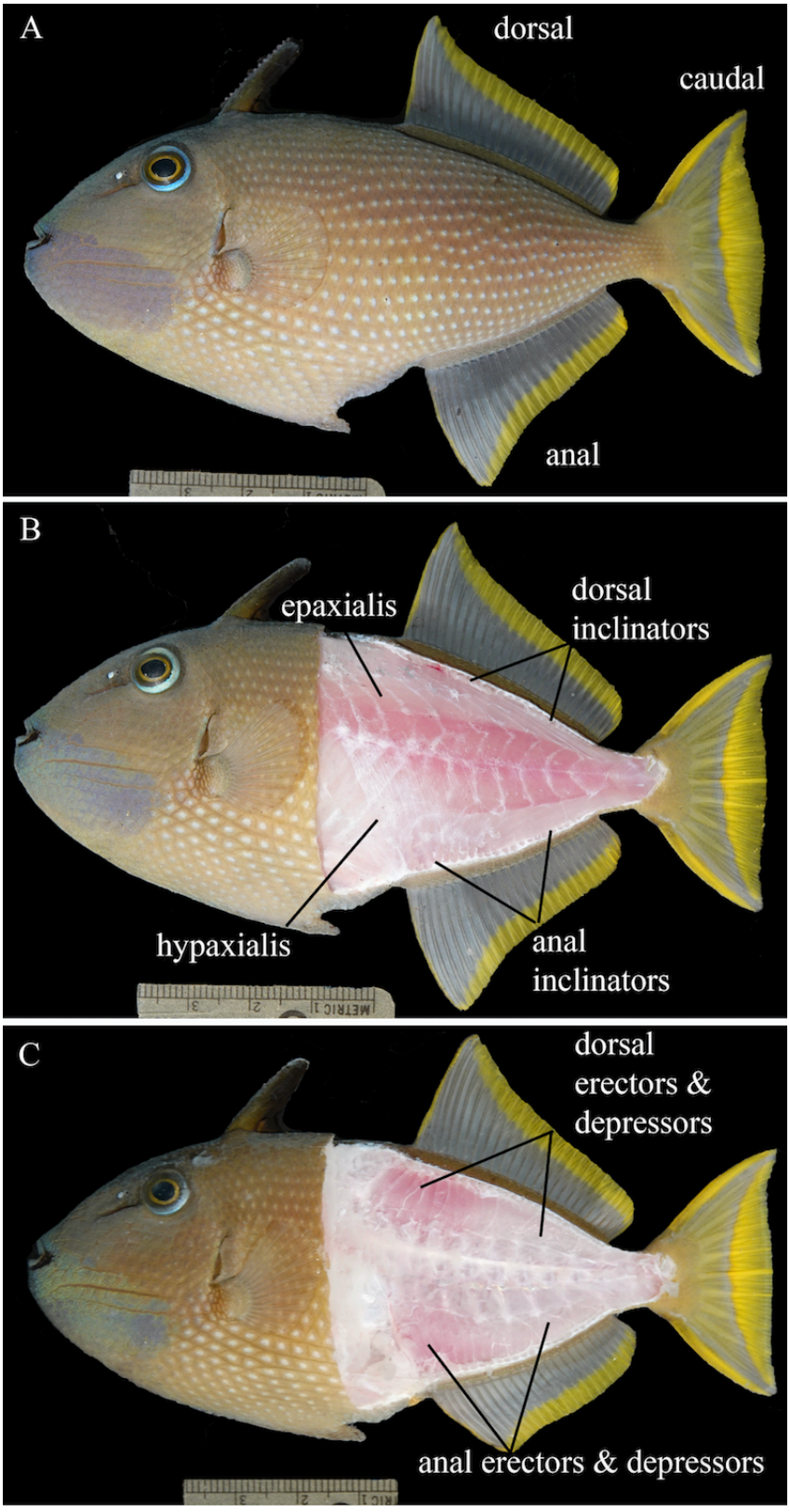

Figure 4.1 continued on page 111.

Figure 4.1. Morphology and locomotor muscle anatomy of *Xanthichthys auromarginatus*. (A) Full body and fin morphology. (B) Skin and connective tissue are removed to reveal superficial epaxial and hypaxial body musculature used to power body/ caudal fin locomotion at high speeds. Small dorsal and anal fin inclinator muscles are also visible. (C) Epaxial and hypaxial muscles are removed to reveal the large, medial dorsal and anal fin erector and depressor muscles used to power balistiform locomotion. Photos provided by Mark Westneat.

Median Fin Kinematics

All three *Xanthichthys auromarginatus* specimens in this study powered steady forward locomotion at 2 total lengths (TL) s^{-1} by undulating sinusoidal waves along their dorsal and anal fins with no contribution from the caudal fin. All studied fin rays along the dorsal and anal fins undulated across the sagittal plane of the fish with the same frequency (mean: 4.38 Hz, SD: 0.49). However, maximum fin ray lateral excursion amplitudes varied significantly both between and along the dorsal and anal fins (Table 4.1, Figure 4.2). Specifically, dorsal and anal fin ray maximum amplitudes decreased from anterior to posterior along each fin ($P = 0.0213$, multiple $R^2 = 0.983$; $P = 0.0298$, multiple $R^2 = 0.975$ for the dorsal and anal fin respectively) (Figure 4.3 A). Additionally, all dorsal fin rays exhibited higher amplitude lateral excursions than their complementary anal fin rays ($t = 3.604$, $df = 52.8$, $P = 0.00207$; $t = 3.916$, $df = 51.8$, $P = 0.000897$; $t = 2.982$, $df = 38.7$, $P = 0.0137$ fin rays 10, 15 and 20, respectively), except for the leading edge fin rays ($t = 0.990$, $df = 52.1$, $P = 0.494$) (Figure 4.3 A). Fin ray lateral velocities showed similar trends to amplitudes, with maximum fin ray velocity decreasing along the anterior-posterior axis ($P = 0.0466$, multiple $R^2 = 0.958$; $P = 0.0323$, multiple $R^2 = 0.973$ for the dorsal and anal fins, respectively) and dorsal fin rays exhibiting faster maximum velocities than their anal fin counterparts ($t = 4.186$, $df = 49.37$, $P = 0.000431$; $t = 6.886$, $df = 49.65$, $P = 4.961 \times 10^{-8}$; $t = 6.141$, $df = 41.39$, $P = 0.000313$; for rays 10, 15 and 20, respectively), with the exception of the leading edge fin rays ($t = 1.798$, $df = 51.239$, $P = 0.153$). Maximum fin ray velocities were achieved as the

fin rays crossed the midline of the body, and minimum fin ray velocities were reached at the point of maximum fin ray amplitude (Figure 4.3 B). Anal fin rays lagged behind their complementary dorsal fin rays by an average of 4.14 s, 8.29 s, 4.83 s, and 7.86 s for the leading edge, ray 10, ray 15, and ray 20, respectively (Figure 4.3 A).

Table 4.1. *Xanthichthys auromarginatus* dorsal and anal fin kinematics

Fin/ Fin Ray	**Frequency (Hz)**	**Lateral Amplitude (mm)**	**Propulsive Effort (mm s^{-1}/ Percent Full Effort)**
Anal Fin Leading Edge	4.40 ± 0.51	15.89 ± 2.63	68.70 ± 6.47 (22.70 ± 1.49)
Dorsal Fin Leading Edge	4.39 ± 0.47	16.53 ± 2.16	72.0 ± 9.69 (23.80 ± 4.03)
Anal Fin Ray 10	4.41 ± 0.48	8.53 ± 1.54	36.84 ± 4.43 (12.17 ± 0.72)
Dorsal Fin Ray 10	4.42 ± 0.45	10.14 ± 1.80	44.41 ± 8.03 (14.67 ± 0.83)
Anal Fin Ray 15	4.37 ± 0.53	5.01 ± 1.34	21.44 ± 4.49 (7.08 ± 1.07)
Dorsal Fin Ray 15	4.35 ± 0.48	6.64 ± 1.80	28.82 ± 8.37 (9.52 ± 1.89)
Anal Fin Ray 20	4.40 ± 0.55	3.02 ± 0.78	12.81 ± 3.90 (4.23 ± 1.88)
Dorsal Fin Ray 20	4.30 ± 0.47	4.06 ± 1.67	17.58 ± 7.98 (5.81 ± 2.83)
Full Anal Fin	4.39 ± 0.51	8.13 ± 5.19	139.99 ± 12.55 (46.50 ± 3.73)
Full Dorsal Fin	4.37 ± 0.46	9.32 ± 5.03	163.13 ± 32.26 (53.50 ± 3.73)

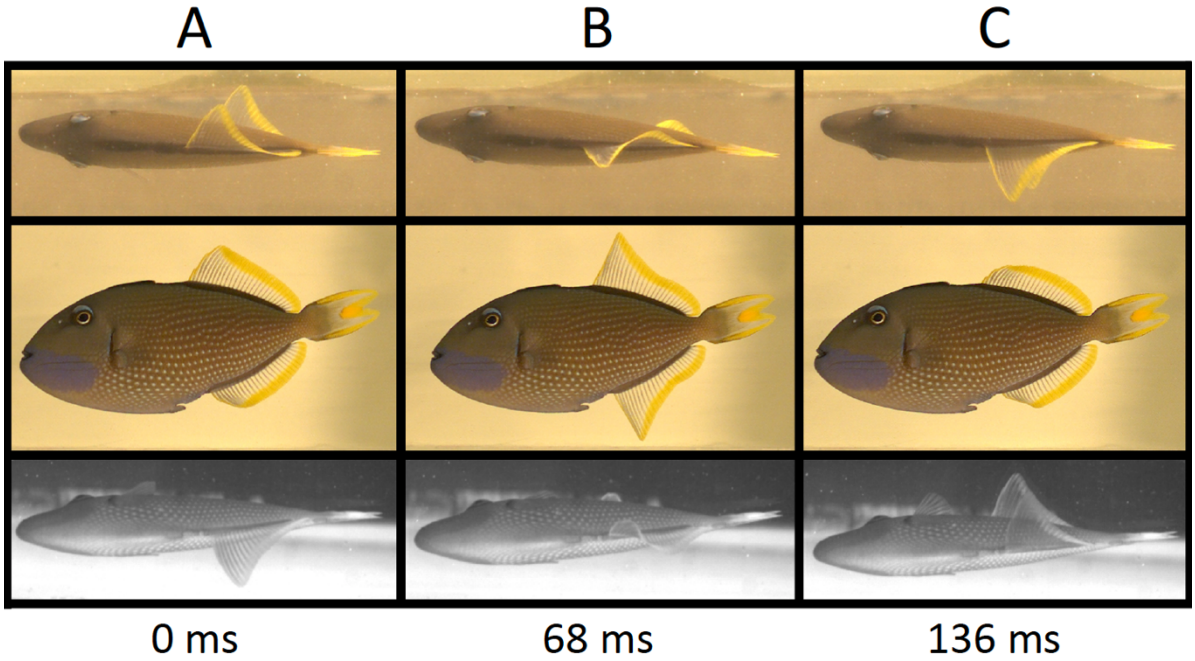

Figure 4.2. Representative *Xanthichthys auromarginatus* dorsal and anal fin wave sequences. (A) Time of maximum dorsal fin leading edge left amplitude. (B) Fin waves as the leading edges cross the midline. (C) Time of maximum dorsal fin leading edge right amplitude.

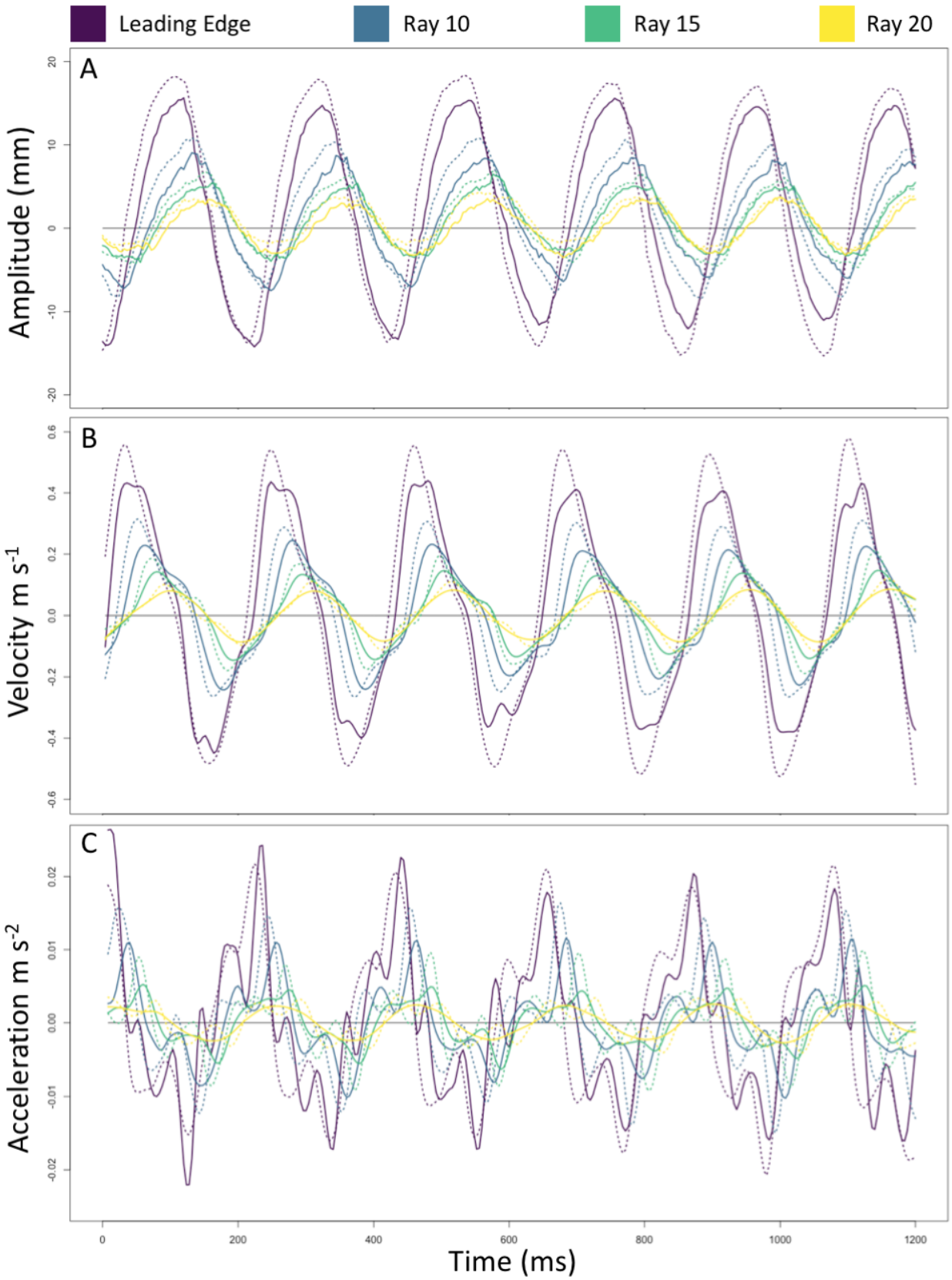

Figure 4.3 continued on Page 114.

Figure 4.3. Dorsal and anal fin ray lateral amplitudes, velocities and accelerations through time. Fin rays are colored by position along the anterior-posterior axis with leading edge rays in purple, tenth fin rays in blue, fifteenth fin rays in green, and twentieth fin rays in yellow. Anal fin rays are represented by solid lines, and dorsal fin rays are represented by dotted lines. All plots are based on data from one *Xanthichthys auromarginatus* individual. (A) Fin ray amplitudes through time. (B) Fin ray velocities through time. (C) Fin ray accelerations through time.

The gilded triggerfish also exhibited differences in fin wave properties between and along the dorsal and anal fins (Table 4.2). The undulatory wave moved faster along the full length of the anal fin (mean: 0.28 m s^{-1}, SD: 0.042) than along the full length of the dorsal fin (mean: 0.23 m s^{-1}, SD: 0.049) ($t = 3.89$, $df = 48.0$, $P = 0.00100$). Wave speed also increased significantly from anterior (mean: 0.25 m s^{-1}; 0.18 m s^{-1}, for the anal and dorsal fins, respectively) to posterior (mean: 0.33 m s^{-1}; 0.28 m s^{-1} for the anal and dorsal fins, respectively) along both the anal ($t = 3.74$, $df = 36.5$, $P = 0.00195$) and dorsal ($t = 6.35$, $df = 48.2$, $P = 3.50 \times 10^{-7}$) fins. The median fins showed similar trends in regards to wavelengths, with the anal fin (mean: 73.6 mm, SD: 24.2) exhibiting a larger average wavelength along the fin than the dorsal fin (mean: 51.9 mm, SD: 8.3) ($t = 4.41$, $df = 32.3$, $P = 0.000409$). Wavelength also increased from anterior to posterior along the median fins ($t = 3.99$, $df = 35.3$, $P = 0.00101$; $t = 6.13$, $df = 45.5$, $P = 8.823 \times 10^{-7}$ for the anal and dorsal fins, respectively). Consequently, the median fins showed significant differences in the number of waves along the fin at any given time, with the dorsal fin exhibiting a significantly higher number of waves (mean: 0.64, SD: 0.068) than the anal fin (mean: 0.43, SD: 0.062) ($t = 5.70$, $df = 9.9$, $P = 0.000713$).

Table 4.2. *Xanthichthys auromarginatus* dorsal and anal fin wave parameters

Fin / Position	Wave Speed (m s^{-1})	Wavelength (mm)
Anterior Anal Fin	0.251 ± 0.056	57.6 ± 12.0
Anterior Dorsal Fin	0.18 ± 0.060	41.3 ± 14.6
Posterior Anal Fin	0.33 ± 0.095	77.5 ± 21.5
Posterior Dorsal Fin	0.28 ± 0.049	62.9 ± 10.6
Full Anal Fin	0.28 ± 0.042	73.6 ± 24.2
Full Dorsal Fin	0.23 ± 0.049	51.9 ± 8.3

In order to compare the relative thrust contributions of each fin ray and whole fin, propulsive effort was calculated for each dorsal and anal fin ray examined in this study. The average total effort of all fin rays combined was 303 mm s^{-1}. Fin ray effort decreased along the anterior-posterior axis of the fins ($P = 0.0215$, multiple $R^2 = 0.98$; $P = 0.0298$ multiple $R^2 = 0.98$ for the dorsal and anal fins, respectively) with the leading edge dorsal and anal fin rays each making up about 23% of the total effort, and twentieth fin rays each making up about 5% of the total effort (Table 4.1). All dorsal fin rays produced higher efforts than their paired anal fin rays ($t = 4.36$, $df = 42.0$, $P = 0.000322$; $t = 4.19$, $df = 42.8$, $P = 0.000495$; $t = 2.83$, $df = 39.2$, $P = 0.0193$ for rays 10, 15, and 20, respectively), except the leading edge rays ($t = 1.51$, $df = 47.1$, $P = 0.244$). Consequentially, the dorsal fin produced a larger total effort (mean: 163 mm s^{-1}, 54%) than the anal fin (140 mm s^{-1}, 46%). The Strouhal numbers based on the average amplitudes and frequencies along the fins were 0.34and 0.28 for the dorsal and anal fins, respectively. When calculated based on leading edge kinematics alone, the Strouhal numbers were 0.60 and 0.58 for the dorsal and anal fins, respectively. No differences were detected between dorsal and anal fin Reynolds numbers ($t = 2.36$, $df = 3.1$, $P = 0.09509$), with means of 8,954 and 7,988 for the dorsal and anal fins, respectively.

Xanthichthys auromarginatus displayed differences in fin ray trajectory shapes, both along and between the dorsal and anal fins across all three body axes (Figures 4.3 - 4.7). All fin rays

followed *U-shaped* fin beat trajectories in frontal planes of the body, with dorsal-ventral depth of the *U* and lateral excursion amplitude decreasing from anterior to posterior fin rays (Figure 4.5). Leading edge fin ray trajectories formed wide *figure-eight* shapes in transverse planes of the body, while more posterior fin rays trajectories showed a decrease in *figure-eight* width along the anterior-posterior axis with some of the most posterior rays following oval-shaped trajectories (Figure 4.6). This shows that anterior fin rays cover a larger range of anterior-posterior positions during a fin beat than posterior fin rays. Along sagittal planes, the fin ray tips made one dorsal-ventrally elongate oval shape on each side of the body (Figure 4.7).

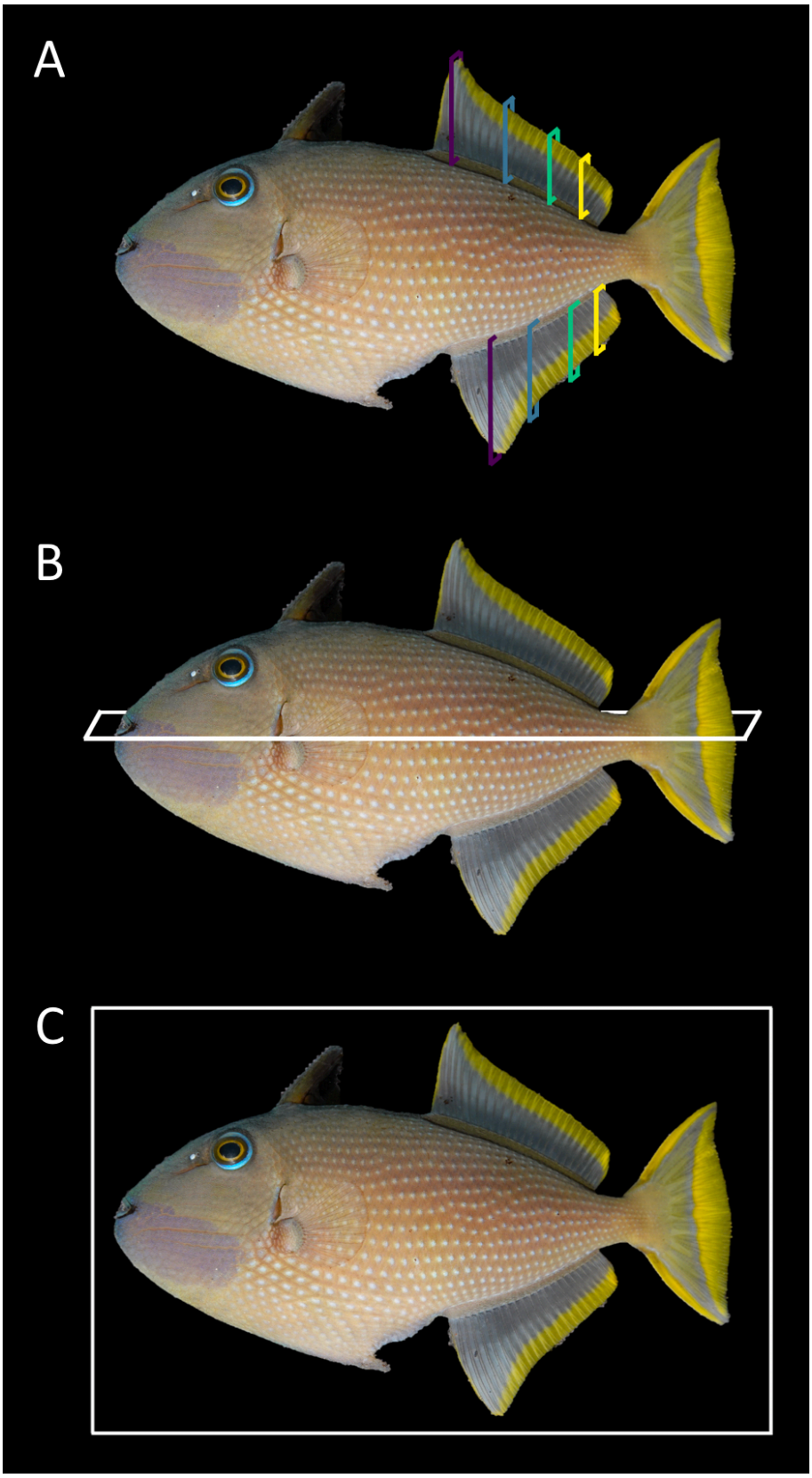

Figure 4.4 continued on page 118.

Figure 4.4. *Xanthichthys auromargninatus* anatomical fin and body planes.
(A) Frontal planes. (B) The transverse plane. (C) The sagittal plane. The colored lines in panel A depict the 8 independent frontal planes depicted in Figure 4.5 with purple lines representing leading edge fin ray planes, blue lines representing tenth fin ray planes, green lines representing fifteenth fin ray planes, and yellow lines representing twentieth fin ray planes. The white lines in panels B and C depict the orientations of the transverse and sagittal body planes depicted in Figures 4.6 and 4.7, respectively.

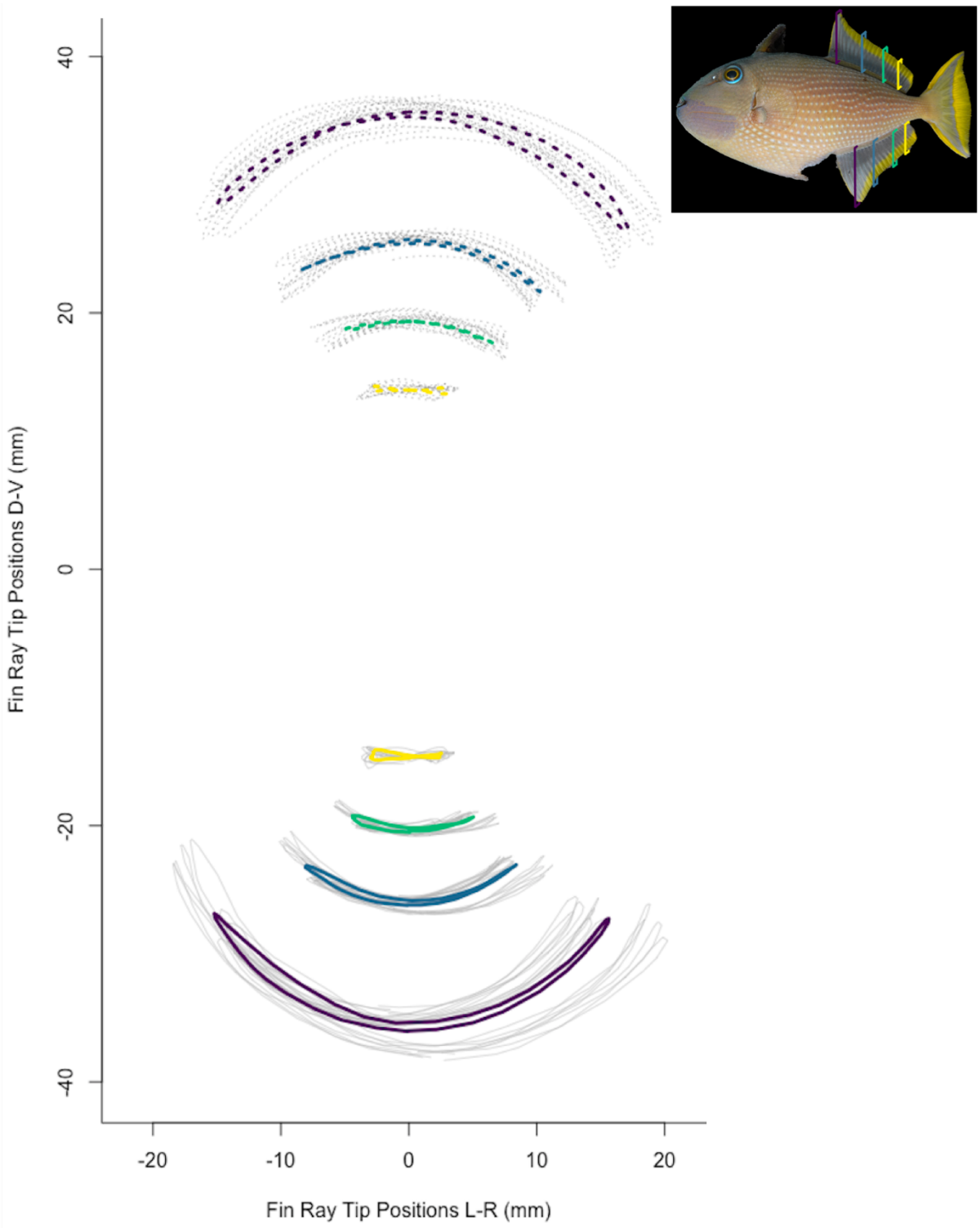

Figure 4.5. Dorsal and anal fin ray tip *U* shaped trajectories in frontal body planes.
Gray lines in the background depict individual fin beat trajectories of each fin dorsal and anal fin ray tip, and average fin ray trajectories for each fin ray are color-coded as in Figure 4.3, with leading edge rays in purple, tenth rays in blue, fifteenth rays in green, and twentieth rays in yellow. Solid lines represent anal fin rays and dotted lines represent dorsal fin rays.

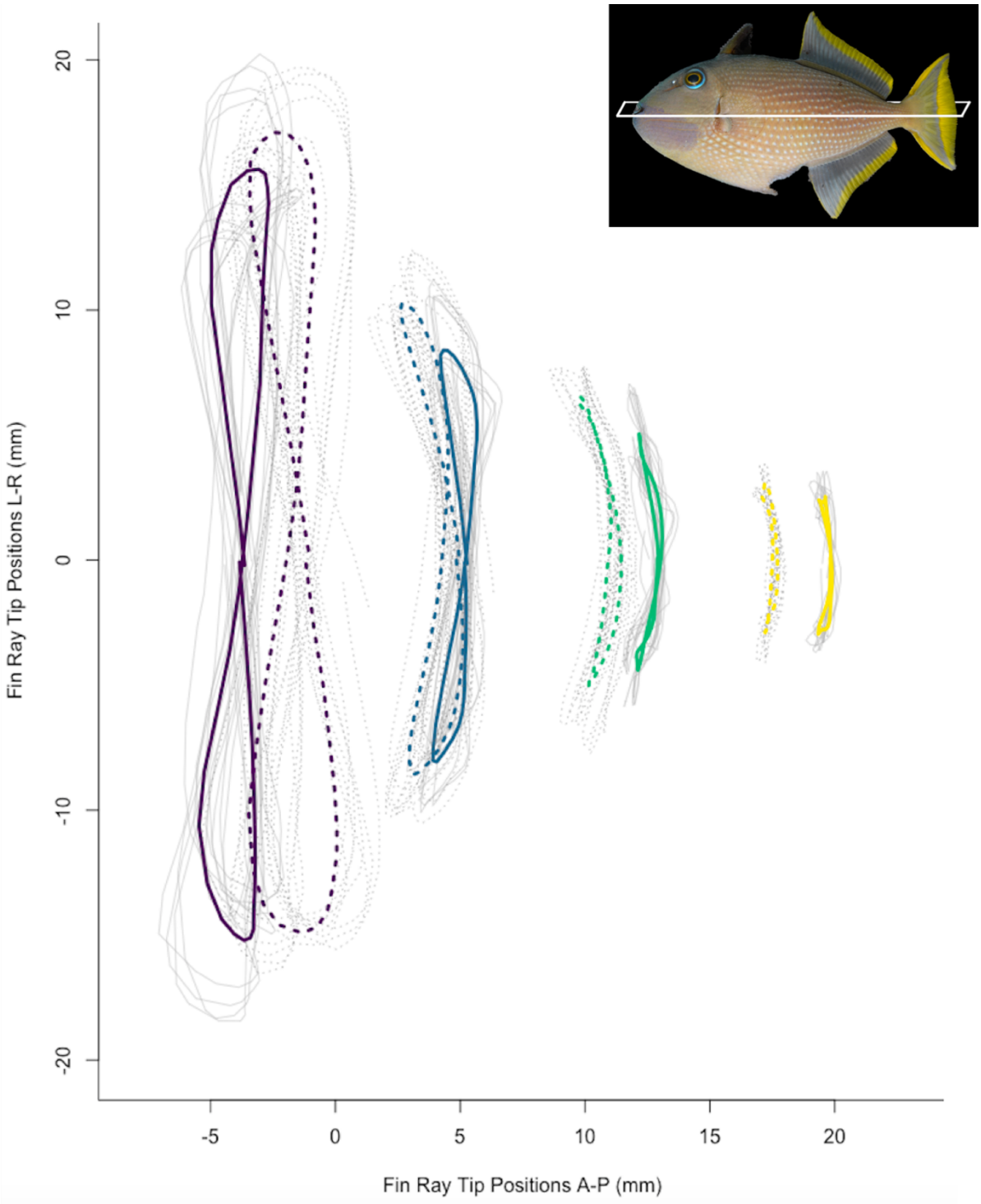

Figure 4.6. Dorsal and anal fin ray tip *figure-eight* trajectories in the transverse body plane. Gray lines in the background depict individual fin beat trajectories of each fin dorsal and anal fin ray tip, and average fin ray trajectories for each fin ray are color-coded as in Figure 4.3, with leading edge rays in purple, tenth rays in blue, fifteenth rays in green, and twentieth rays in yellow. Solid lines represent anal fin rays and dotted lines represent dorsal fin rays.

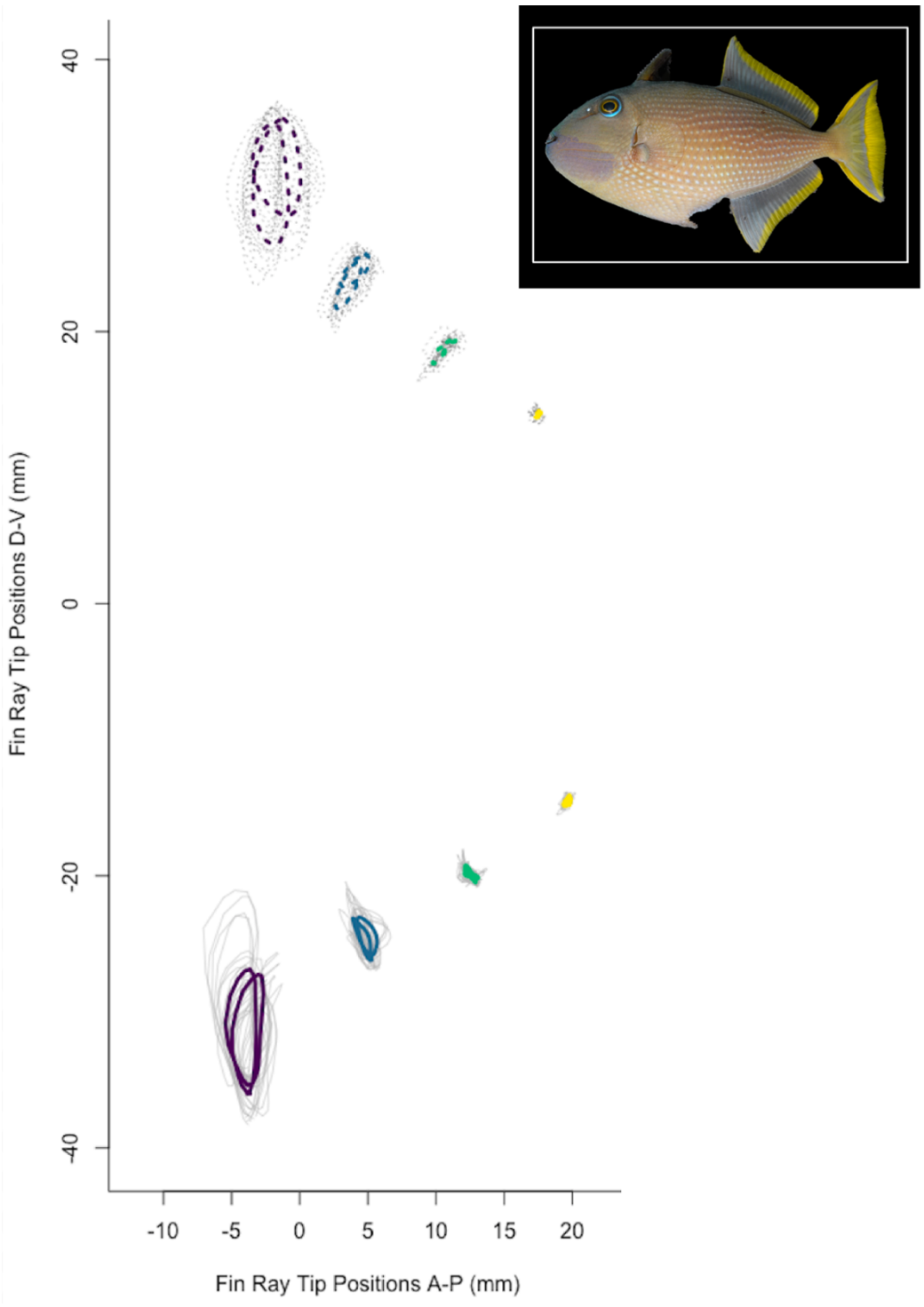

Figure 4.7. Dorsal and anal fin ray tip *double-oval* trajectories in the sagittal body plane. Gray lines in the background depict individual fin beat trajectories of each fin dorsal and anal fin ray tip, and average fin ray trajectories for each fin ray are color-coded as in Figure 4.3, with leading edge rays in purple, tenth rays in blue, fifteenth rays in green, and twentieth rays in yellow. Solid lines represent anal fin rays and dotted lines represent dorsal fin rays.

The significance of these differences in fin ray trajectory shapes between and along fins was assessed using principal components analyses of the Procrustes-aligned three-dimensional shapes. In order to visualize shape changes associated with variation along each major principal component (PC) axis, the 3D PC scores of each fin ray trajectory shape were projected into a series of two-dimensional backtransformation morphospaces (Figure 4.8). Despite considerable overlap in fin ray trajectory morphospace, dorsal fin ray trajectories differed from anal fin ray trajectories along PC1 ($t = 2.45$, $df = 77.1$, $P = 0.0291$). Dorsal fins rays tend to occupy the area of low PC1 morphospace defined by fin ray trajectories that are deeper along the dorsal-ventral axis while the fin ray moves away from the body and shallower during the return stroke (Figure 4.7 A). Conversely, anal fin rays tend to lie on the right side of PC1 morphospace, defined by dorsal-ventrally deep power strokes and shallow return strokes (Figure 4.7 A). Additionally, all fin ray positions (when dorsal and anal fin ray pairs are grouped together) exhibit significantly different trajectory shapes along PC2 (see Table 4.3 for statistical significance of pairwise relationships). The anterior fin rays occupy low PC2 morphospace defined by deep dorsal-ventral U-shaped excursions along the frontal plane (Figure 4.8 A) and rounded *figure-eight* shapes along the transverse body plane (Figure 4.8 B). Conversely, posterior fin rays occupy regions of high PC2 morphospace defined by shallow dorsal-ventral dips along the frontal plane (Figure 4.8 A) and bow-tie shaped trajectories along the transverse body plane (Figure 4.8 B). It should be noted that additional hydrodynamically important differences in fin ray tip shape trajectories including scaling and orientation are not recovered in these geometric morphometric shape analyses because the Procrustes-alignment process removes variation due to size and rotation of the shapes.

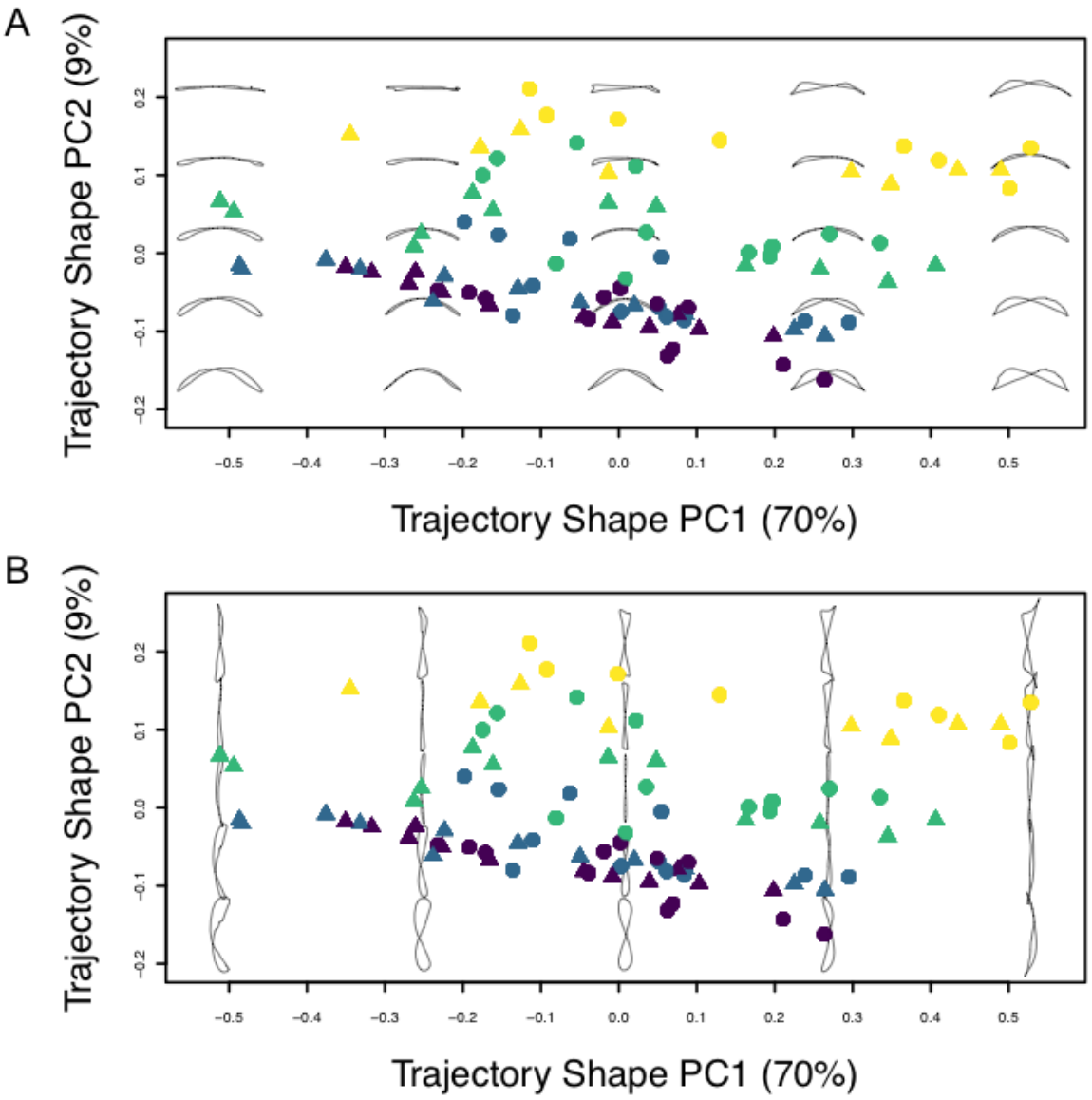

Figure. 4.8. Dorsal and anal fin ray tip trajectory shape backtransformation morphospaces. Principal component scores from three-dimensional shape analyses are projected into two two-dimensional backtransformation morphospaces for visualization. (A) Backtransformation morphospace along the frontal body plane. (B) Backtransformation morphospace along the transverse plane. In both panels, gray shapes in the background represent theoretical fin ray trajectory shapes at each location in morphospace. Each point represents one full fin ray trajectory. Triangles repesent dorsal fin rays, and circles represent anal fin rays. Points are color-coded by fin ray position with leading edge rays in purple, tenth rays in blue, fifteenth rays in green, and twentieth rays in yellow.

Table 4.3. Significant results of three-dimensional fin ray trajectory shape pair-wise principal component scores t-tests.

Relationship	Principal Component Axis	T values	P values
All Dorsal Fin Rays vs All Anal Fin Rays	PC1	2.45	0.029
Leading Edge Fin Rays vs Twentieth Fin Rays	PC1	2.64	0.029
Tenth Fin Rays vs Twentieth Fin Rays	PC1	2.72	0.026
Leading Edge Fin Rays vs Tenth Fin Rays	PC2	2.41	0.031
Leading Edge Fin Rays vs Fifteenth Fin Rays	PC2	8.46	5.21×10^{-10}
Leading Edge Fin Rays vs Twentieth Fin Rays	PC2	17.80	1.08×10^{-17}
Tenth Fin Rays vs Fifteenth Fin Rays	PC2	6.14	5.78×10^{-7}
Tenth Fin Rays vs Twentieth Fin Rays	PC2	14.90	4.97×10^{-16}
Fifteenth Fin Rays vs Twentieth Fin Rays	PC2	7.32	3.26×10^{-8}

Discussion

Xanthichthys auromarginatus power steady forward swimming at 2 TL s^{-1} using coordinated dorsal and anal fins kinematics. Although all dorsal and anal fin rays undulated at the same frequency, nearly every other kinematic parameter differed both along and between the dorsal and anal fins. Anterior fin ray tip trajectories of both the dorsal and anal fins consisted of deep, high amplitude, high velocity, figure-eight shaped motions, while posterior fin ray tip trajectories consisted of shallow, low amplitude, low velocity, bow-tie shaped motions. Wave speeds and wavelengths increased anteriorly to posteriorly along both fins, with the anal fin exhibiting higher values than the dorsal fin for both of these wave parameters. The dorsal fin, on the other hand, exhibited a higher number of waves along the fins and higher fin ray amplitudes and velocities than the anal fin. Overall, the dorsal and anal fin leading edge rays contributed just under half of

the total propulsive effort, and the dorsal fin provided significantly higher propulsive effort than the anal fin.

Median Fin Kinematics Compared to Other Undulatory Fishes

The gilded triggerfish, *X. auromarginatus* possesses high aspect ratio (1.05), posteriorly tapering dorsal fins (George, Chapter 3) and displays dorsal fin kinematics comparable to those of other high aspect ratio triggerfishes and filefishes such as *Melichthys vidua, Odonus niger* and *Stephanolepis hispidus* (Wright 2000). Wright (2000) reported similar *X. auromarginatus* dorsal fin wavelengths, wave speeds and leading edge frequencies for specimens swimming at approximately 2 TL s^{-1} as those measured in the present study. However Wright (2000) found a smaller number of waves along the dorsal fin. Interestingly, the dorsal and anal fin Strouhal numbers measured as the average of all fin rays (0.34 and 0.28 for the dorsal and anal fins, respectively) fit well within the suggested optimal range of Strouhal number (0.24 – 0.35) (Triantafyllou, Triantafyllou, and Grosenbaugh 1993), while the Strouhal numbers measured at the leading edge alone (0.60 and 0.58 or the dorsal and anal fins, respectively) are well above this optimal range, suggesting that triggerfish median fin undulatory hydrodynamics may be more efficient than indicated by the leading edge alone as in Wright (2000).

Among the 11 balistoid species for which dorsal fin kinematic data at swimming speeds of approximately 2 TL s^{-1} exists, *X. auromarginatus* has the third slowest dorsal fin leading edge frequency (mean: 4.4 Hz), just faster than *O. niger* (mean: 3.6 Hz) and slightly slower than *M. vidua* and *S. hispidus* (mean: 4.5 Hz and 4.8 Hz, respectively) (Wright 2000; Korsmeyer, Steffensen, and Herskin 2002; Loofbourrow 2009). Leading edge frequencies of these 11 species (*Balistoides conspicillum, Balistapus undulatus, Cantherhines macrocerus, Melichthys niger, M.*

vidua, O. niger, Pseudobalistes fuscus, Rhinecanthus aculeatus, Sufflamen chrysopterum, S. hispidus, and *X. auromarginatus*) range from 2.7 Hz in *M. niger* to 8.2 Hz in *B. undulatus* with an average of 5.7 Hz (Wright 2000; Loofbourrow 2009). *Xanthichthys auromarginatus* has the second slowest dorsal fin wave speed (mean: 0.23 m s^{-1}) and fourth longest wavelength (52 mm) of these 11 species (mean: 0.29 m s^{-1} and 48 mm for balistoid species dorsal fin wave speed and wavelength, respectively) (Wright 2000; Loofbourrow 2009). Data on dorsal fin amplitudes during steady swimming only exist for one other species (*R. aculeatus*), and comparing these values reveals that *X. auromarginatus* uses much higher amplitude dorsal fin leading edge undulations (mean: 16.5 mm) than *R. aculeatus* (mean: ~10 mm) despite similar fish body sizes (Loofbourrow 2009). This difference is likely largely due to differences in *X. auromarginatus* and *R. aculeatus* dorsal fin morphologies, with *X. auromarginatus* possessing long, high aspect ratio dorsal fins with much longer leading edge fin rays compared to the short, rounded, medium aspect ratio dorsal fins of *R. aculeatus* (George, Chapter 3).

Kinematics of multiple fin rays along the anterior – posterior axis of the fin have only been studied in the dorsal fin of one other balistoid species, *M. niger* (Wright 2000). *Melichthys niger* dorsal fin rays exhibit the same pattern of high amplitude, figure-eight tip trajectories near the leading edge and low amplitude, more oval-shaped fin tip trajectories towards the trailing edge of the fin. *Melichthys niger* has an intermediate dorsal fin aspect ratio (0.66) compared to other balistoid species (George, Chapter 3), suggesting that the kinematic shape trajectory trends described in the present study may be applicable to all balistoid fishes with intermediate to high dorsal fin aspect ratios (0.66 - 1.05).

Notably, balistoid anal fin steady swimming biomechanics have only previously been studied in two species, *O. niger* and *R. aculeatus*, with results reported for *R. aculeatus* only (Blake

1978). This study found that the dorsal fin exhibits faster wave speeds than the anal fin at all swimming speeds in *R. aculeatus*, which is the opposite of the median fin wave speed relationship measured for *X. auromarginatus* in the present study. However, *R. aculeatus* dorsal fins were also reported to have higher power outputs (1.63×10^5 ergs s^{-1}) than anal fins (1.1×10^5 ergs s^{-1}) while swimming at 2.1 lengths s^{-1} (Blake 1978), indicating that the dorsal fin of *R. aculeatus* contributes a greater propulsive effort than the anal fin, following the same median fin propulsive effort relationship calculated for *X. auromarginatus* in the present study. Ultimately, the present study confirms that *X. auromarginatus* dorsal fin kinematics lie on the oscillatory (low frequency, high amplitude, long wave length) end of the undulatory-oscillatory balistiform locomotion kinematic continuum generally occupied by high aspect ratio median fins (Wright 2000). Furthermore, when examined in the context of other balistiform locomotion studies (Blake 1978; George Chapter 3), the results of the present study suggest that triggerfish dorsal fins may play a larger role in thrust production than anal fins across a wide range of median fin morphologies, from the fairly symmetrical, high aspect ratio, posteriorly tapering median fins of *X. auromarginatus* to the fairly asymmetrical, medium aspect ratio, rounded median fins of *R. aculeatus*.

A few other fish species swim using elongate undulatory fins, such as the dorsal fin-powered locomotion of the bowfin, *Amia calva*, (Jagnandan and Sanford 2013), and the anal fin powered locomotion of knifefishes (Youngerman, Flammang, and Lauder 2014; Ruiz-Torres et al. 2013; Shirgaonkar et al. 2008; Blake 1983). Studies of steady forward swimming in bowfin and knifefishes have revealed that these fishes power locomotion using highly undulatory fin kinematics with multiple full waves present along the fins at any given time (Youngerman, Flammang, and Lauder 2014; Ruiz-Torres et al. 2013; Shirgaonkar et al. 2008; Blake 1983; Jagnandan and Sanford 2013). Furthermore, studies that measured kinematic properties of multiple

fin rays found consistent undulatory kinematic properties (frequency, amplitude and wave speed) along the full length of bowfin and knifefish elongate fins at swimming speeds around 1 body length s^{-1} (Jagnandan and Sanford 2013; Ruiz-Torres et al. 2013). This pattern is quite unlike the kinematic pattern observed in triggerfishes *X. auromarginatus* (present study) and *M. niger* (Wright 2000), both of which display differences in fin ray kinematic parameters along their median fins. However, these kinematic differences may be easily explained by morphological differences between these species. Knifefishes and bowfin both power steady swimming with incredibly low aspect ratio median fins in which fin ray length remains relatively constant across upwards of 150 rays along the length of the fins. Conversely, *X. auromarginatus* and *M. niger* have fairly high aspect ratio median fins with much longer fin rays near the leading edges compared to the trailing edges (George Chapter 3). It is not surprising that the different morphologies of the anterior and posterior portions of these triggerfish fins would be associated with kinematic differences, while the morphologically similar leading and trailing edge fin rays of bowfin and knifefish median fins would be associated with similar kinematics. Many filefishes such as *Aluterus* and *Oxymonacanthus* species possess median fins that more closely resemble the elongate, rectangular, low aspect ratio fins of bowfin and knifefishes than the posteriorly tapering, high aspect ratio median fins of *X. auromarginatus* and *M. niger*. Consequently, these very low aspect ratio balistoid species likely possess median fin kinematics that more closely resemble the highly undulatory, anterior-posteriorly consistent kinematics of amiiform and gymnotiform fins than the more oscillatory, posteriorly changing kinematics of *X. auromarginatus.*

Hydrodynamics of Balistiform Swimming

Fishes experience and exert three-dimensional forces during steady swimming. In the dorsal – ventral axis, fishes must offset ventrally oriented body weight forces through production of dorsally oriented lift either by regulating buoyancy with the swim bladder or by generating hydrodynamic lift forces with their fins and bodies (reviewed in Sfakiotakis, Lane, and Davies 1999). In the anterior – posterior axis, fishes must generate enough anteriorly-oriented propulsive thrust to overcome the posteriorly-oriented drag experienced along the fins and body in order to achieve forward locomotion. Fishes also generate left and right lateral forces (sideslip) as well as rotational forces around the center of mass including pitch forces (head tilting up or down), roll forces (clockwise or counterclockwise dorsal - ventral rotation) and yaw forces (turning of the head to the left or right) (Paul W. Webb and Weihs 2015). In the present study, kinematic analyses focused on steady forward locomotion in which fish generated anterior thrust forces approximately equal to the experienced posterior drag forces, and were thus able to maintain their anterior-posterior positions in the flow tank. Similarly, only video sequences in which fishes exhibited minimal vertical and sideslip motions and minimal pitch, yaw and roll were analyzed in this study.

In order to achieve steady swimming and maintain their positions in the flow tank, triggerfish likely counteract the majority of the experienced ventral weight force by regulating their buoyancy with their swim bladders. Balistiform swimmers appear to generate anteriorly directed thrust forces along a continuum from drag-based to lift-based propulsive strategies (Wright 2000; J. Lighthill and Blake 1990; J. Lighthill 1990; Watanabe and Sato 2008). The drag-based forces are primarily driven by added mass forces generated at each fin segment along the fin (Wright 2000; J. Lighthill and Blake 1990) while the lift forces are generated due to asymmetries in fluid flow along the left and right sides of the fins, typically facilitated through fin

angle of attack and camber and are more prevalent in oscillating, stiff fins than in undulating, flexible fins (M. J. Lighthill 1969; Rosenberger 2001; Walker and Westneat 2000; Sfakiotakis, Lane, and Davies 1999). Wright (2000) conducted a series of hydrodynamic modelling and live-animal swimming experiments in order to explore the hydrodynamic forces produced by balistoid dorsal fins of different shapes and found that lower aspect ratio fins are generally more efficient when using highly undulatory (drag-based) kinematics and high aspect ratio fins are more efficient when utilizing oscillatory, flapping (lift-based) kinematics. Additionally, detailed computational and experimental examination of the triggerfish *Melichthys niger* revealed that the hydrodynamics of the intermediate aspect ratio, posteriorly tapering dorsal fins of *M. niger* could not be accurately reproduced by either highly undulatory (J. Lighthill and Blake 1990) or highly oscillatory, flapping (DeLaurier 1993) mathematical models, and instead seems to fall somewhere in between these two extremes. *Xanthichthys auromarginatus* possesses similarly shaped, posteriorly tapering dorsal fins, and the fin rays of both species appear to follow similar trajectories including distinct *figure-eight* shapes in anterior rays and oval shapes in posterior rays (Wright 2000), suggesting that the *X. auromarginatus* fins examined in the present study likely also generate thrust with some combination of lift and drag-based hydrodynamics.

A major goal of this study was to explore biomechanical asymmetries between dorsal and anal fin ray motions that may be caused by the morphological asymmetries exhibited by these fins. Our results revealed differences in fin ray and whole fin kinematics between the dorsal and anal fins, but further research is required in order to achieve a comprehensive understanding of the hydrodynamic consequences of these kinematic differences. One major finding of the present study is that the dorsal fin contributed greater average propulsive effort than the anal fin. Here, I consider potential three-dimensional hydrodynamic consequences of this dorsal-ventral force

generation asymmetry. The posteriorly angled, high aspect ratio dorsal fins of *X. auromarginatus* likely produce forces with components directed in dorsal, posterior and left and right directions as they move left and right across the body. The anal fin likely generates forces with components directed in ventral, posterior and left and right directions.

The left and right forces generated by the dorsal and anal fins are likely canceled out as the fin rays move symmetrically across the left - right axis, thus avoiding the production of yaw, sideslip, and roll. The posteriorly-directed forces generated by the dorsal and anal fins combine to propel the fish forwards through the water column. The dorsally and ventrally directed force components generated by the dorsal and anal fins, respectively, must cancel out in order to avoid pitching the head up or down around the center of mass. As I have demonstrated that the dorsal fin produces a larger propulsive effort than the anal fin, if the dorsal and anal fins were positioned and oriented symmetrically around the fish's center of mass (located anterior to the dorsal and anal fins), these larger dorsal fin forces would likely serve to cause the head of the fish to pitch upwards. However, this pitch motion was not observed, suggesting that the positional and angle of attachment asymmetries observed between *X. auromarginatus* dorsal and anal fins (George Chapter 3) likely serve to cancel out the dorsal-ventral forces produced by these fins around the center of mass. The anal fin is positioned slightly posterior to the dorsal fin, which would likely serve to increase the head-down rotational pitch force generated by the anal fin and offset some of the pitch forces exerted by the dorsal fin. A negative angle of attack of the fish's body (head slightly tilted down relative to the direction of flow) could also serve to offset some of the pitch force generated by the dorsal fin. Further hydrodynamic experiments are required to confirm these hypotheses. Digital particle image velocimetry (DPIV) would be particularly useful in determining the directional components of dorsal and anal fin generated forces, and computed tomography

(CT) scans could be used to accurately determine the fish's center of mass in order to assess rotational consequences of these forces.

Swimming Behavior

All three *Xanthichthys auromarginatus* specimens observed in this study exhibited a wide range of swimming behaviors throughout the filming experiments. The biomechanical results reported above focus only on dorsal and anal fin swimming kinematics during steady swimming sequences in which the fish swam near the center of the working section, away from the walls and exhibited minimal roll, pitch, yaw, lateral and dorsal - ventral movements. However, *X. auromarginatus* individuals tended to swim fairly unsteadily for large portions of the swimming trials. Fish tended to swim near the walls of the working section in order to take advantage of the slower flow in these regions due to the boundary layer effects (Vogel 1994). In some cases fish even chose to swim with their dorsal fins rubbing against the lid above the tank with each fin beat for minutes at a time, certainly altering the dorsal fin kinematics and likely increasing the biomechanical asymmetries between dorsal and anal fins. The fish also exhibited many rolling maneuvers throughout the swimming trials and often swam steadily in the flow tank with their bodies angled about 10° – 30° off of a vertical orientation in the water column. In fact, the fish almost never exhibited a perfectly vertical orientation relative to the bottom of the tank, and were able to maintain their positions in the flow tank at a variety of angles or attack. Furthermore, although *X. auromarginatus* typically beat their dorsal and anal fins relatively synchronously from left to right across the body, these fish occasionally moved the fins largely out of phase during maneuvers, while maintain their positions in the flow tank.

Low amplitude body undulations were occasionally observed during steady swimming while the caudal fin remained in its closed or folded position, suggesting that body undulations may contribute slightly to forward thrust production even at this relatively slow swimming speed before the fish make the gait transition to a gait dominated by caudal fin oscillations (George and Westneat 2019). The pectoral fins were also involved in a variety of maneuvers and occasionally flapped synchronously for multiple consecutive beats, indicating that the pectoral fins may also occasionally be recruited for forward thrust production in additional to the dorsal and anal fins at speeds below the cauda fin recruitment gait transition. Ultimately, the wide variety of swimming behaviors and kinematic strategies observed during the filming experiments reveal that *X. auromarginatus* are capable of maintaining their anterior-posterior position in the flow tank while accomplishing a diverse set of maneuvers involving all fins groups (including the dorsal and anal fins) and even slight body undulations. Coupled with the fact that *X. auromarginatus* rarely chose to swimming steadily in the flow tank, these observations suggest that balistiform steady sustained swimming performance is likely robust to a wide range of biomechanical strategies, and the differences detected between dorsal and anal fin kinematics during the steadiest swimming bouts examined in this study likely do not have serious consequences for swimming stability. This biomechanical robustness is likely beneficial for most balistoid fishes that live in complex coral reef environments in which they constantly experience unsteady, turbulent flows and are likely to regularly experience minor fin tip damage from the rough coral and aggressive interactions with other fishes that may temporarily alter the shapes of their fins.

Evolutionary Patterns of Balistiform Locomotion Biomechanics

Past balistiform locomotion fin kinematic comparisons have been based on dorsal fin leading edge fin ray kinematics alone (Wright 2000). The results of the present study suggest that anal fin biomechanics do not exactly match dorsal fin kinematics, even in a species with fairly symmetrical median fins. Furthermore, the leading edge fin ray kinematics differed from posterior fin ray kinematics in every measured kinematics trait. Even in this high aspect ratio species, leading edge fin ray motions only accounted for about 50% of the total propulsive effort, suggesting it may be necessary to include posterior fin ray kinematics in order to get an accurate understanding of balistiform locomotion biomechanics and thrust production. In fact, the most significant differences between dorsal and anal fin kinematics were found among the most posterior fin rays, with dorsal and anal fin leading edge rays oscillating at the same frequencies and amplitudes.

Balistoid fishes with lower aspect ratio, more rectangular median fins likely exhibit far fewer biomechanical differences between fin rays along the length of the fins, and this suggests that posterior fin rays of low aspect ratio fins likely contribute to a far greater percentage of the total propulsive effort and thrust production compared to high aspect ratio fins. Thus, using only leading edge fin ray kinematics to compare biomechanics across species is likely to result in underestimated thrust production measurements of low aspect ratio median fins compared to higher aspect ratio median fins. Furthermore, some balistoid species such as *Chaetodermis penicilligerus* and some *Rhinecanthus* and *Pseudobalistes* species possess highly rounded median fins in which the longest fin ray is actually located near the middle of the fin, suggesting that leading edge fin ray kinematics may not be a good measure of maximum fin ray propulsive efforts for these species. The morphological differences between balistoid species also likely play a role

in facilitating different hydrodynamic thrust production techniques among these fishes (Wright 2000).

Finally, many balistoid species including *Balistes, Pseudobalistes* and *Rhinecanthus* species possess median fins with far greater morphological asymmetry than that of *X. auromarginatus*, indicating that these species likely exhibit even greater levels of biomechanical asymmetry between their dorsal and anal fins. Balistoid median fin morphological and biomechanical asymmetries may be particularly interesting to study in species that exhibit sexual dimorphism in their median fin shapes, and thus varying intra-specific levels median fin asymmetry, such as *Odonus niger* and *Monacanthus chinensis*. These species could provide unique opportunities to study relationships between morphological and biomechanical asymmetries without confounding factors such as evolutionary relatedness or foraging and habitat use ecologies, known to be associated with balistoid median fin morphologies. Ultimately, the results of this study reveal multiple differences in balistoid dorsal and anal fin kinematics that likely lead to differences in relative thrust production between the fins, suggesting that future comparative research on balistiform locomotion should treat the dorsal and anal fins a functionally and morphologically distinct structures.

CHAPTER FIVE: CONCLUSIONS AND FUTURE DIRECTIONS

The overarching goal of this thesis was to explore the evolution of the unique balistiform swimming mode in the context of triggerfish and filefish functional morphology, ecology, and biomechanics. The results of this thesis demonstrate that balistoid fishes have evolved a wide variety of morphologies with body shapes ranging from slender, elongate forms to rounded, deep bodied forms and median fin shapes spanning nearly an order of magnitude in aspect ratio and displaying widespread morphological convergence throughout the superfamily. These morphological differences are tightly associated with gait transition strategies and endurance swimming performance. Balistoid fishes with high aspect ratio, posteriorly tapering dorsal and anal fins are associated with high endurance swimming performance, facilitating their successful occupations of offshore, pelagic habitats and planktivorous feeding modes. Balistoid fishes with low aspect ratio fins achieve lower overall endurance swimming performance, but are capable of reaching relatively high swimming speeds using the dorsal and anal fin-powered balistiform gait alone, and use this maneuverable gait to occupy nearly every habitat and feeding mode studied. The majority of balistoid fishes possess surprisingly asymmetrical dorsal and anal fin shapes, with triggerfishes generally exhibiting higher levels of fin asymmetry than filefishes. Steady swimming biomechanics experiments revealed that even moderate levels of morphological median fin asymmetry, such as those exhibited by *Xanthichthys auromarginatus*, can lead to significant biomechanical asymmetries between the dorsal and anal fins, suggesting a widespread trend of biomechanically asymmetrical median fin kinematics throughout Balistoidea. In the final chapter of this thesis I will discuss evolutionary, biomechanical and ecomorphological consequences of these finding and describe ongoing comparative field and laboratory studies aimed at improving our understanding of maneuverable, low aspect ratio balistiform swimming.

Evolutionary Biomechanics and Ecomorphology of the Balistiform Swimming Mode

Despite their circumtropical distribution, extensive ecological diversity and vast morphological disparity, all balistoid fishes use their dorsal and anal fins to power aquatic locomotion, clearly demonstrating the ecological and biomechanical versatility of the balistiform swimming mode. Throughout the history of this clade, balistoid fishes have evolved a suite of fin and body forms with associated biomechanical swimming strategies that have allowed their successful occupation of these diverse ecological niches. While some balistoid species spend their days swimming into currents and picking plankton from the water column or cruising through the open ocean using their high aspect ratio, high endurance dorsal and anal fins, other species spend their time precisely plucking away coral polyps while slowly hovering around structurally complex reefs using their low aspect ratio median fins. Still others, such as *Rhinecanthus aculeatus*, use their dorsal and anal fins to slowly swim across barren sand flats in search of food, abruptly transitioning to fast, aerobic, caudal-fin powered locomotion when threatened. Many balistoid species use some combination of the three lifestyle strategies described above, while a few species use different strategies altogether such as the filefish, *Aluterus monoceros*, which, despite possessing very low aspect ratio fins, spends much of its life in the open ocean, where it drifts among patchy rafts of floating *Sargassum* nipping at the diverse invertebrate dominated communities associated with these algal rafts (Lopez-Peralta and Arcila 2002; Ghosh et al. 2011; personal observation).

The results presented here have clearly demonstrated the performance advantages of high aspect ratio median fins, which appear to directly facilitate life in the most energetically demanding habitats and feeding guilds occupied by balistoid fishes. However, I have yet to explain why so many balistoid fishes have convergently evolved low aspect ratio median fins as well as highly asymmetrical median fins. It is clear that balistoid fishes use their dorsal and anal fins for far more

than just steady swimming and prey capture. For instance, many species engage in complex mating behaviors and territorial display that require highly coordinated median fin biomechanics to power intricate displays (Kawase and Nakazono 1996). Some of these competitive mating displays even require one individual to keep up with their forwards swimming competitor while they swim backwards in fast, tight circles (Kawase and Nakazono 1996; George, personal observation)! Other species create nests by blowing wide divets in the sand (Fricke 1980; Gladstone 1994) or by organizing small rocks with their mouths (Fricke 1980; Gladstone 1994), both activities that require hovering, backwards swimming and multiple additional maneuvers. Following spawning, many balistoid species will use a variety of maneuverable behaviors and fast bursts of speed to guard their eggs (Fricke 1980; Gladstone 1994; Ishihara and Kuwamura 1996; Kawase 2003; Kawase and Nakazono 1995; Nakazono and Kawase 1993). Finally, balistoid fishes, like all fishes, require fast, anaerobic, burst swimming performance to escape from predators and chase off competitors. These highly maneuverable mating, escaping, and competitive behaviors are completed by fishes will all sorts of fin and body shapes, but possessing low aspect ratio median fins likely facilitates the wide range of complex fin biomechanics required to complete these maneuvers (Weihs 1973; Paul W. Webb 1982; Walker and Westneat 2002; Blake 1978). Possessing asymmetrical dorsal and anal fins may also facilitate the biomechanical diversity to power these maneuvers, as the results of this thesis have shown that even during steady swimming, the slightly asymmetrical dorsal and anal fins of *Xanthichthys auromarginatus* are coupled with asymmetrical fin biomechanics. In order to test the hypotheses that both low aspect ratio and highly asymmetrical dorsal and anal fins are associated with increased balistoid maneuverability, I have designed and begun to implement three-dimensional videography field behavior experiments on the reefs of French Polynesia.

Future Directions

Balistiform Maneuverability

A general trend in fish swimming biomechanics is that high aspect ratio locomotor fins facilitate high endurance swimming performance, while low aspect ratio median fins facilitate high burst swimming performance and maneuverability (Paul W. Webb 1982). A recent study (Marcoux and Korsmeyer 2019) revealed that the triggerfish *Sufflamen bursa* is capable of station-holding in a turbulent, bi-directional flow environment by quickly switching between forwards and backwards balistiform locomotion, while most other species studies turned their bodies around to face the direction of the flow. One other median/ paired fin swimmer, the acanthurid *Ctenochaetus strigosus*, used the same strategy as *S. bursa* by altering its labriform pectoral fin kinematics to swim backwards rather then turning its whole body around. At high flow-reversal frequencies, the balistiform and labriform swimmers that altered their fin kinematics rather than turning their bodies around, were found to be more energetically-efficient (Marcoux and Korsmeyer 2019). This suggests an energetic advantage to the backwards swimming, stability, and maneuverability of median/ paired fin locomotor modes, including balistiform locomotion compared to body and caudal fin powered locomotion. However interspecific relationships between fin morphologies and degrees maneuverability remain unexplored in balistoid fishes.

In order to study these functional morphology maneuverability relationships, I implemented a baited, three-camera underwater filming rig to induce and capture maximum swimming performance behaviors of multiple triggerfish species during competitive feeding events on the coral reefs of Moorea, French Polynesia. The filming rig consisted of three GoPro Hero 6 cameras in underwater housings, affixed to a custom built iron frame (constructed by Mark Westneat) at approximately 45° lateral angles to one-another and pointed down at the food patch

at approximately 15° each. The cameras filmed at 120 frames per second and were manually synchronized following each filming trial using a powerful laser pointer. The cameras were then calibrated in three-dimensional space using a large checkerboard grid following the methods of George (Chapter 4). The food patch consisted of 3 large shrimp affixed to the top and bottom of a 5 kg dive weight using zip ties. The shrimp affixed to the top of the dive weight were easily accessible to the fishes and served to quickly draw fishes into the arena, while the shrimp affixed to the bottom of the dive weight were difficult for the fishes to access, causing fishes to establish dominance over and defend the food patches until they could flip over the weight. These competitive feeding field trials typically lasted about 30-45 minutes before the fishes were able to access and consume all the food and leave the filming arena.

These baited GoPro filming arenas successfully attracted a wide variety of reef-associated fishes including triggerfishes, wrasses, butterflyfishes, goatfishes, surgeonfishes and even large predators such as jacks among others. The most abundant triggerfish species filmed during these experiments included *Balistapus undulatus, Melichthys vidua,* and *Sufflamen chrysopterum*, and *Rhinecanthus aculeatus*. These triggerfish species range in dorsal fin shapes from low (*B. undulatus*) to medium (*S. chrysopterum* and *R. aculeatus*) to high (*Melichthys vidua*) aspect ratios (George Chapter 3). Additionally, these species exhibit a large range of median fin asymmetries, with *B. undulatus* possessing low aspect ratio dorsal fins, but medium aspect ratio anal fins and *R. aculeatus* exhibiting particularly high levels of full fin shape asymmetry using the Procrustes distance metric (George Chapter 3).

In the vast majority of trials, triggerfishes (typically large *B. undulatus* individuals) quickly asserted dominance over the food patches. The dominant triggerfish individuals displayed a variety of complex maneuvers while feeding on the food patches and attempting to flip over the dive

weight to access the food on the underside including hovering, backwards swimming, and even upside-down swimming and full barrel-rolls! When other species approached the food patches, the dominant triggerfishes typically responded with multiple large, fast, caudal-fin powered bursts and quick, tight turning maneuvers to chase away competitors. Smaller triggerfish individuals would typically hover around the perimeter of the filming area and quickly burst in to bite at the food patch while the dominant individual was distracted by other competitors. Ultimately, these experiments yielded dozens of hours of competitive feeding-induced maximal maneuverability performance videos that can be analyzed in three dimensions using similar calibration and digitization methods as those used to study steady swimming kinematics in the laboratory experiments described in George (Chapter 4). By tracking individual triggerfishes from each species filmed during these field experiments, maneuverability data such as maximum burst swimming speed, maximum backwards swimming speed, maximum turning velocity, minimum turning angle, and maximum roll can be measured and calculated in a manner similar to that of the lab-based comparative maneuverability studies (Gerstner 1999; Paul W Webb and Fairchild 2001). I can then compare these maneuverability metrics across balistoid species and explore functional morphology patterns between median fin morphologies and maneuverability performance.

It is clear from preliminary analyses that triggerfishes, especially the low aspect ratio *B. undulatus*, are capable of using a wide variety of complex maneuvers and fast bust swimming behaviors to assert dominance over and defend food resources from a variety of other fish taxa in their natural reef environments (Figure 5.1). This result suggests that balistiform locomotion may provide some competitive functional advantages over the fish swimming modes utilized by the other reef fishes present in and around the arena including wrasse and surgeonfish labriform locomotion and a variety of body/ caudal fin locomotor modes utilized by most other present taxa.

Once analyzed, the results of this study will provide insight into the ecological utility of low aspect ratio and asymmetrical balistoid fins.

Figure 5.1. Triggerfishes competing over food patches during field experiments in Moorea, FP. The tigerfishes *Balistapus undulatus* and *Melichthys vidua* compete for access to food patches beneath the diving weights. The left panels depict an 8 m deep field site and the right panels depict a shallow 4 m deep field site. *B. undulatus* were dominant in both environments, but *M. vidua* did acquire some food at both sites and was especially successful at the deeper site. Photos depict triggerfishes exhibiting a variety of maneuvers and fast burst swimming bouts.

Balistiform Biomechanics of Low Aspect Ratio and Highly Asymmetrical Median Fins

A second major question raised by the results of this thesis concerns the steady balistiform swimming biomechanics of low aspect ratio and highly asymmetrical dorsal and anal fins. Previous research based on leading edge dorsal fin ray kinematics has revealed that balistoid dorsal fins lie on a biomechanical continuum from highly undulatory to highly oscillatory biomechanical motions (Wright 2000; Blake 1978; Loofbourrow 2009). Furthermore, Wright (2000) revealed that among the ten balistoid species examined, dorsal fin morphology was a good predictor of dorsal fin steady swimming kinematics, with high aspect ratio dorsal fins exhibiting lower frequencies, longer wavelengths, and lower number of waves than low aspect ratio dorsal fins. The anal fins of balistoid fishes likely follow these same functional morphology patterns, although the results of the steady swimming biomechanics study in the present thesis (George Chapter 4) indicate that the specific kinematics and wave form properties of the dorsal and anal fins are unlikely to be identical. Furthermore, the species include in the Wright (2000) study were generally limited to median fin morphologies of either elongate, high area, and high aspect ratio fins or short, low area, low aspect ratio fins. The morphometric studies in this thesis (George Chapter 3), revealed that some balistoid fishes such as the filefishes genera *Aluterus* and *Pervagor* possess highly elongate, low aspect ratio dorsal and anal fins that more closely resemble the dorsal fins of bowfin, *Amia calva*, and the anal fins of knifefishes than the short, low aspect ratio median fins of triggerfishes like *Balistapus undulatus* and *Balistoides conspicillum.* The highly elongate, low aspect ratio median fins of bowfin (Jagnandan and Sanford 2013) and knifefishes (Youngerman, Flammang, and Lauder 2014; Ruiz-Torres et al. 2013; Shirgaonkar et al. 2008; Blake 1983) tend to exhibit much more undulatory median fin kinematics than the most undulatory, low aspect ratio balistoid median fins

described to date (Wright 2000; Blake 1983; Loofbourrow 2009; Korsmeyer, Steffensen, and Herskin 2002).

In order to explore the relationships between dorsal and anal fin aspect ratios and symmetry and balistiform swimming biomechanics, I have selected two additional balistoid species for detailed three-dimensional kinematic experiments. The first species, *R. aculeatus*, possessed short, highly asymmetrical, low aspect ratio median fins (George, chapter 3) and has been extensively studied in the contexts of dorsal fin swimming biomechanics (Blake 1978; Wright 2000; Loofbourrow 2009; Korsmeyer, Steffensen, and Herskin 2002), performance (George and Westneat 2019; Wright 2000) and energetics (Korsmeyer, Steffensen, and Herskin 2002), however anal fin kinematics remain largely unexplored in this species. This species exhibits fairly undulatory dorsal fin kinematics (Wright 2000) and a very low gait transition speed, powering the majority of its endurance swimming speed range using body/ caudal fin locomotion (George and Westneat 2019). Due to these traits, *R. aculeatus* will serve as a nice representative of the body/ caudal fin specialist balistoid gait transition strategy. Furthermore, the wealth of *R. aculeatus* background knowledge will allow me to interpret the kinematics results in a broad biomechanical and physiological context.

The second selected species, *Pervagor janthinosoma*, possesses elongate, fairly symmetrical, low aspect ratio dorsal and anal fins (George Chapter 3) and powers endurance swimming using balistiform locomotion for nearly its entire range of swimming speeds, with a very high gait transition speed and very poor endurance body/ caudal fin performance (George and Westneat 2019). This filefish species is an excellent representative of the balistiform specialist gait transition strategy. In order to study the steady swimming kinematics of these low aspect ratio fishes, I have filmed 2 – 3 individuals from each species swimming in a flow tank using the same

methods described in George (Chapter 4). With the assistance of an undergraduate researcher, I plan to analyze and contrast the dorsal and anal fin kinematics of these species following the method used for *X. auromarginatus* (George Chapter 4).

I hypothesize that *P. janthinosoma* will exhibit the most undulatory fin kinematics ever described among balistoid fishes defined by high frequency fin ray undulations, short wavelengths and a large number of waves. I predict that *R. aculeatus* will also exhibit fairly undulatory fin kinematics based on described dorsal fin kinematics for this species (Wright 2000; Loofbourrow 2009; Blake 1983; Korsmeyer, Steffensen, and Herskin 2002). These hypotheses appear to be supported by preliminary filming studies (Figure 5.2). However, due to the high levels of median fin asymmetry displayed by *R. aculeatus*, including dorsal fins of significantly higher areas compared to anal fins (George, chapter 3; Loofbourrow 2009), I hypothesize that the anal fin will produce far less propulsive effort than the dorsal fin. This hypothesis is further supported by the finding that *R. aculeatus* dorsal fin muscles are capable of higher power outputs than the anal fin muscles (Blake 1978). These predicted highly asymmetrical dorsal and anal fin biomechanics could help explain the low balistiform swimming performance of *R. aculeatus* (George and Westneat 2019).

I predict that both of these low aspect ratio balistoid species will exhibit fairly consistent fin ray kinematics along the anterior-posterior lengths of their dorsal and anal fins due to the regular median fin ray lengths found in these species compared to those of the high aspect ratio, tapering *X. auromarginatus* median fins. Ultimately, in combination with the results of George (Chapter 4), I predict that this ongoing study will reveal widespread biomechanical asymmetries in dorsal and anal fin kinematics across both balistoid families and the nearly the full range of biomechanical strategies.

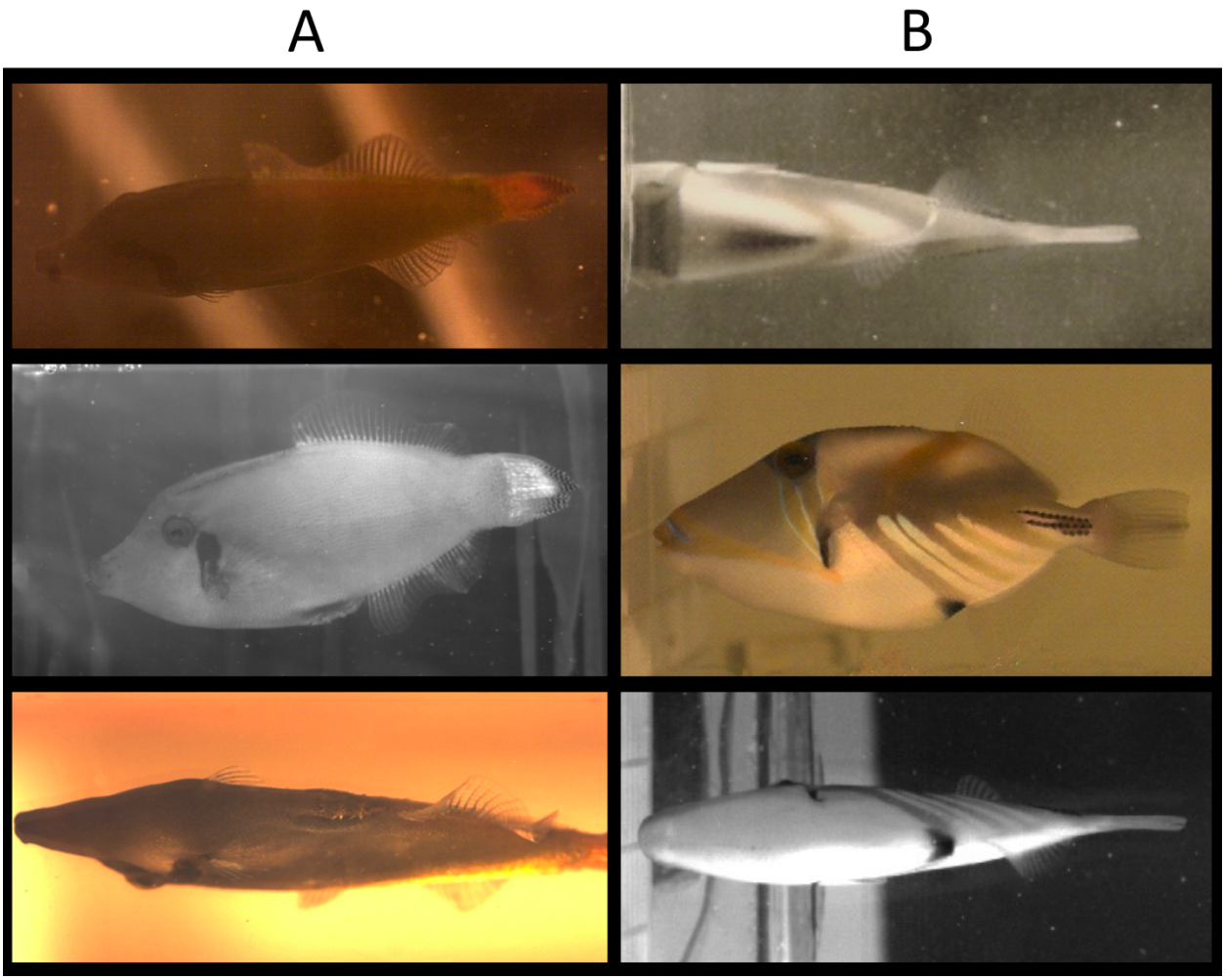

Figure 5.2. *Pervagor janthinosoma* and *Rhinecanthus aculeatus* steady swimming kinematics. (A) Time-synchronized dorsal, lateral and ventral views of the filefish *Pervagor janthinosoma* swimming steadily at 18 cm s^{-1} in a flow tank. Note the highly undulatory dorsal and anal fin wave properties with more than one full undulatory wave present along these elongate fins at this instant in time. (B) Time-synchronized dorsal, lateral and ventral views of the triggerfish *Rhinecanthus aculeatus* swimming steadily at 18 cm s^{-1} in a flow tank. *R. aculeatus* also exhibit fairly undulatory dorsal and anal fin wave properties despite the short lengths of these medium aspect ratio fins.

Balistoid Locomotor Muscle Morphology

The basic muscular anatomy underlying the balistoid swimming apparatus has been described for a number of triggerfish and filefish species (Winterbottom 1974; Davison 1987a; 1987b) and median fin power output has been experimentally measured in *Rhinecanthus aculeatus* (Blake 1978), but detailed studies of muscle lengths, attachment sites and cross-sectional areas have not

yet been performed. In fact, even the set of median fin muscles that power balistiform locomotion has yet to be experimentally confirmed beyond dissection descriptions. In balistoid fishes, each dorsal and anal fin ray possess a pair of erector, depressor, and inclinator muscles, for a total of 6 muscles associated with each fin ray (Winterbottom 1974). This means that balistoid fishes with very elongate median fins such as *Aluterus scriptus* can have over 300 individual muscles playing a role in their balistiform swimming biomechanics!

In the dorsal fin, the paired erector muscles originate on the pterygiophores with one erector muscle attaching to the anterior edges of the right and left sides of each fin ray base. In most fishes, these muscles serve to erect the dorsal fin, but balistoid fishes appear to have co-opted the large erector muscles to power lateral fin ray undulations, and likely also use them in controlling the anterior to posterior *figure eight* trajectories observed in the leading edge fin rays of *Xanthichthys auromarginatus* (George, chapter 4) and *Melichthys niger* (Wright 2000). The dorsal fin depressor muscles originate on the pterygiophores and neural spines and attach to the posterior edges of the right and left fin ray bases (Winterbottom 1974). The large depressor muscles serve to fold the fin down against the body in most fishes, but once again, balistoid fishes appear to have co-opted these muscles to participate in the lateral fin motions that power their locomotion, though the depressors also likely play a role in controlling the anterior-posterior figure eight fin ray motions. Finally, one small inclinator muscle connects to each side of each dorsal fin ray and attaches to the connective tissue overlying the lateral epaxial muscles on the body (Winterbottom 1974; Davison 1987b). Contractions of these small inclinator muscles serve to pull the fin rays from left to right in most fishes, and these muscles likely maintain this ability to a small degree in balistoid fishes, however the larger erector and depressor muscles certainly provide the vast majority of the thrust powering the fin ray motions of balistiform locomotion. The anal fins possess their own sets of fin

ray muscles (erectors, depressors and inclinators) that perform the same tasks and attach to the same relative position on the fin rays as their dorsal fin counterparts. The anal fin erector and depressor muscles originate on the pterygiophores and haemal spines, and the small inclinator muscles originate from facia overlaying the hypaxial muscles (Winterbottom 1974).

Dorsal and anal fin rays can be modeled as lever systems, with the short lateral extensions at the base of each paired fin ray hemitrich serving as the in-levers and the long dorsal/ ventral extensions of each hemitrich representing the out-lever. Accurately modelling the fin ray lever systems that power balistiform locomotion would require (1) detailed fin ray-specific kinematic data, as collected in George (chapter 4), (2) detailed anatomical data on balistoid dorsal and anal fins and fin rays, and (3) anatomical and physiological properties of the erector, depressor and inclinator muscles controlling each fin ray. The collection of this data would allow for the estimation of fin ray (and total fin) force production during steady swimming using a computer model that treats each fin ray apparatus as a paired lever system.

Muscle physiology research using the filefish *Meuschenia scaber* has shown that the epaxial body musculature of this species is composed almost entirely of white (fast glycolytic) muscle fibers, while the dorsal and anal fin muscles contain red (slow oxidative), white, and pink (intermediate) fiber types (Davison 1987b). Power output research that combined kinematics and physiological experiments in *R. aculeatus* revealed that the dorsal fin muscles produce greater power output than the anal fin muscles. Outside of these two species, the anatomy and physiology of balistoid median fin muscles remains largely unexplored. However, gross examination of these balistoid muscles indicates large differences in median fin muscle lengths, fiber types (colors) and orientations between species (Figure 5.3). Fin ray associated erector and depressor muscles decrease in length along the anterior-posterior length of each fin. Keeping in mind that these

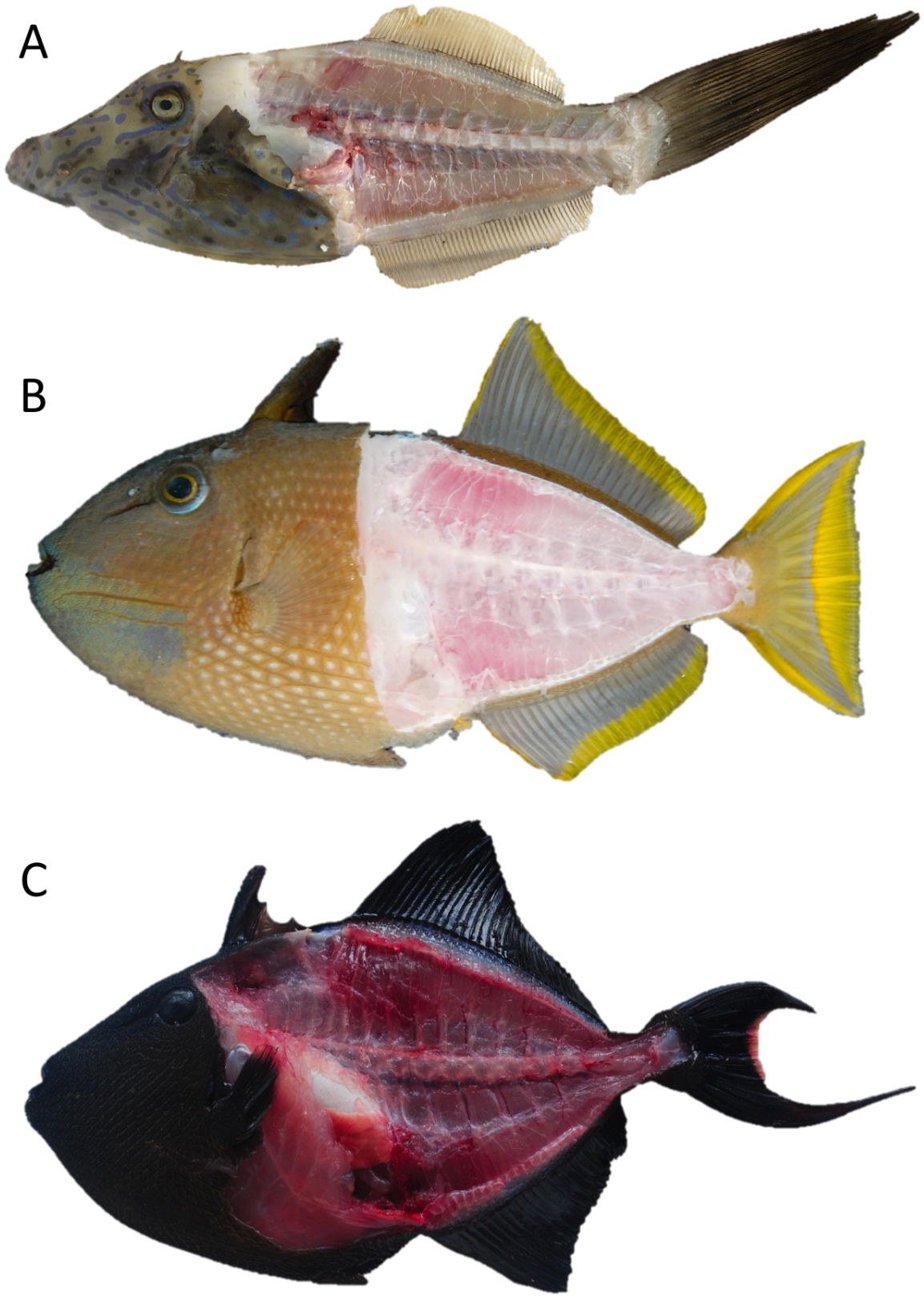

Figure 5.3. continued on page 150.

Figure 5.3. Comparative balistoid dorsal and anal fin erector and depressor muscles. (A) *Aluterus scriptus* (B) *Xanthichthys auromarginatus* (C) *Odonus niger*. Note the darker red coloration of the large erector and depressor muscles of the anterior dorsal and anal fin rays in each species and the paler white colors of the posterior erector and depressor muscles.

preliminary trends are based on dissection photos and notes alone, it appears that the leading edge dorsal fin rays of all 6 examined balistoid species, *Aluterus scriptus*, *Balistoides conspicillum*, *Melichthys vidua*, *Odonus niger, R. aculeastus,* and *X. auromarginatus*, are associated with large red or pink colored erector and depressor muscles (probably aerobic) while the posterior fin rays are associated with shorter, white colored erector and depressor muscles (Figure 5.3). This trend seems to hold across median fin shapes from high (*M. vidua, O. niger,* and *X. auromarginatus*) to low (*A. scriptus*, *B. conspicillum*) aspect ratio fins as well as across balistoid families. Additionally, the planktivorous species (*O. niger*, *M. vidua*, and *X. auromarginatus*) appear to have deeper red erector and depressor musculature (Figure 5.3 B and C) than the other species, while fishes that use their bodies and caudal fins for greater portions of their endurance swimming range (*R. aculeatus* and *S. bursa*) seem to have deeply red epaxial and hypaxial muscles compared to balistiform specialists such as *A. scriptus*. Comprehensive histochemistry and electron scanning microscopy studies of these muscles need to be performed in order to confirm these patterns. However, preliminary examination suggests that balistoid fin and body musculature has evolved diverse anatomical and physiological properties that facilitate efficient, aerobic locomotion using each species' preferred gait transition strategies, and allow balistoid species to occupy a wide range of habitat and feeding ecologies.

Concluding Remarks

The morphologically, ecologically and biomechanically diverse balistoid fishes have served as an excellent group in which to study patterns of functional morphology and ecomorphology associated with the evolution of a novel swimming mode. These charismatic fishes use a wide variety of biomechanical strategies and behaviors to successfully occupy nearly every marine habitat, and even within most habitats, morphologies and lifestyles vary greatly between species. The inclusion of the filefishes (Monacanthidae) in this research has been particularly valuable for illuminating previously undescribed morphological disparity and associated swimming biomechanical diversity of balistoid fishes. Indeed, given the overwhelming focus on triggerfishes (Balistidae) in past comparative balistoid swimming performance, biomechanics, physiology, and functional morphology studies, further exploration of monacanthid functional morphology and evolution is likely to be especially enlightening.

REFERENCES

Adams, D. C., M. L. Collyer, A Kaliontzopoulou, and E Sherratt. 2017. *Geomorph: Software for Geometric Morphometric Analyses.* (version 3.0.5). R. https://cran.r-project.org/package=geomorph.

Aiello, Brett R., Aaron M. Olsen, Chris E. Mathis, Mark W. Westneat, and Melina E. Hale. 2019. "Pectoral Fin Kinematics and Motor Patterns Are Shaped by Fin Ray Mechanosensation during Steady Swimming in Scarus Quoyi." *Journal of Experimental Biology*, January. https://doi.org/10.1242/jeb.211466.

Alexander, R. M. 1989. "Optimization and Gaits in the Locomotion of Vertebrates." *Physiological Reviews* 69 (4): 1199–1227. https://doi.org/10.1152/physrev.1989.69.4.1199.

Alsop, D., and C. Wood. 1997. "The Interactive Effects of Feeding and Exercise on Oxygen Consumption, Swimming Performance and Protein Usage in Juvenile Rainbow Trout (*Oncorhynchus mykiss*)." *Journal of Experimental Biology* 200 (17): 2337–46.

Arreola, Veronica I, and Mark W. Westneat. 1996. "Mechanics of Propulsion by Multiple Fins: Kinematics of Aquatic Locomotion in the Burrfish (*Chilomycterus schoepfi)*." *Proceedings of the Royal Society of London. Series B: Biological Sciences* 263 (1377): 1689–96. https://doi.org/10.1098/rspb.1996.0247.

Benjamini, Yoav, and Yosef Hochberg. 1995. "Controlling the False Discovery Rate: A Practical and Powerful Approach to Multiple Testing." *Journal of the Royal Statistical Society: Series B (Methodological)* 57 (1): 289–300. https://doi.org/10.1111/j.2517-6161.1995.tb02031.x.

Biewener, A. A. 2003. *Animal Locomotion*. Oxford Animal Biology Series. Oxford ; New York: Oxford University Press.

Binning, S. A., and C. J. Fulton. 2011. "Non-Lethal Measurement of Pectoral Fin Aspect Ratio in Coral-Reef Fishes." *Journal of Fish Biology* 79 (3): 812–18. https://doi.org/10.1111/j.1095-8649.2011.03070.x.

Blake, R. W. 1978. "On Balistiform Locomotion." *Journal of the Marine Biological Association of the United Kingdom* 58 (1): 73–80. https://doi.org/10.1017/S0025315400024401.

———. 1983. "Swimming in the Electric Eels and Knifefishes." *Canadian Journal of Zoology* 61 (6): 1432–41. https://doi.org/10.1139/z83-192.

Blob, R. W., R. Rai, M. L. Julius, and H. L. Schoenfuss. 2006. "Functional Diversity in Extreme Environments: Effects of Locomotor Style and Substrate Texture on the Waterfall-

Climbing Performance of Hawaiian Gobiid Fishes." *Journal of Zoology* 268 (3): 315–24. https://doi.org/10.1111/j.1469-7998.2005.00034.x.

Breder, Charles M. 1926. "The Locomotion of Fishes." *Zoologica : Scientific Contributions of the New York Zoological Society.* 4 (5): 159–297.

Brett, J. R. 1964. "The Respiratory Metabolism and Swimming Performance of Young Sockeye Salmon." *Journal of the Fisheries Research Board of Canada* 21 (5): 1183–1226. https://doi.org/10.1139/f64-103.

Bushnell, D. M., and K. J. Moore. 1991. "Drag Reduction in Nature." *Annual Review of Fluid Mechanics* 23 (1): 65–79. https://doi.org/10.1146/annurev.fl.23.010191.000433.

Cannas, M., J. Schaefer, P. Domenici, and J. F. Steffensen. 2006. "Gait Transition and Oxygen Consumption in Swimming Striped Surfperch *Embiotoca lateralis* Agassiz." *Journal of Fish Biology* 69 (6): 1612–25. https://doi.org/10.1111/j.1095-8649.2006.01225.x.

Davison, William. 1987a. "The Median Fin Muscles of the Leatherjacket, *Parika scaber* (Pisces: Balistidae)." *Cell and Tissue Research* 248 (1): 131–35. https://doi.org/10.1007/BF01239973.

———. 1987b. "Arterioles in the Swimming Muscles of the Leatherjacket *Parika scaber* (Pisces: Balistidae)." *Cell and Tissue Research* 248 (3): 703–8. https://doi.org/10.1007/BF00216502.

DeLaurier, J. D. 1993. "An Aerodynamic Model for Flapping-Wing Flight." *The Aeronautical Journal of the Royal Aeronautical Society* 97: 125–30.

Denny, Christopher M. 2005. "Distribution and Abundance of Labrids in Northeastern New Zealand: The Relationship between Depth, Exposure and Pectoral Fin Aspect Ratio." *Environmental Biology of Fishes* 72 (1): 33–43. https://doi.org/10.1007/s10641-004-4178-5.

Dornburg, Alex, Francesco Santini, and Michael E. Alfaro. 2008. "The Influence of Model Averaging on Clade Posteriors: An Example Using the Triggerfishes (Family Balistidae)." *Systematic Biology* 57 (6): 905–19. https://doi.org/10.1080/10635150802562392.

Dornburg, Alex, Brian Sidlauskas, Francesco Santini, Laurie Sorenson, Thomas J. Near, and Michael E. Alfaro. 2011. "The Influence of an Innovative Locomotor Strategy on the Phenotypic Diversification of Triggerfish (Family: Balistidae)." *Evolution* 65 (7): 1912–26. https://doi.org/10.1111/j.1558-5646.2011.01275.x.

Drucker, E., and J. Jensen. 1996. “Pectoral Fin Locomotion in the Striped Surfperch. II. Scaling Swimming Kinematics and Performance at a Gait Transition.” *Journal of Experimental Biology* 199 (10): 2243–52.

Dudley, Robert. 2000. *The Biomechanics of Insect Flight: Form, Function, Evolution*. Princeton University Press. https://doi.org/10.2307/j.ctv301g2x.

Evans, K. M., L. Y. Kim, B. A. Schubert, and J. S. Albert. 2019. “Ecomorphology of Neotropical Electric Fishes: An Integrative Approach to Testing the Relationships between Form, Function, and Trophic Ecology.” *Integrative Organismal Biology* 1 (1): 1–16. https://doi.org/10.1093/iob/obz015.

Farlinger, S., and F. W. H. Beamish. 1977. “Effects of Time and Velocity Increments on the Critical Swimming Speed of Largemouth Bass (Micropterus Salmoides).” *Transactions of the American Fisheries Society* 106 (5): 436–39. https://doi.org/10.1577/1548-8659(1977)106<436:EOTAVI>2.0.CO;2.

Feilich, Kara L. 2016. “Correlated Evolution of Body and Fin Morphology in the Cichlid Fishes.” *Evolution* 70 (10): 2247–67. https://doi.org/10.1111/evo.13021.

———. 2017. “Swimming with Multiple Propulsors: Measurement and Comparison of Swimming Gaits in Three Species of Neotropical Cichlids.” *Journal of Experimental Biology* 220 (22): 4242–51. https://doi.org/10.1242/jeb.157180.

Fierstine, Harry L., and Vladimir Walters. 1968. *Studies in Locomotion and Anatomy of Scombroid Fishes*. [Los Angeles,: Southern California Academy of Sciences]. https://doi.org/10.5962/bhl.title.146943.

Fish, F. E. 1990. “Wing Design and Scaling of Flying Fish with Regard to Flight Performance.” *Journal of Zoology* 221 (3): 391–403. https://doi.org/10.1111/j.1469-7998.1990.tb04009.x.

Fontanella, Janet E., Frank E. Fish, Elizabeth I. Barchi, Regina Campbell-Malone, Rachel H. Nichols, Nicole K. DiNenno, and John T. Beneski. 2013. “Two- and Three-Dimensional Geometries of Batoids in Relation to Locomotor Mode.” *Journal of Experimental Marine Biology and Ecology* 446 (August): 273–81. https://doi.org/10.1016/j.jembe.2013.05.016.

Fox, John, and Sanford Weisberg. 2011. *An {R} Companion to Applied Regression*. Second. Thousand Oaks, CA: Sage. http://socserv.socsci.mcmaster.ca/jfox/Books/Companion.

Fricke, Hans W. 1980. “Mating Systems, Maternal and Biparental Care in Triggerfish (Balistidae).” *Zeitschrift Für Tierpsychologie* 53 (2): 105–22. https://doi.org/10.1111/j.1439-0310.1980.tb01043.x.

Friedman, S. T., S. A. Price, A. S. Hoey, and P. C. Wainwright. 2016. "Ecomorphological Convergence in Planktivorous Surgeonfishes." *Journal of Evolutionary Biology* 29 (5): 965–78. https://doi.org/10.1111/jeb.12837.

Froese, R., and D. Pauly. 2019. "FishBase." World Wide Web electronic publication. FishBase. 2019. www.fishbase.org.

Fulton, Christopher J., and David R. Bellwood. 2002. "Ontogenetic Habitat Use in Labrid Fishes: An Ecomorphological Perspective." *Marine Ecology Progress Series* 236: 255–62. http://dx.doi.org/10.3354/meps236255.

Fulton, Christopher J., and David R. Bellwood. 2004. "Wave Exposure, Swimming Performance, and the Structure of Tropical and Temperate Reef Fish Assemblages." *Marine Biology* 144 (3): 429–37. https://doi.org/10.1007/s00227-003-1216-3.

Fulton, Christopher J., David R. Bellwood, and Peter C. Wainwright. 2001. "The Relationship between Swimming Ability and Habitat Use in Wrasses (Labridae)." *Marine Biology* 139 (1): 25–33. https://doi.org/10.1007/s002270100565.

George, Andrew B., and Mark W. Westneat. 2019. "Functional Morphology of Endurance Swimming Performance and Gait Transition Strategies in Balistoid Fishes." *Journal of Experimental Biology* 222 (8). https://doi.org/10.1242/jeb.194704.

Gerry, S. P., J. Wang, and D. J. Ellerby. 2011. "A New Approach to Quantifying Morphological Variation in Bluegill *Lepomis macrochirus*." *Journal of Fish Biology* 78 (4): 1023–34. https://doi.org/10.1111/j.1095-8649.2011.02911.x.

Gerstner, Cynthia L. 1999. "Maneuverability of Four Species of Coral-Reef Fish That Differ in Body and Pectoral-Fin Morphology." *Canadian Journal of Zoology* 77 (7): 1102–10. https://doi.org/10.1139/z99-086.

Ghosh, Shubhadeep, R. Thangavelu, Gulshad Mohammed, H. Dhokia, Mahendrasinh Zala, Y. Savaria, J. Polara, and A. Ladani. 2011. "Sudden Emergence of Fishery and Some Aspects of Biology and Population Dynamics of Aluterus Monoceros (Linnaeus, 1758) at Veraval." *Indian Journal of Fisheries* 58 (1): 31–34.

Gladstone, William. 1994. "Lek-like Spawning, Parental Care and Mating Periodicity of the Triggerfish *Pseudobalistes flavimarginatus* (Balistidae)." *Environmental Biology of Fishes* 39 (3): 249–57. https://doi.org/10.1007/BF00005127.

Gordon, Malcolm S., Jay R. Hove, Paul W. Webb, and Daniel Weihs. 2000. "Boxfishes as Unusually Well-Controlled Autonomous Underwater Vehicles." *Physiological and Biochemical Zoology* 73 (6): 663–71. https://doi.org/10.1086/318098.

Gross, Juergen, and Uwe Ligges. 2015. *Nortest: Tests for Normality.* (version 1.0-4). R. https://CRAN.R-project.org/package=nortest.

Hale, Melina E., Ryan D. Day, Dean H. Thorsen, and Mark W. Westneat. 2006. "Pectoral Fin Coordination and Gait Transitions in Steadily Swimming Juvenile Reef Fishes." *Journal of Experimental Biology* 209 (19): 3708–18. https://doi.org/10.1242/jeb.02449.

Hiatt, Robert W., and Donald W. Strasburg. 1960. "Ecological Relationships of the Fish Fauna on Coral Reefs of the Marshall Islands." *Ecological Monographs* 30 (1): 65–127. https://doi.org/10.2307/1942181.

Holm, Sture. 1979. "A Simple Sequentially Rejective Multiple Test Procedure." *Scandinavian Journal of Statistics* 6 (2): 65–70.

Hove, J. R., L. M. O'Bryan, M. S. Gordon, P. W. Webb, and D. Weihs. 2001. "Boxfishes (Teleostei: Ostraciidae) as a Model System for Fishes Swimming with Many Fins: Kinematics." *Journal of Experimental Biology* 204 (8): 1459–71.

Hu, Tianjiang, Guangming Wang, Lincheng Shen, and Fei Li. 2006. "A Novel Conceptual Fish-like Robot Inspired by Rhinecanthus Aculeatus." In *Robotics and Vision 2006 9th International Conference on Control, Automation*, 1–5. Singapore. https://doi.org/10.1109/ICARCV.2006.345100.

Hutchins, J. B., and R. Swainston. 1985. "Revision of the Monacanthid Fish Genus Brachaluteres." *Records of the Western Australian Museum* 1: 57–78.

Ishihara, Masahiro, and Tetsuo Kuwamura. 1996. "Bigamy or Monogamy with Maternal Egg Care in the Triggerfish, *Sufflamen chrysopterus*." *Ichthyological Research* 43: 307–13.

Jagnandan, Kevin, and Christopher P. Sanford. 2013. "Kinematics of Ribbon-Fin Locomotion in the Bowfin, *Amia Calva*." *Journal of Experimental Zoology Part A: Ecological Genetics and Physiology* 319 (10): 569–83. https://doi.org/10.1002/jez.1819.

Jamon, Marc, Sabine Renous, Jean Pierre Gasc, Vincent Bels, and John Davenport. 2007. "Evidence of Force Exchanges during the Six-Legged Walking of the Bottom-Dwelling Fish, *Chelidonichthys lucerna.*" *Journal of Experimental Zoology. Part A, Ecological Genetics and Physiology* 307 (9): 542–47. https://doi.org/10.1002/jez.401.

Karpouzian, G., G. Spedding, and H. K. Cheng. 1990. "Lunate-Tail Swimming Propulsion. Part 2. Performance Analysis." *Journal of Fluid Mechanics* 210 (January): 329–51. https://doi.org/10.1017/S0022112090001318.

Kawase, Hiroshi. 2003. "Spawning Behavior and Biparental Egg Care of the Crosshatch Triggerfish, *Xanthichthys mento* (Balistidae)." *Environmental Biology of Fishes* 66 (3): 211–19. https://doi.org/10.1023/A:1023978722744.

Kawase, Hiroshi, and Akinobu Nakazono. 1995. “Predominant Maternal Egg Care and Promiscuous Mating System in the Japanese Filefish, *Rudarius ercodes* (Monacanthidae).” *Environmental Biology of Fishes* 43 (3): 241–54. https://doi.org/10.1007/BF00005856.

———. 1996. “Two Alternative Female Tactics in the Polygynous Mating System of the Threadsail Filefish, *Stephanolepis cirrhifer* (Monacanthidae).” *Ichthyological Research* 43 (3): 315–23. https://doi.org/10.1007/BF02347603.

King, Heather M., Neil H. Shubin, Michael I. Coates, and Melina E. Hale. 2011. “Behavioral Evidence for the Evolution of Walking and Bounding before Terrestriality in Sarcopterygian Fishes.” *Proceedings of the National Academy of Sciences* 108 (52): 21146–51. https://doi.org/10.1073/pnas.1118669109.

Klaczko, Julia, Emma Sherratt, and Eleonore Z. F. Setz. 2016. “Are Diet Preferences Associated to Skulls Shape Diversification in Xenodontine Snakes?” *PLoS ONE* 11 (2): e0148375. https://doi.org/10.1371/journal.pone.0148375.

Klingenberg, Christian Peter, Marta Barluenga, and Axel Meyer. 2002. “Shape Analysis of Symmetric Structures: Quantifying Variation Among Individuals and Asymmetry.” *Evolution* 56 (10): 1909–20. https://doi.org/10.1111/j.0014-3820.2002.tb00117.x.

Kolok, A. S. 1999. “Interindividual Variation in the Prolonged Locomotor Performance of Ectothermic Vertebrates: A Comparison of Fish and Herpetofaunal Methodologies and a Brief Review of the Recent Fish Literature.” *Canadian Journal of Fisheries and Aquatic Sciences* 56 (4): 700–710. https://doi.org/10.1139/f99-026.

Korsmeyer, Keith E., John Fleng Steffensen, and Jannik Herskin. 2002. “Energetics of Median and Paired Fin Swimming, Body and Caudal Fin Swimming, and Gait Transition in Parrotfish (*Scarus schlegeli*) and Triggerfish (*Rhinecanthus aculeatus*).” *Journal of Experimental Biology* 205 (9): 1253–63.

Larouche, Olivier, Miriam L. Zelditch, and Richard Cloutier. 2017. “Fin Modules: An Evolutionary Perspective on Appendage Disparity in Basal Vertebrates.” *BMC Biology* 15 (1): 32. https://doi.org/10.1186/s12915-017-0370-x.

Lighthill, James. 1969. “Hydromechanics of Aquatic Animal Propulsion.” *Annual Review of Fluid Mechanics* 1 (1): 413–46. https://doi.org/10.1146/annurev.fl.01.010169.002213.

———. “Aquatic Animal Propulsion of High Hydromechanical Efficiency.” *Journal of Fluid Mechanics* 44 (2): 265–301. https://doi.org/10.1017/S0022112070001830.

———. 1990. “Biofluiddynamics of Balistiform and Gymnotiform Locomotion. Part 4. Short-Wavelength Limitations on Momentum Enhancement.” *Journal of Fluid Mechanics* 213 (April): 21–28. https://doi.org/10.1017/S0022112090002191.

Lighthill, James, and Robert Blake. 1990. “Biofluiddynamics of Balistiform and Gymnotiform Locomotion. Part 1. Biological Background, and Analysis by Elongated-Body Theory.” *Journal of Fluid Mechanics* 212 (March): 183–207. https://doi.org/10.1017/S0022112090001926.

Lindsey, C. C. 1978. “Form, Function, and Locomotory Habits in Fish.” In *Fish Physiology*, edited by W. S. Hoar and D. J. Randall, 7:1–100. Locomotion. Academic Press. https://doi.org/10.1016/S1546-5098(08)60163-6.

Loofbourrow, H. 2009. “Hydrodynamics of Balistiform Swimming in the Picasso Triggerfish, *Rhinecanthus aculeatus*.” Master’s Thesis, Vancouver, Canada: University of British Columbia.

Lopez-Peralta, R. H., and C. A. T. Arcila. 2002. “Diet Composition of Fish Species from the Southern Continental Shelf of Colombia.” *Naga, Worldfish Center Quarterly* 25 (3–4): 23–29.

MacLeod, Norm. 2009. “Form & Shape Models.” *Palaeontology Newletter* 18: 1–11.

Marcoux, Travis M., and Keith E. Korsmeyer. 2019. “Energetics and Behavior of Coral Reef Fishes during Oscillatory Swimming in a Simulated Wave Surge.” *Journal of Experimental Biology* 222 (4). https://doi.org/10.1242/jeb.191791.

Martinez, Christopher M., F. James Rohlf, and Michael G. Frisk. 2016. “Re-Evaluation of Batoid Pectoral Morphology Reveals Novel Patterns of Diversity among Major Lineages.” *Journal of Morphology* 277 (4): 482–93. https://doi.org/10.1002/jmor.20513.

Mathis, Alexander, Pranav Mamidanna, Kevin M. Cury, Taiga Abe, Venkatesh N. Murthy, Mackenzie Weygandt Mathis, and Matthias Bethge. 2018. “DeepLabCut: Markerless Pose Estimation of User-Defined Body Parts with Deep Learning.” *Nature Neuroscience* 21 (9): 1281–89. https://doi.org/10.1038/s41593-018-0209-y.

McCord, Charlene L., and Mark W. Westneat. 2016a. “Evolutionary Patterns of Shape and Functional Diversification in the Skull and Jaw Musculature of Triggerfishes (Teleostei: Balistidae).” *Journal of Morphology* 277 (6): 737–52. https://doi.org/10.1002/jmor.20531.

———. 2016b. “Phylogenetic Relationships and the Evolution of BMP4 in Triggerfishes and Filefishes (Balistoidea).” *Molecular Phylogenetics and Evolution* 94 (January): 397–409. https://doi.org/10.1016/j.ympev.2015.09.014.

McKenzie, David J., John F. Steffensen, Edwin W. Taylor, and Augusto S. Abe. 2012. “The Contribution of Air Breathing to Aerobic Scope and Exercise Performance in the Banded Knifefish *Gymnotus carapo* L.” *Journal of Experimental Biology* 215 (8): 1323–30. https://doi.org/10.1242/jeb.064543.

Meyer, David L. 1985. “Evolutionary Implications of Predation on Recent Comatulid Crinoids from the Great Barrier Reef.” *Paleobiology* 11 (2): 154–64. https://doi.org/10.1017/S0094837300011477.

Meyers, R. F. 1991. *Micronesian Reef Fishes: A Practical Guide to the Identification of the Coral Reef Fishes of the Tropical Central and Western Pacific*. 2nd ed. Guam, USA: Coral Graphics.

Millard, Steven. 2013. *EnvStats: An R Package for Environmental Statistics*. R. New York: Springer. http://www.springer.com.

Nakazono, Akinobu, and Hiroshi Kawase. 1993. “Spawning and Biparental Egg-Care in a Temperate Filefish, *Paramonacanthus japonicus* (Monacanthidae).” *Environmental Biology of Fishes* 37 (3): 245–56. https://doi.org/10.1007/BF00004632.

Norberg, Ulla M. 1981. “Allometry of Bat Wings and Legs and Comparison with Bird Wings.” *Philosophical Transactions of the Royal Society of London. Series B, Biological Sciences* 292 (1061): 359–98.

Norberg, Ulla M., and Michael James Lighthill. 1981. “Allometry of Bat Wings and Legs and Comparison with Birds Wings.” *Philosophical Transactions of the Royal Society of London. B, Biological Sciences* 292 (1061): 359–98. https://doi.org/10.1098/rstb.1981.0034.

Nursall, J. R. 1958. “The Caudal Fin as a Hydrofoil.” *Evolution* 12 (1): 116–20. https://doi.org/10.1111/j.1558-5646.1958.tb02937.x.

Olsen, Aaron M. 2017. “Feeding Ecology Is the Primary Driver of Beak Shape Diversification in Waterfowl.” *Functional Ecology* 31 (10): 1985–95. https://doi.org/10.1111/1365-2435.12890.

Olsen, Aaron M., and Mark W. Westneat. 2015. “StereoMorph: An R Package for the Collection of 3D Landmarks and Curves Using a Stereo Camera Set-Up.” *Methods in Ecology and Evolution* 6 (3): 351–56. https://doi.org/10.1111/2041-210X.12326.

Orme, David, Rob Freckleton, Gavin Thomas, Thomas Petzoldt, Susanne Fritz, Nick Isaac, and Will Pearse. 2013. *Caper: Comparative Analyses of Phylogenetics and Evolution in R*. R. https://CRAN.R-project.org/package=caper.

Pace, C. M., and A. C. Gibb. 2009. “Mudskipper Pectoral Fin Kinematics in Aquatic and Terrestrial Environments.” *Journal of Experimental Biology* 212 (14): 2279–86. https://doi.org/10.1242/jeb.029041.

Paradis, Emmanuel, Julien Claude, and Korbinian Strimmer. 2004. “APE: Analyses of Phylogenetics and Evolution in R Language.” *Bioinformatics* 20 (2): 289–90. https://doi.org/10.1093/bioinformatics/btg412.

Peristiwady, T., and P. Geistdoerfer. 1991. “Biological Aspects Of *Monacanthus tomentosus* (Monacanthidae) in the Seagrass Beds of Kotania Bay, West Seram, Moluccas, Indonesia.” *Marine Biology* 109 (1): 135–39. https://doi.org/10.1007/BF01320240.

Plaut, Itai, and Tamar Chen. 2003. “How Small Puffers (Teleostei: Tetraodontidae) Swim.” *Ichthyological Research* 50 (2): 149–53. https://doi.org/10.1007/s10228-002-0153-3.

R Core Team. 2016. *R: A Language and Environment for Statistical Computing*. Vienna, Austria: R Foundation for Statistical Computing. https://www.R-project.org/.

Rade, Cristina. 2013. “Functional Morphology of Aquatic Substrate-Based Locomotion in Walking Batfishes (Lophiiformes; Ogcocephalidae).” M.S., United States -- New York: Adelphi University. https://search.proquest.com/docview/1372277467/abstract/35C108F329524A92PQ/1.

Randall, John E. 1955. “Fishes of the Gilbert Islands.” http://repository.si.edu//handle/10088/6126.

———. 1964. “A Revision of the Filefish Genera Amanses and Cantherhines.” *Copeia* 1964 (2): 331–61. https://doi.org/10.2307/1441027.

———. 1985. *Guide to Hawaiian Reef Fishes*. Newtown Square, PA : Kaneohe, HI: Harrowood Books ; copublished and distributed in Hawaii by Treasures of Nature.

———. 2007. *Reef and Shore Fishes of the Hawaiian Islands*. Honolulu: Sea Grant College Program, University of Hawai‘i.

Randall, John E, Gerald R. Allen, and Roger C. Steene. 1997. *Fishes of the Great Barrier Reef and Coral Sea, Revised and Expanded Edn.* Honolulu, HI: University of Hawaii Press.

Randall, John. E., and W. D. Hartman. 1968. “Sponge-Feeding Fishes of the West Indies.” *Marine Biology* 1 (3): 216–25. https://doi.org/10.1007/BF00347115.

Randall, John E., Keiichi Matsuura, and Akira Zama. 1978. “A Revision of the Triggerfish Genus Xanthichthys, with Description of a New Species.” *Bulletin of Marine Science* 28 (October): 688–706.

Revell, Liam J. 2012. “Phytools: An R Package for Phylogenetic Comparative Biology (and Other Things).” *Methods in Ecology and Evolution* 3 (2): 217–23. https://doi.org/10.1111/j.2041-210X.2011.00169.x.

Rosenberger, Lisa J. 2001. “Pectoral Fin Locomotion in Batoid Fishes: Undulation versus Oscillation.” *The Journal of Experimental Biology* 204: 379–94.

Rouleau, Sébastien, Hélène Glémet, and Pierre Magnan. 2010. "Effects of Morphology on Swimming Performance in Wild and Laboratory Crosses of Brook Trout Ecotypes." *Functional Ecology* 24 (2): 310–21. https://doi.org/10.1111/j.1365-2435.2009.01636.x.

Ruiz-Torres, Ricardo, Oscar M. Curet, George V. Lauder, and Malcolm A. MacIver. 2013. "Kinematics of the Ribbon Fin in Hovering and Swimming of the Electric Ghost Knifefish." *Journal of Experimental Biology* 216 (5): 823–34. https://doi.org/10.1242/jeb.076471.

Sano, Mitsuhiko, Makoto Shimizu, and Yukio Nose. 1984. *Food Habits of Teleostean Reef Fishes in Okinawa Island, Southern Japan*. The University Museum, The University of Tokyo, Bulletin No. 25. Tokyo: University of Tokyo Press.

Santini, Francesco, Laurie Sorenson, and Michael E. Alfaro. 2013. "A New Multi-Locus Timescale Reveals the Evolutionary Basis of Diversity Patterns in Triggerfishes and Filefishes (Balistidae, Monacanthidae; Tetraodontiformes)." *Molecular Phylogenetics and Evolution* 69 (1): 165–76. https://doi.org/10.1016/j.ympev.2013.05.015.

Savile, D. B. O. 1957. "Adaptive Evolution in the Avian Wing." *Evolution* 11 (2): 212–24. https://doi.org/10.2307/2406051.

Schoenfuss, Heiko L., and Richard W. Blob. 2003. "Kinematics of Waterfall Climbing in Hawaiian Freshwater Fishes (Gobiidae): Vertical Propulsion at the Aquatic–Terrestrial Interface." *Journal of Zoology* 261 (2): 191–205. https://doi.org/10.1017/S0952836903004102.

Sfakiotakis, M., D.M. Lane, and J.B.C. Davies. 1999. "Review of Fish Swimming Modes for Aquatic Locomotion." *IEEE Journal of Oceanic Engineering* 24 (2): 237–52. https://doi.org/10.1109/48.757275.

Shirgaonkar, Anup A., Oscar M. Curet, Neelesh A. Patankar, and Malcolm A. MacIver. 2008. "The Hydrodynamics of Ribbon-Fin Propulsion during Impulsive Motion." *Journal of Experimental Biology* 211 (21): 3490–3503. https://doi.org/10.1242/jeb.019224.

Sprinkle, Brennan, Rahul Bale, Amneet Pal Singh Bhalla, Malcolm A. MacIver, and Neelesh A. Patankar. 2017. "Hydrodynamic Optimality of Balistiform and Gymnotiform Locomotion." *European Journal of Computational Mechanics* 26 (1–2): 31–43. https://doi.org/10.1080/17797179.2017.1305160.

Svendsen, Jon C., Christian Tudorache, Anders D. Jordan, John F. Steffensen, Kim Aarestrup, and Paolo Domenici. 2010. "Partition of Aerobic and Anaerobic Swimming Costs Related to Gait Transitions in a Labriform Swimmer." *Journal of Experimental Biology* 213 (13): 2177–83. https://doi.org/10.1242/jeb.041368.

Swaddle, John P., and Mark S. Witter. 1998. “Cluttered Habitats Reduce Wing Asymmetry and Increase Flight Performance in European Starlings.” *Behavioral Ecology and Sociobiology* 42 (4): 281–87.

Thomas, Adrian L. R. 1993. “The Aerodynamic Costs of Asymmetry in the Wings and Tail of Birds: Asymmetric Birds Can’t Fly Round Tight Corners.” *Proceedings: Biological Sciences* 254 (1341): 181–89.

Tobalske, Bret W. 2007. “Biomechanics of Bird Flight.” *Journal of Experimental Biology* 210 (18): 3135–46. https://doi.org/10.1242/jeb.000273.

Triantafyllou, G. S., M. S. Triantafyllou, and M. A. Grosenbaugh. 1993. “Optimal Thrust Development in Oscillating Foils with Application to Fish Propulsion.” *Journal of Fluids and Structures* 7 (2): 205–24. https://doi.org/10.1006/jfls.1993.1012.

Vijay Anand, P., and N.G.K Pillai. 2005. “Community Organization of Coral Reef Fishes in the Rubble Sub-Habitat of Kavaratti Atoll, Lakshadweep, India.” *Journal of the Marine Biological Association of India* 47 (1): 77–82.

Vogel, S. 1994. *Life in Moving Fluids: The Physical Biology of Flow*. 2nd ed. Princeton, NJ: Princeton University Press.

Wainwright, Peter C., David R. Bellwood, and Mark W. Westneat. 2002. “Ecomorphology of Locomotion in Labrid Fishes.” *Environmental Biology of Fishes* 65 (1): 47–62. http://dx.doi.org/10.1023/A:1019671131001.

Walker, Jeffrey A., and Mark W. Westneat. 2000. “Mechanical Performance of Aquatic Rowing and Flying.” *Proceedings of the Royal Society of London. Series B: Biological Sciences* 267 (1455): 1875–81. https://doi.org/10.1098/rspb.2000.1224.

———. 2002. “Performance Limits of Labriform Propulsion and Correlates with Fin Shape and Motion.” *Journal of Experimental Biology* 205 (2): 177–87.

Watanabe, Yuuki, and Katsufumi Sato. 2008. “Functional Dorsoventral Symmetry in Relation to Lift-Based Swimming in the Ocean Sunfish *Mola mola*.” *PLoS ONE* 3 (10). https://doi.org/10.1371/journal.pone.0003446.

Webb, Paul W. 1982. “Locomotor Patterns in the Evolution of Actinopterygian Fishes.” *American Zoologist* 22 (2): 329–42. https://doi.org/10.1093/icb/22.2.329.

Webb, Paul W. 1984. “Body Form, Locomotion and Foraging in Aquatic Vertebrates.” *American Zoologist* 24 (1): 107–20. https://doi.org/10.1093/icb/24.1.107.

Webb, Paul W, and Antonia Gardiner Fairchild. 2001. "Performance and Maneuverability of Three Species of Teleostean Fishes." *Canadian Journal of Zoology* 79 (10): 1866–77. https://doi.org/10.1139/z01-146.

Webb, Paul W., and Daniel Weihs. 2015. "Stability versus Maneuvering: Challenges for Stability during Swimming by Fishes." *Integrative and Comparative Biology* 55 (4): 753–64. https://doi.org/10.1093/icb/icv053.

Weihs, D. 1973. "The Mechanism of Rapid Starting of Slender Fish." *Biorheology* 10 (3): 343–50. https://doi.org/10.3233/BIR-1973-10308.

Whoriskey, F. G., and R. J. Wootton. 1987. "The Swimming Endurance of Threespine Sticklebacks, *Gasterosteus aculeatus* L., from the Afon Rheidol, Wales." *Journal of Fish Biology* 30 (3): 335–39. https://doi.org/10.1111/j.1095-8649.1987.tb05757.x.

Wiktorowicz, A. M., D. V. Lauritzen, and M. S. Gordon. 2010. "Powered Control Mechanisms Contributing to Dynamically Stable Swimming in Porcupine Puffers (Teleostei: Diodon Holocanthus) (Ed. G. K. Taylor, M. S. Triantafyllou and C. Tropea),." In *Animal Locomotion*, edited by G. K. Taylor, M. S. Triantafyllou, and C. Tropea, 87–97. Berlin: Springer.

Wilson, Anthony B., Alexandra Wegmann, Ingrid Ahnesjö, and Jorge M. S. Gonçalves. 2020. "The Evolution of Ecological Specialization across the Range of a Broadly Distributed Marine Species." *Evolution* n/a (n/a). https://doi.org/10.1111/evo.13930.

Winterbottom, Richard. 1974. "The Familial Phylogeny of the Tetraodontiformes (Acanthopterygii: Pisces) as Evidenced by Their Comparative Myology." *Smithsonian Contributions to Zoology*, no. 155: 1–201. https://doi.org/10.5479/si.00810282.155.

Wright, Wright. 2000. "Form and Function in Aquatic Flapping Propulsion: Morphology, Kinematics, Hydrodynamics, and Performance of the Triggerfishes (Tetraodontiformes: Balistidae)." Doctoral Thesis, Chicago, IL: University of Chicago.

Xin, ZhiQiang, and ChuiJie Wu. 2013. "Shape Optimization of the Caudal Fin of the Three-Dimensional Self-Propelled Swimming Fish." *Science China Physics, Mechanics and Astronomy* 56 (2): 328–39. https://doi.org/10.1007/s11433-013-4994-8.

Youngerman, Eric D., Brooke E. Flammang, and George V. Lauder. 2014. "Locomotion of Free-Swimming Ghost Knifefish: Anal Fin Kinematics during Four Behaviors." *Zoology (Jena, Germany)* 117 (5): 337–48. https://doi.org/10.1016/j.zool.2014.04.004.

Yuan, Michael L., Marvalee H. Wake, and Ian J. Wang. 2019. "Phenotypic Integration between Claw and Toepad Traits Promotes Microhabitat Specialization in the Anolis Adaptive Radiation." *Evolution* 73 (2): 231–44. https://doi.org/10.1111/evo.13673.